Acoustic Levitation

- Optimization of instrumental parameters of the LevMac instrument for protein crystallization applications

LUNDS
UNIVERSITET
Lunds Tekniska Högskola

LTH School of Engineering at Campus Helsingborg

Bachelor thesis:
Maria Knutsson

LTH School of Engineering
Lund University
Box 882
SE-251 08 Helsingborg
Sweden

LTH Ingenjörshögskolan vid Campus Helsingborg
Lunds Universitet
Box 882
251 08 Helsingborg

Printed in Sweden
Media-Tryck
Biblioteksdirektionen
Lunds University
Lund 2006

Abstract

The LevMac is an analytical instrument under development that makes use of levitated droplets in the 100 nL-2μL range. By the use of the levitated droplets, with the only contacting surface being the surrounding gaseous medium, the LevMac avoids the most common problems associated with miniaturization of analytical techniques, e.g. contamination of the sample by desorption from container walls, adsorption of the analyte to the walls of the vessel and interfaces leading to a decrease in recovery, and optical interference at the walls of the sample container disturbing the detection.

Additions to the levitated droplet can be made in the pL volume range and reactions in the levitated droplet can be monitored by different spectroscopic techniques. After analysis, the droplet can be transferred to, e.g. a separation system for further analysis of its constituents or it can be stored, frozen inside a glass capillary.

In this thesis, the instrumental parameters of the LevMac were screened and optimized with the aim of developing a method for 2D membrane protein reconstitution in the levitated droplets. A reliable positioning technique capable of easy positioning of droplets in the levitator without air bubble introduction was developed. The GELoader tip was shown to be a suitable positioning technique, results showing it robust, reproducible, and reliable. A quick method for the prediction of physical properties of reagent solutions was found by using glass capillaries. Instrumental performance were investigated and established through different experiments. Limit of detection for volume measurements by the LevMac was found to be 0.03 μL, and for the scattering measurements 0.1 A.U.

A method for 2D crystallization of membrane proteins using cyclodextrin for the detergent removal was developed and optimized with promising results. By using a higher concentration of cyclodextrin the reconstitution process starts almost immediately and proceeds quickly, providing aggregates. By using more and more diluted cyclodextrin solutions as the reaction proceeds, the reconstitution process is slowed down and levels off.

Keywords: LevMac, levitation, miniaturization, 2D crystallization, reconstitution, membrane proteins.

Sammanfattning

LevMacinstrumentet är ett analysinstrument under utveckling som utnyttjar leviterade droppar på 100 nl – 2 µl. Genom att använda leviterade droppar med den omgivande atmosfären som enda kontaktyta, undviker LevMac'en de vanligaste problemen associerade med miniatyrisering av analytiska tekniker, t.ex. kontaminering av provet genom desorption från provbehållaren eller andra gränsytor, adsorption av analyten till omgivningen med minskat utbyte som följd, och optisk interferens vid väggarna av provbehållaren vilket resulterar i störningar av detektionen.

Tillsatser till den leviterade droppen kan göras i pl-området och reaktioner i droppen kan följas med olika spektroskopiska tekniker. Efter analysen kan droppen överföras, t.ex. till ett separationssystem för vidare analys av dess innehåll eller till en glasskapillär för lagring i fryst tillstånd.

I det här examensarbetet screenades och optimerades LevMac-instrumentets instrumentella parametrar med syftet att utveckla en metod för 2D rekonstitution av membranprotein i de leviterade dropparna. En pålitlig positioneringsteknik kapabel att smidigt placera dropparna i levitatorn utan att introducera luftbubblor utvecklades. GELoader spetsen visade sig vara en passande positioneringsteknik som var robust, reproducerbar och pålitlig. En snabb metod för att förutsäga lösningars fysikaliska egenskaper togs fram genom att använda glaskapillärer. Instrumentell prestanda undersöktes och fastställdes genom olika experiment. Detektionsgränsen för mätningarna av volymen med LevMac instrumentet sattes till 0.03 µL och för mätningarna av spridningsvärdena till 0.1 A.U.

En metod för 2D kristallisering av membranprotein genom att använda cyklodextrin som detergentborttagare utvecklades och optimerades med lovande resultat. Genom att använda höga koncentrationer av cyklodextrin startar rekonstituerings processen nästan direkt och fortskrider snabbt. Genom använda mer och mer utspädda cyklodextrin lösningar när reaktionen fortskrider, saktas reaktionen ner och planar ut.

Nyckelord: LevMac, levitering, miniatyrisering, 2D kristallisation, rekonstitution, membranprotein.

Foreword

The work in this thesis was a part of a Bachelor of Science in Chemical Engineering at LTH School of Engineering, Lund University, Campus Helsingborg and was carried out during the spring of 2006 at Crystal Research AB, Lund. Sabina Santesson was the supervisor, and Margareta Sandahl the examiner.

The aim of this work was to optimize the instrumental parameters of the LevMac instrument and to develop a method for 2D crystallization of membrane proteins in order to make future predictions of suitable instrumental and experimental settings using complex protein solutions.

List of contents

APPENDIX

1 Introduction

The analytical-chemical problems facing the modern researchers in biochemical, biological, medicinal, and drug areas are becoming more and more advanced. Different ways of analyzing the function, localization, and interaction of certain molecules involvement in diseases are areas of interest for the Life Sciences. There is an increasing need of analytical techniques able to monitor biological processes on the molecular and cellular level and the development of new analysis instruments for this area of science are of great importance.

1.1 Miniaturization

In recent years, there has been a miniaturization drive in analytical chemistry inspired by the search for improved analytical performance. This has led to the development of e.g. down-scaled separation techniques such as micro column liquid chromatography, capillary electrophoresis, and capillary electro chromatography. Further miniaturization of all the steps of the analytical chain, from sampling to detection, has led to the micro total analysis system.

The main reasons for the expanding interest in miniaturization have been the growing need of higher throughput and the problems associated with very small sample amounts, especially in the growing field of protein crystallography – this because no amplification technique such as PCR exists in the protein world, which render sensitivity and dynamic range critical parameters.

The protein world is also very diverse. Protein size can range from a few tens of amino acids to several MDa, and the amount of sample that can be obtained is often limited.

For the analysis of very small sample volumes, miniaturization is a must since minimal dead volumes and sample losses are required. Beneficial effects of down-scaling are decreased requirements of sample and reagent volumes. Miniaturized analysis systems are also more cost effective since the analysis time is reduced in smaller systems, and because more runs can be performed on the same sample amount.

When a system is scaled down, with all the system parameters decreased uniformly, the changes in length, area, and volume ratios alter the relative influence of various physical effects that determine the overall operation [1]. The surface area to volume ratio is bigger in a miniaturized system compared

to a large scale analytical system which can sometimes be a disadvantage [1]. For example, the relatively large surface may cause contamination of the sample solution by desorption from the container walls or adsorption of the analyte to the container walls and interfaces, leading to a decrease in recovery. Another problem with miniaturization can be optical interference at the walls of the sample container, disturbing the detection [1]. These problems exist in normal sized systems as well but are more troublesome in miniaturized systems when dealing with small sample amounts since the losses can be considerable.

The number of significant properties increases as a system gets smaller. Temperature, substrate material properties, liquid properties, electrical, and magnetical properties all need to be taken into consideration. When dealing with miniaturized systems it is also important to have control of surface tension, surface chemistry, bubble formation, and liquid evaporation, since fast evaporation is associated with the large surface to volume ratios [2, 3, 4, 5, 6, and 7].

1.1.1 The LevMac instrument

In this thesis an analytical instrument under development, the LevMac instrument, has been used. In order to circumvent the problems associated with miniaturization, the LevMac makes use of levitated droplets in the 100 nL – 2 µL volume range (figure 1).

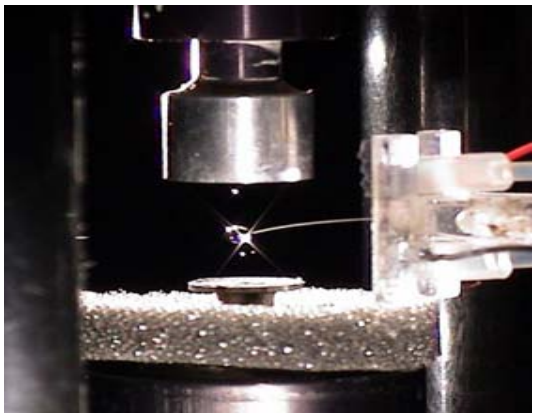

Figure 1: A droplet in the LevMac.

Additions to the levitated droplet can be made in the pL volume range and reactions in the levitated droplet can be monitored by different spectroscopic techniques. After analysis, the droplet can be transferred to e.g. a separation system for further analysis of its constituents or it can be stored, e.g. frozen inside a glass capillary.

The levitated droplet method exhibits the same miniaturization benefits as the more common chip approach, such as diversity of application, and low reagent and sample consumption. The levitated droplet, in addition, also comprises the advantage of preventing the chemical and thermal contamination that accompanies contact between droplets and external objects, since the only contacting surface is the surrounding gaseous medium, commonly air. The sample droplet makes out its own “container” and different substances can be introduced into the droplet in a contact-less way through the usage of flow-

through dispensers. The use of levitated droplets also has the benefit of increased sensitivity of detection, since no walls disturb the detection [8].

1.1.1.1 The ultrasonic levitator

The central part of the LevMac instrument, is the ultrasonic levitator which can be seen in figure 2.

For a levitation technique to be useful as a bioanalytical technique it must combine biological compatibility with ease of handling, stable sample position, easy access to the sample, low costs for supply and operation, all requirements fulfilled by acoustic levitation [1].

Ultrasonic (or acoustic) levitation requires no specific physical properties of the sample, in contrast to most other levitation techniques, such as those based on electrostatic or magnetic fields [9]. Ultrasonic levitation is a promising tool for miniaturization of entire analysis procedures beginning at the sampling stage. Sample volumes of a few microliters can be handled in a contact-less way and protected from the loss of analyte through adsorption, memory effects, and contamination from container walls [10].

The technique has previously been applied to investigate the evaporation, drying, temperature, and stability of liquid droplets [11]. It has also been used to monitor the formation of ice particles, as well as in titration and crystallization studies of pharmaceuticals and proteins [11]. Acoustic levitation is well suited for analytical chemistry because surface tension and density of the sample droplet are the only properties that determine the viability of the method [10].

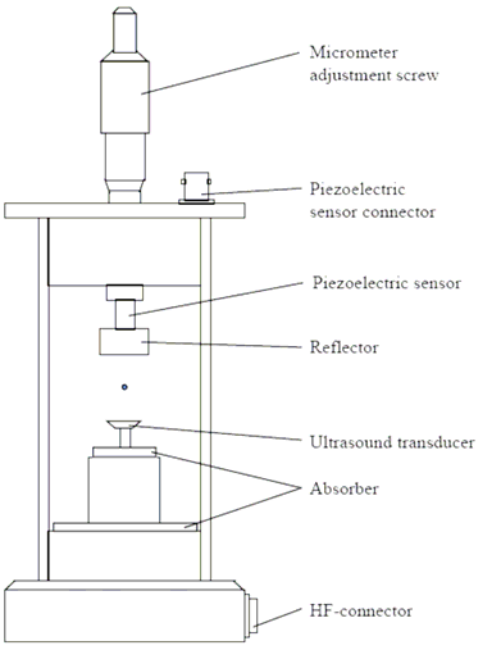

Figure 2: Schematics of the acoustic levitator.

In the LevMac instrument sample droplets are positioned in the nodes of an ultrasonic standing wave. This standing wave has equally spaced nodes and antinodes, generated as a result of multiple reflections of the sound pressure and velocity amplitude between an ultrasonic transducer and a solid, concave reflector [12].

There are generally four to five pressure nodes generated but only the inner two or three can be used for stable

levitation since the outer nodes are influenced by destabilizing effects from the transducer and the reflector.

To levitate a droplet, the ultrasound intensity has to be strong enough to overcome gravity so that the droplet does not fall down. The behavior of droplets in ultrasonic levitators is governed by the interaction between gravity and capillary forces, as well as the sound radiation pressure [13].

Excessive ultrasonic power yields a significant drop deformation while optimal setting of the HF-power gives a spherical shape of the levitated sample. With increasing sound intensity the droplet will be spheroidally deformed with a continuous growth of its horizontal diameter, i.e., the droplet forms an ellipsoid. If the sound pressure level becomes too high the droplet disintegrates into smaller droplets, since the capillary forces become too weak to keep it intact [13].

The maximum diameter of a levitated sample is a function of the ultrasonic wavelength and is about half the wavelength under ambient atmospheric conditions. Usually a levitator operates with ultrasonic frequencies of 15-100 kHz, resulting in wavelengths of 2.2 - 0.34 cm [9]. For wavelengths exceeding 8 mm, the maximum volume is related to physical properties of the droplet, like surface tension and specific density. The minimum droplet volume is also restricted. At a certain minimum volume, droplets tend to be displaced from their rest position in the nodal point of the stationary ultrasonic field and are easily blown away by the gas flow induced by the ultrasonic field [10].

If the liquid evaporates significantly and the droplet becomes smaller, the surface tension force becomes more dominant than the acoustic radiation stress and the droplet gets more spherical. For droplets that do not change in volume during the time of experiments, e.g., glycerol droplets or droplets with replenishing additions, the shape of the droplets are not changed because the acoustic pressure remains constant.

Strong ultrasonic fields can be damaging for sensitive samples such as proteins, and the ultrasonic power should thus be kept as low as possible. Stabilization of the levitated droplet is achieved by adjusting the distance between the transducer and the reflector, and by proper setting of the ultrasonic power (the HF-power). The required transducer amplitude increases with sample size and is proportional to the sample density [12].

1.1.1.2 The flow-through dispenser

Stable levitation of a liquid sample of a given size requires a regulating circuit of a solvent replenish and a size measurement module to keep the volume

constant when the droplet evaporates. The droplet size can be determined by means of light scattering, while solvent fill-up can be carried out with piezoelectric flow-through dispensers, which are also suitable for sample enrichment of levitated droplets [10].

Ink-jet printing technology originally formed the basis for the development of the flow-through dispensers, but with the drawback of generating droplets from enclosed volumes of liquids [14]. This made it difficult to insert them in the flow line of flow-through systems for on-line sample deposition.

Problems associated with these kinds of dispensers were clogging, air trapping, and extensive cleaning difficulties.

Therefore the flow-through dispensers were developed at the department of Electrical Measurements, Lund University, Lund, Sweden.

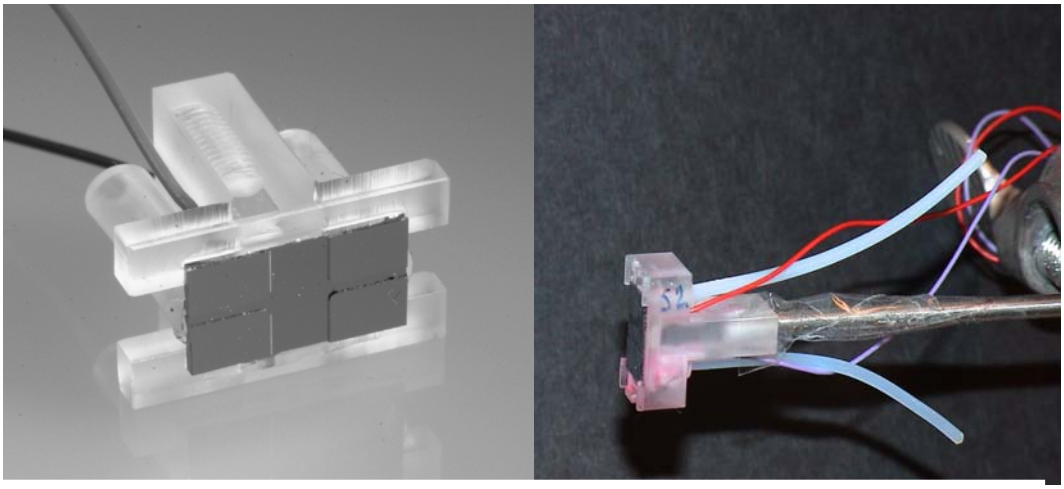

Figure 3: The piezoelectric flow-through dispenser.

The main advantages of the flow-through dispenser are the possibility of dispensing samples from flowing liquids, the high precision non-contact mode of sample supply, the small size of the droplets, and the high droplet ejection frequency [8]. By having a flow-through channel, cleaning procedures and removal of trapped air bubbles are made easier since the washing solution does not have to pass exclusively through the small orifice of the dispenser.

The piezoelectric flow-through dispensers are dispensing exactly one droplet at a time at a repetition rate of 1 to 9000 droplets per second [8]. In the LevMac, they are used for the addition of water, crystallization agents, or other solutions in the pL-scale to the levitated droplet [15]. The droplets ejected from the dispensers are transmitted to the levitated sample in a non-contact manner from a flow-through channel formed by joining two micro structured silicon plates, 13 mm long, 6 mm wide, and 250 µm thick each.

The flow-through channel measures 8 mm × 1 mm × 50 µm and has a volume of 400 nL. In the center of the channel a protruding pyramid-shaped nozzle is formed.

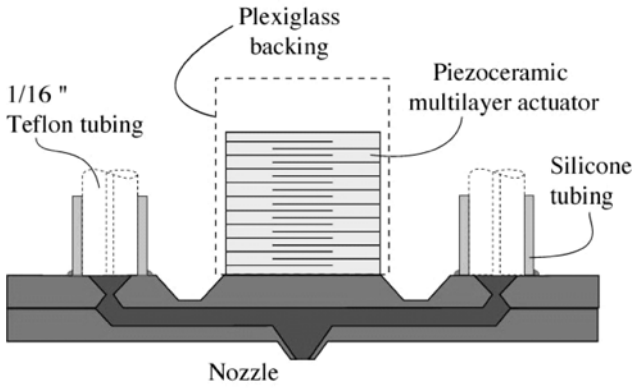

Figure 4: Schematics of the flow-through dispenser construction.

To obtain stable droplet formation, it is essential that the orifice front surface is kept free from liquid deposits, crystals, and particles. The pyramid-shape helps to ensure this since the front surface area is only a few micrometers wide. Liquid and particles that might be deposited there are more likely to stick to the side walls of the nozzle, with no adverse effect on the formation of droplets [14].

In the flow-through channel wall, opposite to the orifice, a multilayer piezoelectric element is connected to a push-bar, as shown in figure 5. A piezoelectric material has the capacity of generating a voltage when pressure is laid on it, and *vise versa* it has the ability of changing shape when exposed to an electric voltage. By applying a short voltage pulse across the piezoelectric element of the flow-through dispenser, it elongates and pushes into the channel, generating a pressure pulse in the liquid.

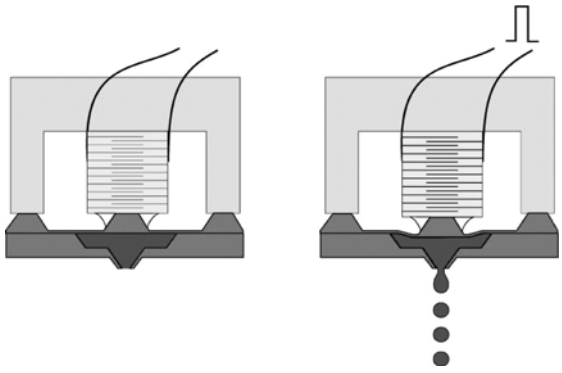

Figure 5: The working principle of the dispenser.

The increased pressure accelerates the liquid in the nozzle and a droplet is ejected. It is important that the pressure build-up in the flow-through channel is rapid in order to create a high acceleration of the liquid in the nozzle. If the velocity of the liquid at the exit is too low, the liquid will wet the front area because of surface tension, causing reduced stability and directional control of droplet formation. A rapid pressure build-up is facilitated by making the physical dimensions of the dispenser small [14]. To form a droplet, the pressure pulse must overcome the surface tension force at the nozzle exit and viscous losses within the nozzle itself, as well as accelerating the mass of the liquid [16].

The volume of the ejected droplets, typically in the range of 50-100 pL, is dependent on the size of the nozzle, the shape on the voltage pulse, and liquid

parameters such as surface tension, viscosity, and density [15]. This also means that not all solutions are suited for use with the dispensers. Such liquids have to be metered in an alternative way if they are going to be used in the instrument.

A problem that can arise with the dispensers if they are used with incorrect settings, unsuitable liquids, or if handling them wrongly is the formation of satellite droplets.

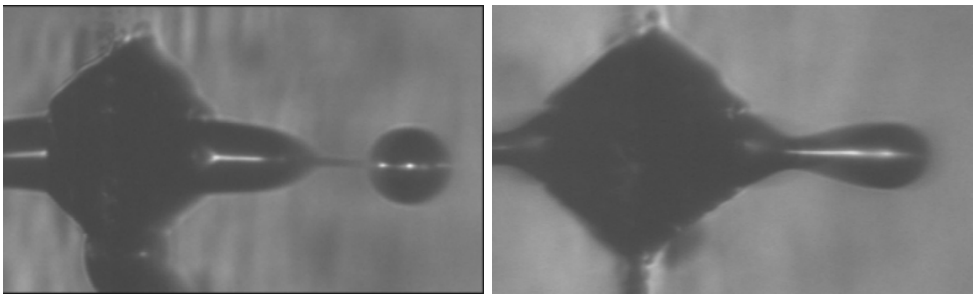

Figure 6: In the left picture, a satellite droplet is formed from the tail of the original droplet. The right picture is showing a droplet being ejected without any satellite droplet formation.

A satellite droplet is a part of the original droplet, formed from the tail of the original droplet as shown in figure 6. Depending on the amplitude and duration of the applied pulse, the tail may get relatively long and one or more satellite droplets may be formed.

The size, velocity, and trajectory of these satellite droplets are different from the main dispenser droplet and will not hit the levitated sample, making it impossible to know the amount of solution added.

Varying fluid properties will affect droplet velocity, droplet size, and satellite droplet formation and care must be taken when driving conditions like pulse amplitude and pulse length are selected for a given situation [16].

To get a satellite free droplet formation, the shape of the pressure pulse must be adjusted to the liquid parameters [14], and the piezoelectric micro dispensers have to be tested for every solution needed in the procedure.

1.1.1.3 Detection systems for the LevMac

In order to truly benefit from the use of levitated droplets, remote and non-invasive detection protocols are important. Several remote detection systems, especially varieties of spectroscopic techniques have previously been tried, e.g. fluorescence imaging detection, Raman spectrometry, and X-ray diffraction detection [17]. The detection system is chosen depending on the

application. In this thesis, right angle light scattering detection (RALS) has been the choice of detection system.

1.2 Protein crystallization

1.2.1 The goal of protein crystallography

In modern biotechnology, one of the main goals is the development of new and more efficient pharmaceuticals. Obtaining drugs and medicines, which work specifically on the disease in question, will not only give a more efficient treatment but will also reduce the number of secondary effects. For this to be possible, the underlying mechanisms behind the disease must be very well understood. To understand these functions and processes correctly it has to be known how the microscopic components that are the keys to biology look like.

The three-dimensional structure of proteins has to be known, since the structure mirrors their function in the body. The best way to obtain structural information of these kinds of molecules is by the method of single crystal X-ray diffraction which relies on the growth of pure, large, and flawless protein crystals [18].

1.2.2 Protein crystallization

To grow a protein crystal, enough protein molecules must be obtained and then the proper conditions for molecules to form a crystal of sufficient size must be found.

The making of the protein crystal is the most time-consuming step in protein crystallography and is the final stage in a long chain of purifying steps. The availability of fast methods which consume small amounts of protein would be of great value.

Proteins are only active when the polypeptide chain is in its native, correctly folded state, so the macromolecules have to be crystallized from aqueous solutions under conditions where they do not denaturize. In solution protein molecules repel each other. Crystallization is initiated by addition of suitable precipitating agents which lead to supersaturation of the protein, followed by precipitation or crystallization.

There are four general categories of protein precipitation agents; salts, volatile organic solvents, polymers, and nonvolatile organic alcohols. Examples of solutions from each group are ammonium sulfate, ethanol, polyethylene glycol, and MPD, respectively [19].

The choice of precipitant is dependent on type of protein, protein concentration and what the goals of the experiment are. Ammonium sulfate is frequently used and gives crystals satisfactory for diffraction work but can be subjected to microbial growth when stored [18]. Organic solvents have been used with some success but the crystals must be kept in low temperature storage [18]. Polyethylene glycol, (PEG), is a common precipitant and is particularly good with proteins that have low intrinsic solubility [18].

The birth of a crystal, the nucleation process, is the biggest problem in protein crystallization partly due to the fact that the mechanisms are not completely understood. The mechanisms leading to the formation of clusters of molecules displaying translational and rotational order have their own rules completely different from those of crystal growth [20]. This nucleation step controls the structure of the crystallizing phase, the number of particles appearing, and thus the size of the crystal.

Protein crystals develop slowly because of slow diffusion, and due to collisions and rotations of the large molecules. The molecules must collide at just the right angle to interact with each other in the appropriate way in order to form a homogenous crystal, otherwise amorphous precipitation (figure 7) will take place instead.

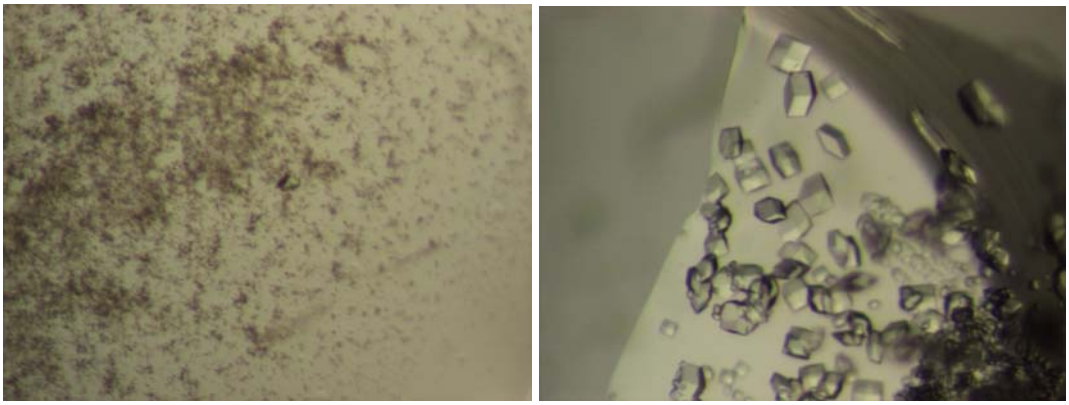

Figure 7: Lysozyme precipitate and crystals formed in a levitated droplet experiment. Amorphous precipitation is shown in the left picture. The right picture is showing protein crystals.

To form a crystal the aggregate must first exceed a specific size, the critical size, defined by the competition ratio of the surface area of the aggregate to its volume. Once the critical size is exceeded, the aggregate becomes a supercritical nucleus capable of further growth. If the nucleus on the other hand decreases in size so that it is smaller than the critical size, spontaneous dissolution will occur.

The process of formation of non-specific aggregates and non-crystalline precipitation from a supersaturated solution does not involve the competition between surface area and volume (*n*-mers add to the aggregate chain in a head to tail fashion, forming a linear arrangement) and thus generally occurs on a much faster time scale than crystallization.

The degree to which nucleation occurs is determined by the degree of supersaturation of the solutes in the solution. The extent of supersaturation is in turn related to the overall solubility of the crystallizing molecule. Supersaturation changes the conditions in the solution so that the repulsive interactions no longer exist and instead a slightly attractive interaction takes place between the molecules. Clusters begin to form and in some of these, the protein molecules start to arrange themselves in the most favorable energy state, the crystalline state.

Higher solubility allows for a greater number of diffusional collisions, thus higher degrees of supersaturation produce more stable aggregates (due to higher probability of collision of diffusing molecules) and therefore increase the likelihood of stable nuclei formation. In the case of a finite number of solute molecules, this condition generally results in the production of a large number of small crystals. At lower solute concentrations the formation of individual stable nuclei is increasingly rare, thus favoring the formation of single crystals [21].

To avoid amorphous precipitation and get large, flawless crystals, you attempt to minimize the opportunity for nucleation of crystal formation while maximizing the degree of supersaturation. These are incompatible factors and it is common to use a system that result in a gradual decrease in volume as the crystals form, so as to maintain a fairly high degree of supersaturation. By removing protein from solution as the crystals form, the remaining solution loses its supersaturation and it is thus necessary to reduce its volume to increase the concentration again. An alternative to reducing the volume is to continually add more precipitant to keep the solution in a supersaturated state until most of the protein has crystallized.

1.2.3 The crystallization process

There is a huge number of variables that can be explored in the search for crystallization conditions. All crystallization experiments are influenced by and depend on physical-, chemical-, and biochemical factors.

Some of the physical factors are temperature, rate of equilibration, vibration, and homogenous or heterogeneous nucleants. The chemical factors include precipitant type and concentration, pH, protein concentration, detergents, and

impurities. Among the biochemical factors are protein purity, ligands, aggregation state, posttranslational modification, genetic modification, and history.

Obviously there is a challenge in deciding how much variation to explore within each factor; much, little or none. A factor that is usually held constant during the screening is the size of the droplet, limiting the size of the crystals that can be grown.

A classical crystallization process is separated into two stages; screening and optimization [22].

In the screening process, lead crystallization conditions which will support nucleation and crystal growth are discovered and typically micro crystals, thin rods, or thin plates are produced. All proteins behave individually and differ in their optimal crystallization conditions, which are found by “pure luck” or with a very tedious and time consuming trial-and-error procedure [18]. This is the reason why screening experiments are designed for the determination of initial crystallization parameters so that as many experimental parameters as possible are varied within the multi-dimensional space of crystallization conditions [18].

After the screening procedure the crystallization conditions are optimized by varying parameters such as concentration and pH of the most successful conditions from the screening phase to find improved conditions in which the best crystals can be grown.

1.2.4 Methodologies

There are several methodologies for mixing the precipitation solutions with the protein, the ones most commonly used being the sitting drop, hanging drop, and micro batch techniques [22].
In each of these methods, a droplet is formed by the mixing of small volumes of protein and crystallization solution. For the hanging drop technique, the mixed droplet is placed on a cover slide that is inverted and sealed above a well containing the undiluted crystallization solution.

In the case of the sitting drop, the droplet is placed directly on a shelf adjacent to a well containing crystallization solution and the entire tray is sealed to prevent evaporation.

In the micro batch technique, the mixed droplet is placed in a well or depression and covered with oil to prevent or reduce evaporation.

In the sitting and hanging drop methods, the droplet equilibrates with the well solution through vapor diffusion. This results in a gradual concentration of the ingredients which will lead to supersaturation and crystallization. For the micro batch technique, gas permeability of the oil layer can be adjusted to allow for slow evaporation of the drop resulting in a similar concentration effect.

The LevMac instrument is an alternative for screening purposes. In the LevMac, levitated droplets of known protein concentrations can be injected with crystallizing agents using piezoelectric flow-through dispensers. With its ability of varying the droplet volume by evaporation and replenishing, and thus changing the concentrations of the droplet constituents, a wide range of possible crystallization conditions can be screened using one single droplet of protein solution [15].

When performing a screening procedure within the LevMac, a camera and a computer program is used to achieve continuous control of the droplet volume. Calculations are performed giving the concentrations of all components in the droplet at any time during the experiment, and right angle light scattering is used to monitor the precipitation or crystal formation in the levitated droplet [15]. Precipitation graphs can then be constructed giving the protein/crystallization agent concentration boundaries between the minimum and the maximum detectable protein precipitation.

The incubation time varies from protein to protein ranging from hours to months, and at a variety of temperatures. The search for crystals is usually done by inspecting the mixtures of proteins and crystallization solutions through a microscope to decide which mixtures contain crystals or show the most promise for use in further optimization.

1.2.5 Membrane proteins

Membrane protein structural biology is an important area of modern research. [23]. Integral membrane proteins, such as channels, transporters, and receptors are critical components of many fundamental biological processes and cellular functions, such as ion regulation and transport, molecular recognition and response, and energy transduction. 20-25% of the proteins encoded by the genome of an organism are integral membrane proteins, also, many membrane proteins are important in biomedical and biotechnological applications; the majority of drug targets being integral membrane proteins [24].

Integral membrane proteins are embedded in biological membranes *in vivo* and have to be treated in a different way than water-soluble proteins (described in the previous section) during the crystallization process.

The understanding of the functions of this broad range of proteins is highly restricted by a lack of structural information, due to the difficulty with obtaining crystals suitable for X-ray diffraction [24].

Integral membrane proteins are more difficult to isolate than water-soluble proteins. The native membrane surrounding the protein must be disrupted and replaced with detergent molecules of similar characteristics to keep the membrane protein in solution without causing any denaturation [24]. The hydrophobic tail of the detergent molecule binds to the hydrophobic areas of the protein which are usually embedded in the membrane, thus solubilizing these areas through the exposed hydrophilic head-groups of the detergent molecules [21].

The aggregation properties of detergents are described in terms of the hydrophobic effect, an entropy-driven process. Every detergent possesses a critical micelle concentration (CMC). The CMC is a function of the specific detergent and will also vary according to the composition of the solvent. At concentrations below the CMC, the detergent is in solution as a monomer. At a concentration equal to the CMC, the detergent spontaneously aggregates into a micelle. At concentrations above the CMC, there is an equilibrium between monomers and an increasing concentration of micelles.

In the presence of membrane proteins, three states of the detergent are in equilibrium; detergent monomers, protein-free detergent micelles, and detergent bound to the protein. The detergent bound to the protein is micelle-like in that it is a hydrophobic effect-driven aggregation of detergent molecules that sequester the non-polar portions of the detergent and protein away from aqueous solvent. This protein-detergent complex (PDC) is the entity that is crystallized, and both the protein and detergent properties are important. The use of different detergents can yield different crystal forms [23].

The solubility of a protein is a critical parameter in the crystallization process. The solubility dependence of factors such as the ionic strength, and pH has been well-characterized for water-soluble proteins. But factors influencing the solubility of integral membrane proteins, most notably the detergent, are poorly characterized [24], and the growing of three-dimensional crystals is relatively infrequent as compared to water soluble proteins [25].

Reconstitution of membrane proteins into lipid bilayers, to form crystals confined to two dimensions (2D crystals) is a viable alternative to 3D crystallization to get structures out of membrane proteins. However, as any

crystallization strategy, one of the main limitations of 2D crystallography is to produce crystals of high enough quality [25].

More about methodologies for 2D crystallization of membrane proteins are described in chapter 4.

2 Materials and methods

2.1 Materials

2.1.1 Chemicals

Water purified with a Milli-Q-system was used for all solutions, and for cleansing procedures of the levitator and the flow-through dispensers.

For the instrumental optimization of the LevMac, the following solutions of crystallographic grade (Hampton Research, Laguna Niguel, USA) were used:

- 100% 2-methyl-2.4-pentanediol (MPD)
- 100% v/v polyethylene glycol (PEG) 400
- 50% w/v PEG 1000
- 50% w/v PEG 1500
- 50% w/v PEG 6000
- 50% w/v PEG 10000
- 3.0 M sodium chloride
- 3.5 M ammonium sulfate
- 3.4 M sodium malonate (pH 6)

For the 2D membrane protein crystallization experiments, aqueous solutions of methyl-β-cyclodextrin (MBCD) with concentrations 3, 1, 0.5, 0.25, 0.1, 0.005, 0.0025, and 0.001% were used.
Liquid nitrogen was used to freeze the protein samples.

2.1.2 Protein and detergent samples for 2D crystallization

- HasAHasR DDM DLPC LPR1
- HasAHasR DDM EC LPR1
- HasAHasR C8E4 EC LPR1
- HasAHasR C8E4 DLPC LPR1

HasAHasR (protein)
DLPC, diauroylphosphatidylcholine (lipid)
C8E4, tetra-oxyethylene octyl ether (detergent)
DDM, N-dodecyl-β-d-maltoside (glycol-detergent)
LPR (lipid-to-protein ratio)

2.1.3 Material

- LevMac instrument, Crystal Research AB, Lund, Sweden, comprising a levitator, APOS BA 10, Dantec Dynamics GmbH, Erlangen, Germany, a flow-through dispenser, department of Electrical Measurements, Lund University, Lund, Sweden, and a light scattering detection system comprising a light source and a camera.
- Levitator, APOS BA 10, Dantec Dynamics
- Flow-through dispenser, department of Electrical Measuremnts, LU, Lund
- 1 ml LUER-LOK™ Syringe, Becton Dickinson, Singapore
- 10 ml LUER-LOK™ Syringe, Becton Dickinson, Franklin Lakes, USA
- NUNC™ Brand Products Disposable Conical Tubes, Nalge Nuncs International Corp, Naperville, USA
- GELoader tips 0.5-20 µL Original Eppendorf, Eppendorf AG, Hamburg, Germany
- Microsyringe, MICROLITER® # 701, Hamilton-Bonaduz, Schweiz
- 2 µL automatic pipette, Pipet·Lite, Rainin, USA
- 10 µL automatic pipette, Eppendorf
- Cold light source, FIBEROPTIC-HEIM LQ 1100, Zwitzerland
- Glass capillaries 5 µL, glass capillaries 25 µL, BLAUBRAND, intraMARK

2.2 Methods

2.2.1 Instrumental setup

The LevMac Instrument, (Crystal Research AB, Lund, Sweden) was used to make evaporation experiments, precipitation experiments with ammonium sulfate and for the 2D crystallization of membrane proteins.

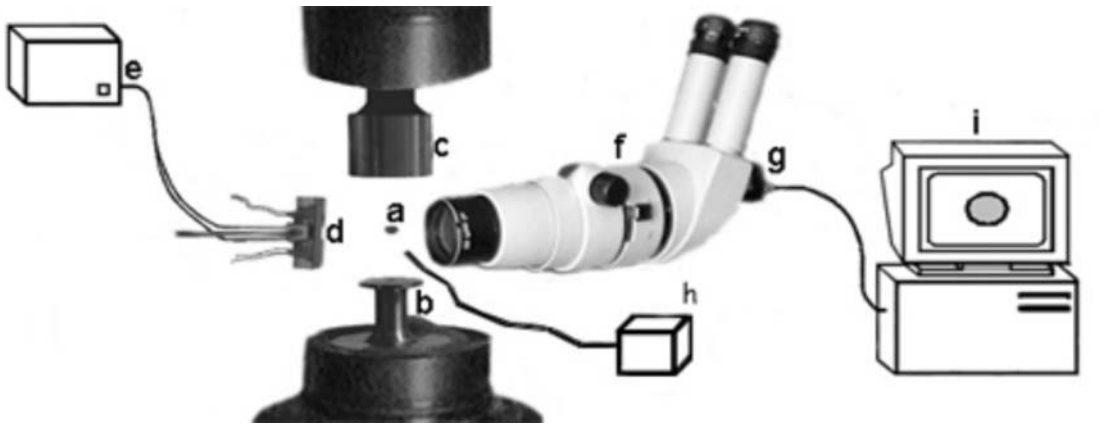

Figure 8: Overview of the instrumental setup: a) a levitated droplet, b) the transducer of the levitator, c) the reflector, d) the flow-through dispenser, e) power supply box for the dispenser, where slope and amplitude are chosen, f) represents the objective, g) the camera, h) the RALS system, i) the computer.

Additional flow-through dispensers, (department of Electrical Measurements, LU, Lund, Sweden), were used for experiments with various solutions.

The pulse length of the dispensers was 70 µs throughout the experiments, the pulse frequency was varied between 14 and 50 Hz. The maximum value of the slope (P1) was 10.4 V, and the maximum value of the amplitude (P2) was 28.4V.

A separate ultrasonic levitator APOS BA 10, (Dantec Dynamics GmbH, Erlangen, Germany), was used to practice positioning of droplets, and was used for protein experiments left over night.

2.2.2 Experimental design

In the first phase of the work basic instrumental principles were to be studied and standard measurements were to be performed with water and other solutions commonly used in protein crystallization applications.

- In order to find a simple and reliable positioning technique for droplets, an automatic pipette with two different plastic tips, and a Hamilton syringe were used. Droplets were positioned in a pressure node in the levitator and different positioning techniques were evaluated with regard to introduced air bubble formation, and the strength of the HF-power needed to detach a droplet from the tip. (Section 3.1)

- To optimize the dispenser settings for different solutions the shape of the tension pulse was varied and intervals were found where stable beams of dispenser droplets could be achieved. (Section 3.2.1.2)

- A quick way of predicting physical properties of various solutions was developed using glass capillaries. (Section 3.2.2)

- In order to get a hint of how long an intermission with the dispenser could last and still get it to work after a restart; different solutions were tried during intermissions of variable length. (Section 3.2.3)

- The LevMac was used to perform evaporation experiments of various liquids in order to find an average evaporation speed. (Section 3.3.1)

- Compensation of evaporation was studied by finding dispenser ejection frequencies that made up for the liquid losses due to evaporation. (Section 3.4)

- Prevention of evaporation was studied using glycerol to cover the droplets. (Section 3.5)

- Optimization of the light source intensity was made and the limit of detection for the instrument was found. (Section 3.6)

In the second phase of the work in this thesis a methodology for 2D crystallization of membrane proteins was to be developed for use in the LevMac.

- Evaporation studies were made on protein and protein/MBCD mixtures for calculating the evaporation speeds and the concentrations in the droplets. (Section 4.1)

- Tests on the prevention of evaporation using glycerol mixtures to cover the protein samples were made. (Section 4.2)

- Tests on detergent removal using MBCD addition by dispenser were made. (Section 4.3)

3 Results and discussion

3.1 Droplet positioning techniques

In order to perform a levitation experiment, a technique able to position the droplet in a node of the levitator in an easy and reproducible way is needed. Basically any kind of syringe, pipette, or capillary may be used for droplet positioning in the ultrasonic field, provided that small enough droplets can be produced.

The Bernoulli forces induced by the ultrasound attract the liquid and detach it from the needle. Hamilton syringes with a metal tip have previously been used to position droplets in the LevMac instrument. Two major drawbacks with the use of these syringes have been previously reported; unwanted introduction of air bubbles into the droplet, and differences in the introduced droplet volume.

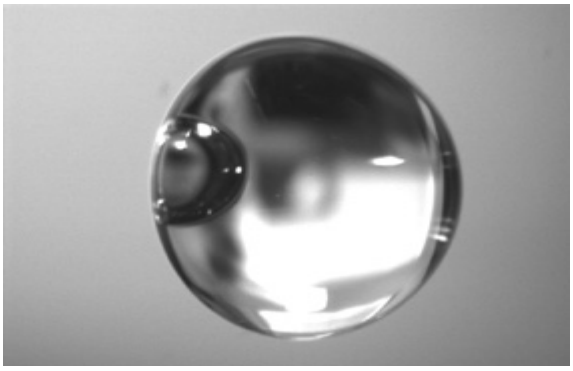

Figure 9: Air bubble in a levitated droplet.

Introduced air can lead to false volume measurements, in turn leading to incorrect calculations of the concentrations of the droplet constituents. Also, trapped air bubbles provide additional interface surfaces where unwanted reactions may occur. Droplets of different volumes give poor reproducibility. Another disadvantage is the disturbance of levitation by inserting the syringe metal needle into the ultrasonic field.

Difficulties in droplet detachment increase with decreased surface tension and/or viscosity of the liquid. To aid droplet detachment from the tip, it can be coated with a hydrophobic substance. Operating at increased ultrasonic power during the positioning enhances detachment but can be fatal for the protein sample and also enhances bubble formation.

A methodology for positioning of levitated droplets without the introduction of air bubbles and at as low HF-power as possible is therefore needed and was to be developed in this thesis work.

Figure 10: The GELoader tip.

The positioning experiments were performed in the LevMac instrument with the transducer/reflector distance set at 3.345 mm. A Hamilton syringe with a metal tip and an automatic pipette (2 µL)

with two different tips (ordinary plastic tips, and GELoader tips) were used in the tests. The GELoader tip (Fig 9) has 15 mm capillary with a defined diameter of less than 0.3 mm, and the material is specially suited for use with protein solutions.

3.1.1 Evaluation of different tips

To evaluate which of the three positioning techniques gave the best results, twenty attempts of positioning a droplet were made with each tip. The results were inserted into table I.

For a result to be considered OK, the droplet would detach from the tip without any air bubble formation. Where a "–" is shown, the droplet was either not detached from the tip or it was detached but with air bubbles introduced inside it, that is, an unsatisfactory result.

Table I: Table showing droplet positioning using different techniques. An OK means droplet detachment without air bubble formation while a "–" means either no detachment or introduced air bubbles.

Test	Ordinary tip	Hamilton syringe	GELoader
1	-	OK	OK
2	-	OK	OK
3	-	OK	OK
4	OK	OK	OK
5	-	-	OK
6	-	-	OK
7	-	-	OK
8	-	-	OK
9	-	-	OK
10	-	OK	OK
11	-	OK	OK
12	-	OK	OK
13	-	OK	OK
14	OK	OK	OK
15	-	-	OK
16	-	-	OK
17	-	-	OK
18	OK	-	OK
19	-	-	OK
20	-	OK	OK

The ordinary dimensioned plastic tip gave successful positioning results in only 15% of the cases. This is probably dependent on the wide opening of the tip giving the droplet a large contact area making the adhesive tendencies towards the tip considerable.

The Hamilton syringe gave acceptable results in only 50% of the cases because of the disadvantage of air bubble introduction.

The GELoader gave 100% successful results. No air was introduced and the droplet was easily detached from the tip.

Since the GELoader tip gave 100% successful results it was used in further evaluation tests.

3.1.2 Minimum HF-power

In order to make a droplet detach from the Hamilton syringe previously used for droplet positioning in the LevMac, the HF-power had to be maximized in the moment of detachment and then reseated in order to obtain a stable droplet in the levitator node. But, ultrasonic fields can be damaging for protein solutions and should therefore be kept as low as possible at all times. Also, air bubble formation is facilitated with the usage of high ultrasonic power.

In a first test the GELoader tip was compared with a Hamilton syringe. The droplet was introduced into the acoustic field and the HF-power was turned up until droplet detachment from the tip took place. The results from this test can be seen in table II.

Table II: The HF-power needed for droplet detachment using a Hamilton syringe, and a GELoader tip, respectively (n = 20).

	Min HF-power	Average HF-power needed	Units from minimum	Standard Deviation
GELoader	4.9	4.9	0	0.1
Hamilton syringe	4.9	8.7	3.8	1.4

Results show that the GELoader tip is a good choice of positioning technique also from the point of view of requiring minimum HF-power.

Because of the good result with water, more tests were performed with the GELoader tip on different solutions commonly used for protein crystallization purposes. Thirteen different solutions (A-M) were tested twenty times each, and the HF-power needed to detach a droplet from a GELoader tip was investigated.

The average values from these results were put together in table III. (For a complete table over the experiments, see appendix 1.)

Table III: The minimum HF-power read of the power supply box, average HF-power needed for detachment of a droplet, units from the minimum HF-power, and the standard deviation of the 20 tests. The letters corresponding to the different solutions are explained in table IV.

	Min HF-power	Average HF-power Needed	Units from min	Standard deviation
A	4.9	4.9	0	0.1
B	5.2	5.2	0	0.0
C	4.8	4.8	0	0.1
D	4.8	4.9	0.1	0.1
E	4.9	4.9	0	0.0
F	4.9	4.9	0	0.0
G	4.8	4.8	0	0.0
H	4.9	5.1	0.2	0.2
I	4.9	4.9	0	0.1
J	4.9	4.9	0	0.0
K	4.9	4.9	0	0.0
L	4.8	4.8	0	0.0
M	4.9	6.8	1.9	0.5

Table IV: Explanation of the letters A-M seen in table III.

A	Water	**H**	100% PEG 400
B	Ethanol	**I**	50% PEG 1000
C	100% MPD	**J**	20% PEG 1500
D	3.5 M Ammonium sulfate	**K**	25% PEG 6000
E	3.4 M Sodium malonate	**L**	25% PEG 10 000
F	2 M Sodium chloride	**M**	1% MBCD
G	50% PEG 400		

The results clearly show that the GELoader tip needs less HF-power to detach a droplet than does the Hamilton syringe. All solutions except the 1% MBCD solution were able to detach with none or very little increase of the HF-power. MBCD is a surfactant and the different result with this solution can depend on its lower surface tension.

In conclusion, the GELoader tip is a suitable positioning technique for droplets in future work with the LevMac. The results show that the technique is robust, reproducible, and reliable. It is also a technique able to provide reproducible droplet volumes.

3.2 Dispenser experiments

Electronic parameters (the form of the tension pulse) of the flow-through dispenser for a broad selection of solutions with different physical properties and concentrations were to be studied for protein crystallization purposes.

The aim of the experiments was to find settings for the dispensers where a single beam of dispenser droplets would form, without satellite droplet formation, and get the beam to hit a selected node in the ultrasonic field of the levitator when placed at a certain distance from the dispenser nozzle.

Viscosity and surface tension are of great importance when working with the flow-through dispensers. Viscosity arises from the forces between molecules. Strong intermolecular forces hold molecules together and do not let them move past one another easily, making the solution viscous.

The surface of a liquid is smooth because intermolecular forces tend to pull the molecules together and inward. The surface tension of a liquid is the net inward pull. The surface tension of water is about three times higher than of most other common liquids, as a result of its strong hydrogen bonds.

A surfactant is a substance which lowers the surface tension of the medium in which it is dissolved, and/or the interfacial tension with other phases, and accordingly is positively adsorbed at the liquid-vapor or other interfaces. The presence of polymers can also have influence on surface forces and the resulting effect depend on structure, length, and composition of the polymer.

The attraction between water and materials such as glass accounts for capillary action, the rise of liquids up narrow tubes. The liquid rises because there are favorable attractions between its molecules and the tube's inner surface. These are forces of adhesion, forces that bind a substance to a surface, as distinct from the forces of cohesion, the forces that bind the molecules of a substance together to form a bulk material. Narrow tubes and high adhesive forces result in tall columns of liquids. Equilibrium occurs when the force of gravity balances this force due to surface tension.

3.2.1 Experiments with separate dispensers

A flow-through dispenser coupled to its voltage supply was mounted at a 15 mm distance from a levitator. A cold light source was placed behind the dispenser in order to be able to detect the beam of dispenser droplets and any possible satellite droplets.

3.2.1.1 Introductory experiment

In a first test water was compared with solutions of 50% and 100% PEG 400 with the purpose of seeing if the same settings could be used for the PEG solutions as for water.

The results (table V) made it clear that the same settings could not be used on solutions of different physical properties.

Table V: Beam lengths of the dispenser droplets and settings for the comparison of water with 50% and 100% of PEG 400 solution, P1 being the slope, and P2 being the amplitude.

Solution	Length (mm)	P1 (V)	P2 (V)
Water	15	7.9	15.6
50% PEG 400	5	7.9	15.6
50% PEG 400	15	7.8	17.8
100% PEG 400	-	7.9	15.6
100% PEG 400	-	7.8	17.8
100% PEG 400	14	10.4	28.4

If the same pulse and amplitude were used for the 50% PEG 400 solution as for water, the beam of droplets became shorter and did not reach all the way to the node. When applying a higher amplitude the beam became long enough and was able to hit the selected node.

When the 100% PEG 400 solution was exposed to the same treatment, neither of the settings used for water and 50% PEG 400 solution gave a beam of droplets long enough. Turning the supply box to its maximum value (28.4 V) was not enough to get a stable beam of sufficient length. The 100% PEG 400 solution gave no stable beam of dispensed droplets and was assumed to be too viscous to be used with the flow-through dispensers.

The conclusion of the experiment was that different settings have to be used for solutions of different properties and more experiments had to be performed in order to get more information for future settings.

3.2.1.2 Dispenser settings for different solutions

There are multiple combinations of settings possible with the dispensers. In order to quickly find settings suitable for a certain solution, min–max amplitudes and slope intervals giving a stable beam of droplets 15 mm long were established for water, 50% PEG 400, 25% PEG 1000, 3.5 M ammonium sulfate, 3.4 M sodium malonate, and 50% MPD.

The solutions were tested by keeping one parameter (slope or amplitude) constant while varying the other.

Table VI: Table showing min-max intervals of slope and amplitude giving a 15 mm dispenser beam for solutions of different properties

Water	**Slope**	**Amplitude Min**	**Amplitude Max**	**Amplitude**	**Slope Min**	**Slope Max**
	7	15.9	17.4	**15**	7.2	10.4
	8	12.5	16.6	**16**	6.5	10.4
	9	14.9	15.9	**17**	6.2	7.1
	10	15.4	16.8	**18**	6.2	6.5
				19	6.1	6.2
				20	6.3	6.3
50% PEG 400	**Slope**	**Amplitude Min**	**Amplitude Max**	**Amplitude**	**Slope Min**	**Slope Max**
	8	16.7	18.4	**17**	7.6	10.4
	9	16.7	18	**18**	6.9	10.4
	10	16.6	18	**19**	6.9	10.4
				20	6.8	10.4
				21	6.7	8
				22	6.7	7.2
25% PEG 1000	**Slope**	**Amplitude Min**	**Amplitude Max**	**Amplitude**	**Slope Min**	**Slope Max**
	7	17.1	18	**16**	7.8	10.4
	8	16.1	17.5	**17**	7.1	7.2
	9	16.1	17.5	**18**	6.2	6.3
	10	17.3	17.3	**19**	6.2	6.4
Ammonium sulfate 3.5 M	**Slope**	**Amplitude Min**	**Amplitude Max**	**Amplitude**	**Slope Min**	**Slope Max**
	8	18.1	18.4	**18**	9.2	10.4
	9	18	21.2	**19**	7.4	8.1
	10	20.9	21.5	**20**	6.7	6.8
3.4 M Sodium Malonate	**Slope**	**Amplitude Min**	**Amplitude Max**	**Amplitude**	**Slope Min**	**Slope Max**
	8	16.9	17.3	**19**	8.4	10.4
	9	16.3	16.8	**20**	6.9	7.2
	10	16.4	16.9			
50% MPD	**Slope**	**Amplitude Min**	**Amplitude Max**	**Amplitude**	**Slope Min**	**Slope Max**
	7	16.5	17.1	**15**	7.7	10.4
	8	15.2	15.7	**16**	7	8
	9	14.7	15.4	**17**	6.7	7.2
	10	15.4	15.5	**18**	6.5	6.7
				19	6.3	6.4
				20	6.2	6.2

In the given intervals the dispenser droplets formed a single beam without formation of satellite droplets. (The values in table VI are average values of three measurements. The complete results are presented in appendix 2.)

Finding possible intervals for every potential solution is a time consuming procedure. So, the question was, is there an easy way of predicting which settings to be used with different solutions?

3.2.2 Quick prediction of dispenser settings

A method for the prediction of dispenser settings can make use of different physical properties of solutions. In order to get a hint of the fluid properties of a selection of solutions commonly used in the LevMac instrument, the solutions were examined by pouring them, to the same level, into a beaker wherein a 5 µL glass capillary was lowered down into the solution and kept stable for a period of 120 seconds. Three replicates were made with each sample and the average values are shown in diagram 3.1.

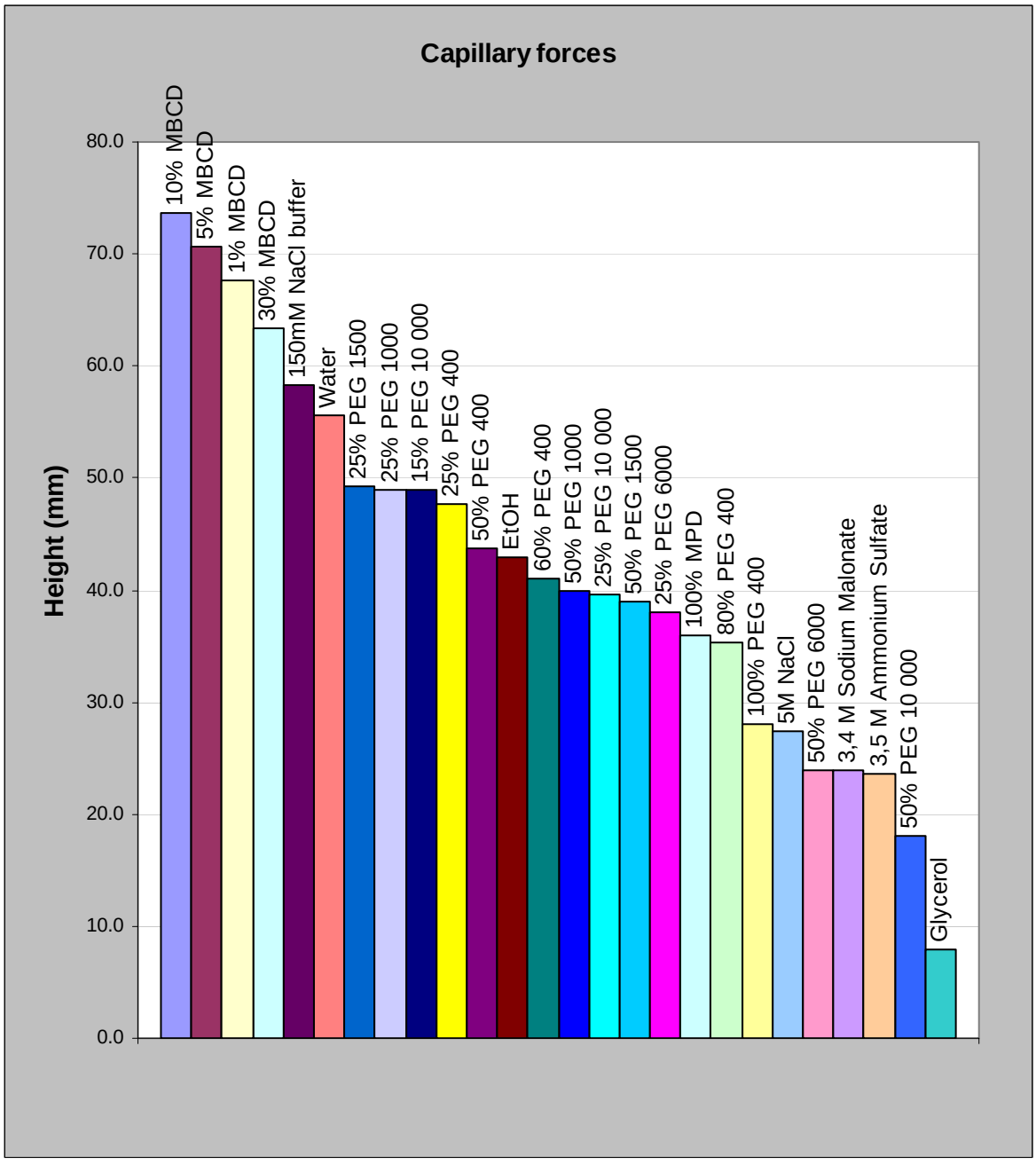

Diagram 3.1: Overview of the capillary rise for a selection of solutions used for protein crystallization purposes.

This method of measuring the capillary forces by no means constitutes an exact measurement of the true capillary forces found in literature. However, it was shown to be an excellent and easy-to-use tool to quickly get a hint of the physical properties of the liquids. For predicting suitable dispenser settings the results from this experiment should be used in combination with the intervals presented in section 3.2.1.2.

3.2.3 The time dependence of dispensers

When performing an experiment in the instrument, the dispenser sometimes comes to a halt for different reasons. Reasons for an intermission can be due to clogging of the system, crystallization of molecules in the nozzle, or if air is trapped inside the dispenser pluming. The dispenser may also need to be switched off for a period of time in order to stop the addition, or when changing reagent solutions in the dispenser.

To see if the dispenser could be restarted after such an intermission the following experiments were made. Commonly used solutions were selected. A dispenser with the solution in question was started and a stable beam of dispenser droplets was found by proper settings of pulse and amplitude. The power was then switched off and the solution was left in the dispenser for periods of variable length. After the intermission the power was switched on in order to see if a stable beam could still be formed. The results are presented in table VII.

For a result to be considered OK, the beam of dispenser droplets would after the intermission hit the selected node and be stable in order to produce a levitated droplet. Where a "–" is shown, the dispenser was not able to start after the intermission, or the beam of dispensed droplets did not hit the node in question, i.e., the beam was too short or instable.

Concerning the different PEG solutions, two conclusions can be drawn from the results. The smaller the PEG molecule and the less concentrated the solution, the better the flow-through dispenser was ejecting droplets.

In the case of PEG 400, the 50% solution gave satisfactory results but, with increasing concentration the solution became too viscous to produce droplets and the system was clogged.

PEG 1000 and PEG 1500 showed a similar pattern but at lower concentrations. As expected, PEG 1000 could be used at a slightly higher concentration than PEG 1500, depending on the smaller polymer size.

Table VII: Table showing if the dispenser could provide a stable beam after having been switched off for different periods of time. Where OK is shown, the beam hit the node in question after the intermission. Where "–" is found, the beam was either unstable, too short or the system was clogged.

Type of precipitant	Direct	2 min	5 min	10 min	15 min
PEG 400 50%	OK	OK	OK	OK	OK
PEG 400 60%	OK	OK	-	-	-
PEG 400 80%	-	-	-	-	-
PEG 400 100%	-	-	-	-	-
PEG 1000 25%	OK	OK	OK	OK	OK
PEG 1000 50%	OK	-	-	-	-
PEG 1500 20%	OK	OK	OK	OK	OK
PEG 1500 30%	OK	OK	-	-	-
PEG 1500 40%	-	-	-	-	-
PEG 1500 50%	-	-	-	-	-
PEG 6000 15%	OK	OK	-	-	-
PEG 6000 20%	OK	-	-	-	-
PEG 6000 25%	OK	-	-	-	-
PEG 6000 50%	-	-	-	-	-
PEG 10000 15%	OK	-	-	-	-
PEG 10000 25%	-	-	-	-	-
3.5 M Ammonium sulfate	OK	OK	OK	-	-
3.4 M Sodium malonate	OK	OK	OK	OK	OK
MPD 50%	OK	OK	OK	OK	OK

In the case of PEG 6000 and PEG 10000, however, the results were unacceptable even at low concentrations. An explanation of this could be the size of the polymers which are not suitable for the small (40 × 40 μm) nozzle size. The big polymer molecules tend to get stuck in the nozzle or hold the fluid back and the phenomenon was increased after a halt in the flow.

A solution with high salt concentration can also affect the dispenser negatively as a result of crystallization of the salt molecules in the nozzle. When the dispenser is shut down, some evaporation in the nozzle is occurring, thus leading to a local rise of the salt concentration which can lead to crystallization. Ammonium sulfate has a water solubility of 5.8 M while the water solubility of sodium malonate is 14.8 M, which can be the explanation of why sodium malonate can handle the intermission better than ammonium sulfate can.

3.3 Evaporation experiments

Evaporation processes of suspended liquid droplets in a gaseous environment can be described by a linear decrease of the surface area S with time t;

$$S = S_0 - K_t$$

where the proportionality factor K is a function of the liquid density ρ_l, the molecular mass M, the binary gas-diffusion coefficient D_{ab} of the vapor in the surrounding gas, the partial vapor pressure p, and the temperature T at the drop surface (subscript s) and in the gaseous environment (subscript ∞):

$$K = \frac{8\pi D_{ab} M}{\rho_l R}\left(\frac{P_s}{T_s} - \frac{P_\infty}{T_\infty}\right)\frac{Sh}{2}$$

where R is the universal gas constant and Sh is the Sherwood number, describing the ratio of mass transfer with and without convection in the gas. Within the stationary ultrasonic field in the acoustic levitator acoustic streaming leads to a higher mass transfer.

As can be seen above evaporation is a complicated process dependent on both environmental and liquid characteristics. To be able to calculate accurate concentrations of the droplet constituents during an experiment in the LevMac, the evaporation speed has to be known. Evaporation takes place at the surface of the liquid where some of the molecules with the highest kinetic energies are escaping into the gas phase. The ease with which a liquid vaporizes depends on the temperature and on the strength of the intermolecular forces within the liquid.

3.3.1 Droplet evaporation experiments

Droplets of a selection of liquids with different physical properties in the volume range of 0.5-1.6 µL were suspended in a pressure node of the stationary ultrasonic field of the levitator. Measurements on the droplet volume were made every tenth second and evaporation graphs were plotted from these measurements. The experiments were performed under an ambient temperature of 20-25ºC.

Several experiments were performed on water droplets of different volumes. For clarity only three samples are shown in diagram 3.2. (More evaporation diagrams can be seen in appendix 3.)

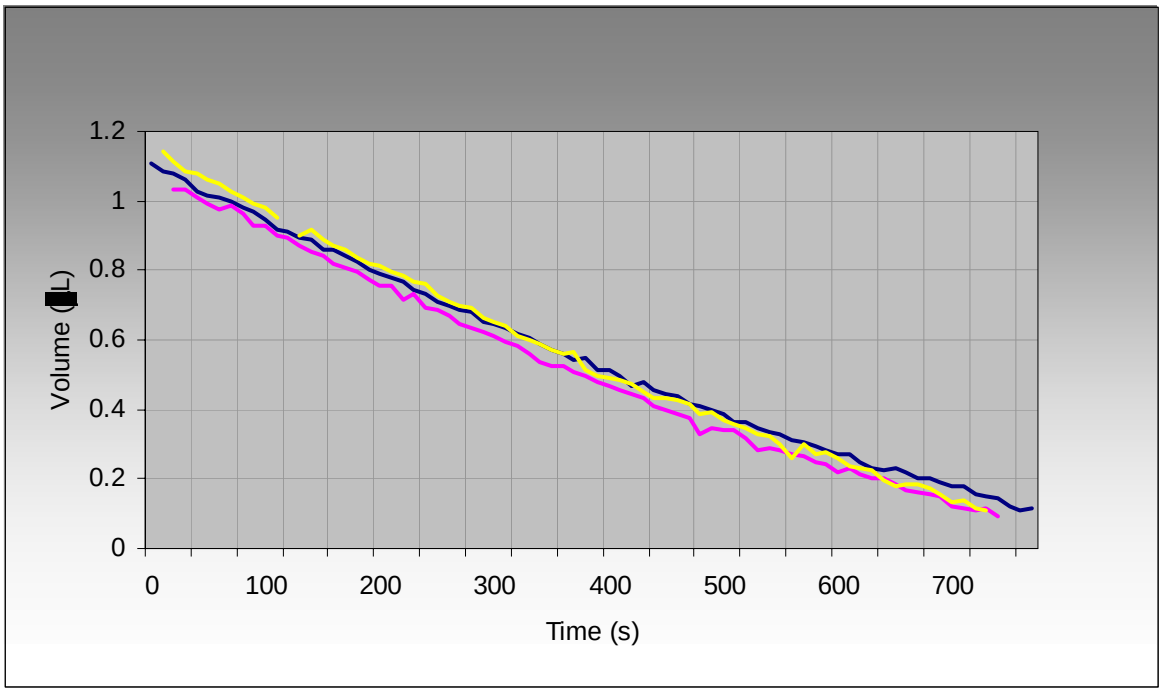

Diagram 3.2: The evaporation graphs of three different water droplets.

The evaporation graphs were fitted with regression lines trough the method of least squares. Table VIII shows the results for the three individual samples.

Table VIII: Table of the data for the water samples in the evaporation experiments shown in diagram3.2.

	Water 1	**Water 2**	**Water 3**
Function of the regression line	Y= -0.0013x +1.057	y=-0.0014x+1.044	y=-0.015x+ 1.120
R^2	0.992219	0.986062	0.981221
Speed of evaporation	0.0013 µL/s	0.0014 µL/s	0.0015 µL/s

The average evaporation speed of water was calculated to 0.001 µL/s. The appearance of the graphs showed similar characteristics which was a good sign for the reproducibility of volume measurements by the LevMac instrument.

The evaporation process is not a completely linear function. This is clearly shown in diagram 3.3 where the evaporation of water droplets of three different volumes, 0.5, 1, and 1.5 µL are shown.

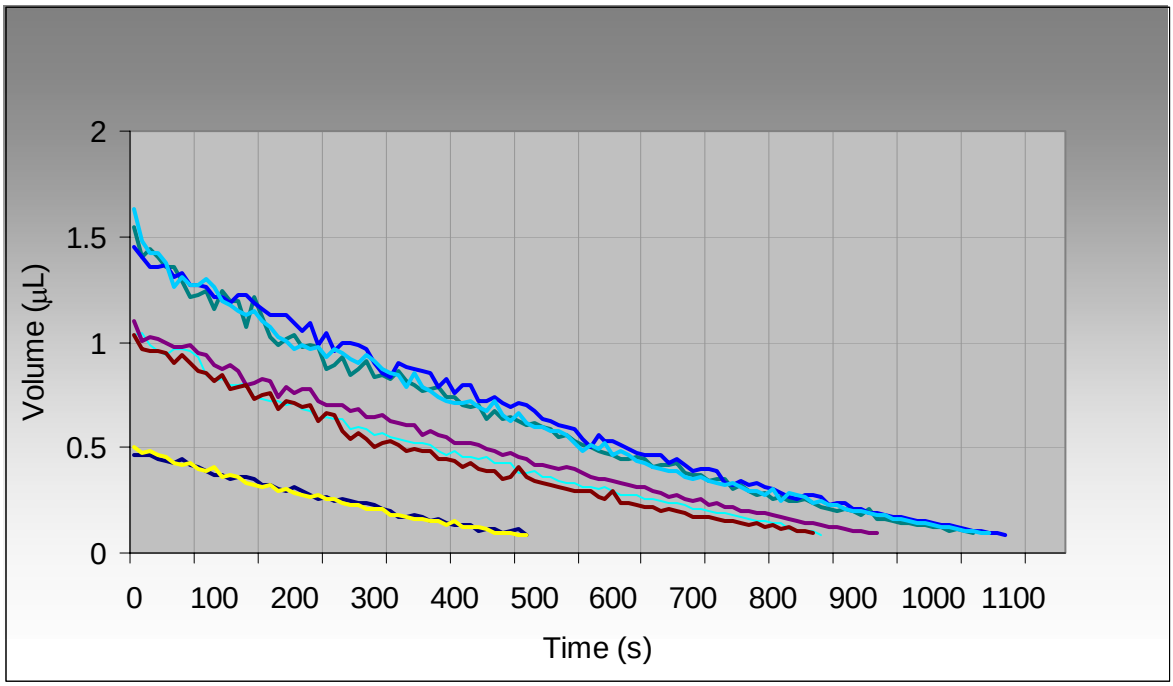

Diagram 3.3: Diagram showing the evaporation of 0.5, 1, and 1.5 µL droplets. Three runs were made of each volume.

Since evaporation takes place at the surface of the droplet, the process is dependent on the surface area of the droplet and therefore on the volume. Results show that the larger the surface area, the faster the evaporation of the droplet. Diagram 3.4 shows three graphs of droplet evaporation for water droplets with volumes 0.5, 1, and 1.5 µL.

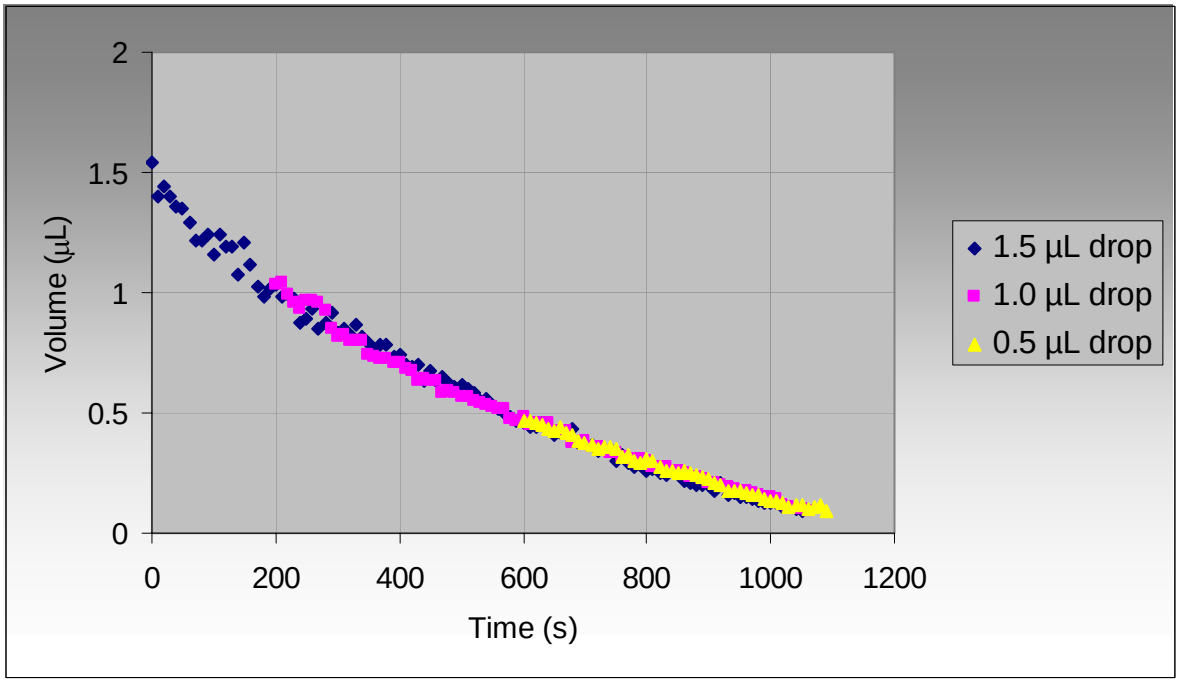

Diagram 3.4: Three droplets of different volumes put together into one graph.

In order to find a reliable evaporation speed for use in future calculations, droplets of different volumes were studied one by one.

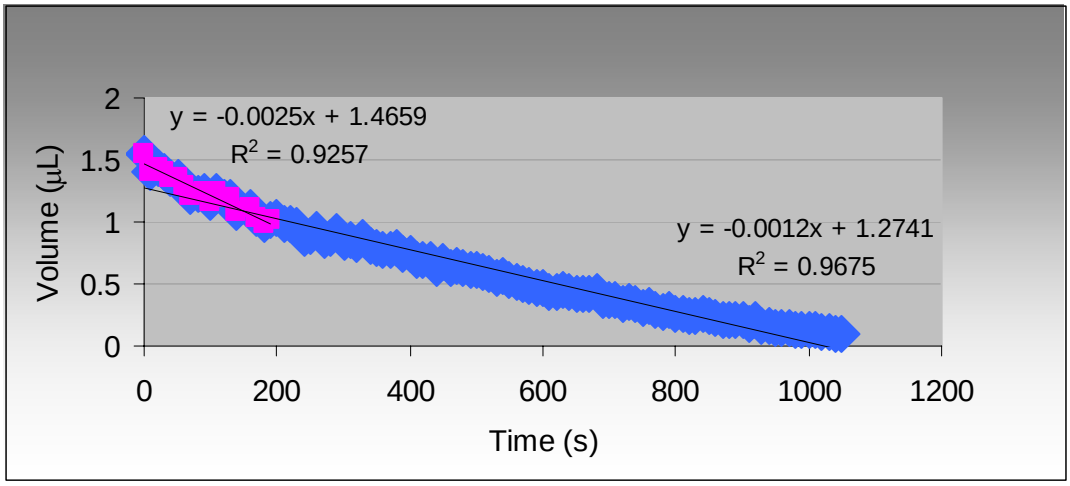

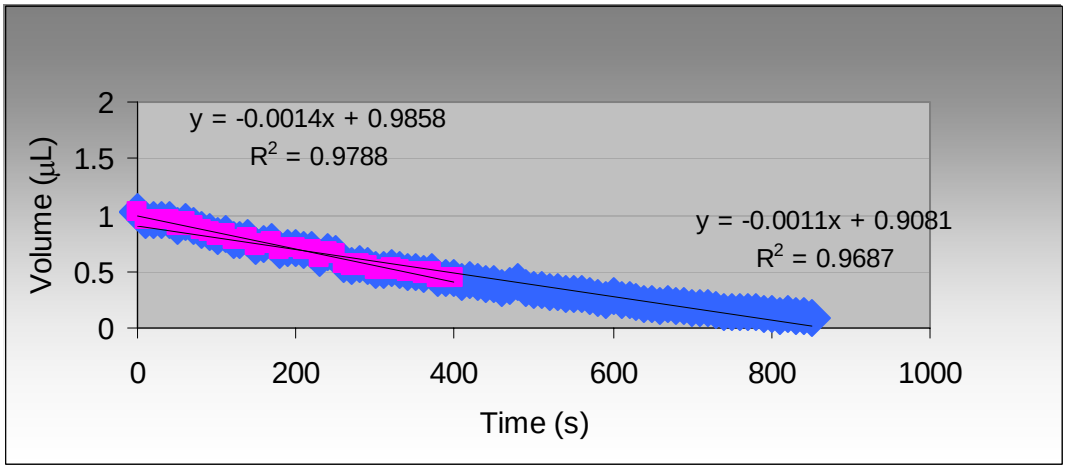

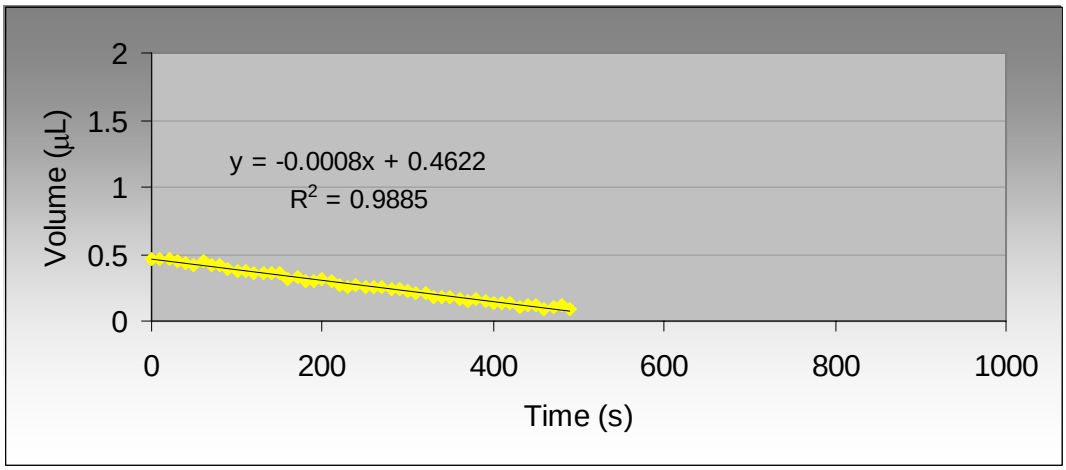

Diagram 3.5a-c: Evaporation of droplets of different volumes. The regression lines showing the linearity of the evaporation at different stages of the evaporation process.

As can be seen in diagram 3.5 a and b, the beginning of the evaporation curves is steeper, that is, has a higher evaporation rate than the rest of the curve. The

phenomenon is most obvious in the evaporation of the 1.5 µL droplet due to its larger surface area.

The evaporation speed in the beginning of the process, from 1.5 µL down to 1 µL is 0.003 µL/s compared with the over all evaporation speed of 0.001 µL/s.

The evaporation of a 1 µL droplet shows more agreement to linearity than a 1.5 µL droplet. The first part of the curve, from 1 µL to 0.5 µL is almost completely linear with an evaporation speed of 0.001 µL/s.

The 0.5 µL droplet in diagram 3.5 c shows the most linear evaporation process of them all but with a slightly lower evaporation rate because of its smaller surface area.

Conclusions that can be drawn from the evaporation experiments so far is that since most droplets used during an experiment in the LevMac instrument are in the range of 0.5-1 µL, an approximation of the evaporation as a linear function with an evaporation speed of 0.001 µL/s can be made.

To see if the same approximation of the evaporation speed could be made for other solutions, the following experiments were made. Three samples of a 150 mM sodium chloride buffer were left to evaporate and the volume measurements were inserted into diagram 3.6.

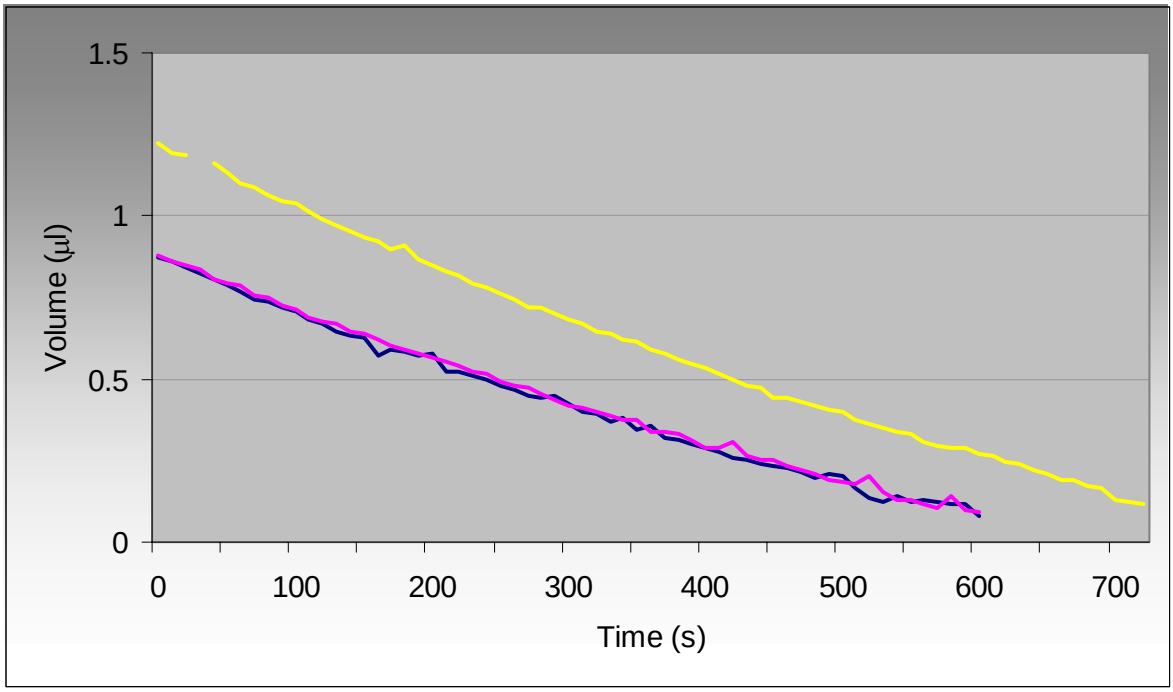

Diagram 3.6: The evaporation of three droplets of 150 mM NaCl buffer.

The volatility of a solution decreases as the concentration of non-volatile dissolved substances increases so theoretically the salt solution should be less volatile than pure water.

The three sodium chloride evaporation curves were fitted with regression lines and the results were inserted into table IX.

Table IX: Data of the evaporation experiments of the NaCl buffer droplets shown in diagram 3.6.

	NaCl buffer 1	NaCl buffer 2	NaCl buffer 3
Function of the regression line	Y= -0.0013x+0.828	y=-0.0013x+0.84	Y=-0.016x+1.189
R^2	0.990135	0.992547	0.976726
Speed of evaporation	0.0013 µL/s	0.0013 µL/s	0.0016 µL/s

The average speed of evaporation of the sodium chloride buffer droplets was 0.001 µL/s, the same as for water, which shows that the salt additive did not affect the evaporation speed, probably due to its low concentration.

Polyethylene glycol (PEG) is a water soluble, waxy solid condensation polymer of ethylene oxide and water with the general formula of $H(OCH_2CH_2)_nOH$, where n is the average number of repeating oxyethylene groups typically ranging from 4 to 180. The abbreviation (PEG) is termed in combination with a numeric suffix which indicates the average molecular weights. As the molecular weight of PEG increases, viscosity and freezing point increase.

Unsaturated PEG behaves as a Newtonian fluid, with strain rates proportional to applied stress. PEG is often used in biological research as a precipitating agent for proteins. It has been approved for a wide range of biomedical applications, as they are biocompatible, nontoxic, and non immunogenic.

Evaporation studies were performed on PEG 400 and PEG 10 000 solutions of different concentrations.

A pure solution of 100 % PEG 400 showed no tendency to evaporate as can be seen in diagram 3.7. This phenomenon can be explained by the strong intermolecular forces between the polymer molecules and by the high viscosity of the solution.

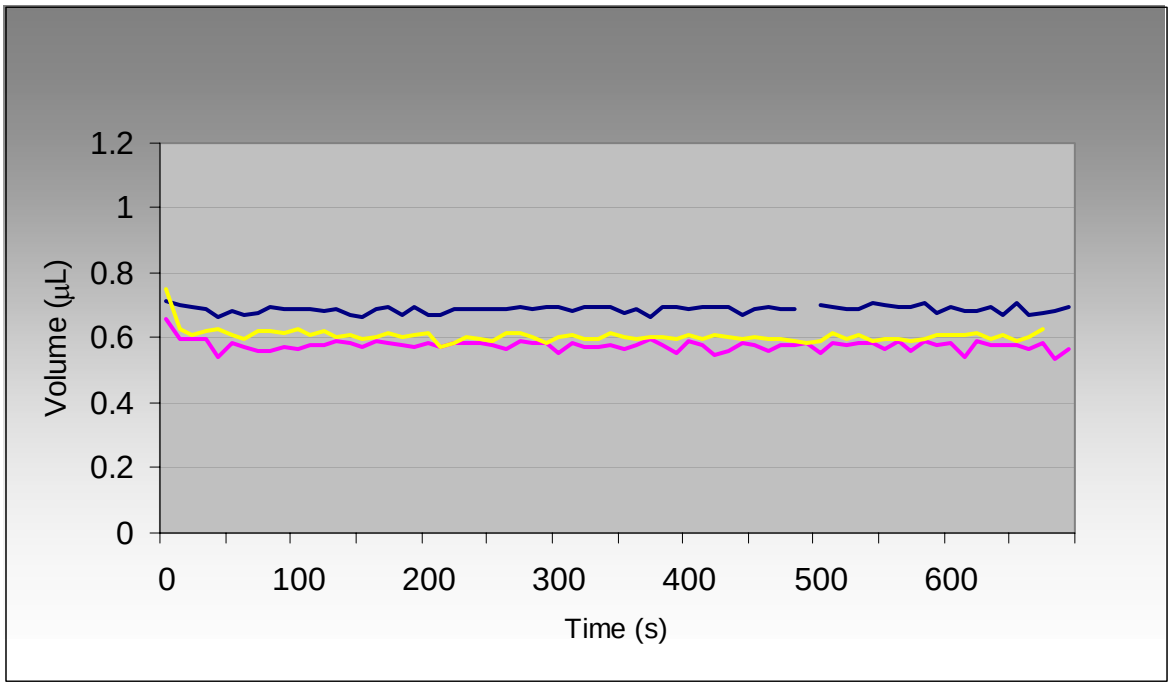

Diagram 3.7: A graph showing an attempt to evaporate 100% PEG 400.

The evaporation graphs of 50% PEG 400 have two distinct areas which are clearly shown in diagram 3.8.

In the first area, the water content of the droplet evaporates, and then the remaining PEG comes to equilibrium which halts the evaporation process.

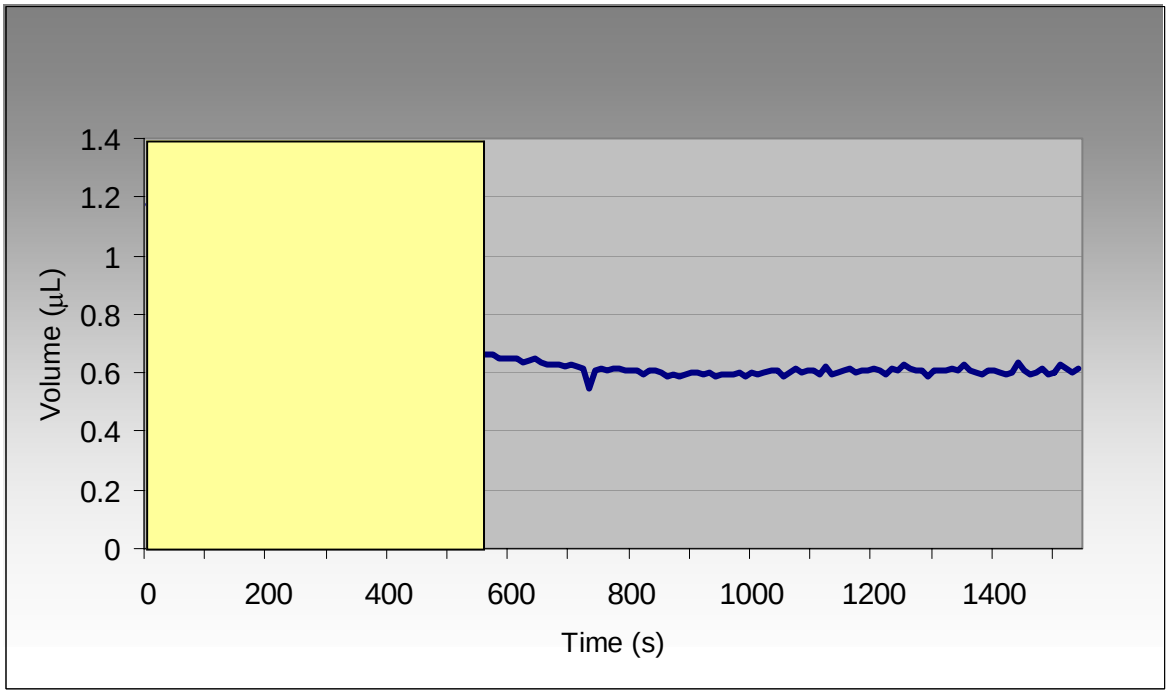

Diagram 3.8: A graph showing the two distinct areas of the evaporation of 50% PEG 400 solution.

Three samples droplets of 50% PEG 400 were examined for evaporation in order to verify the results. The three samples showed good agreement with each other which can be seen in diagram 3.9.

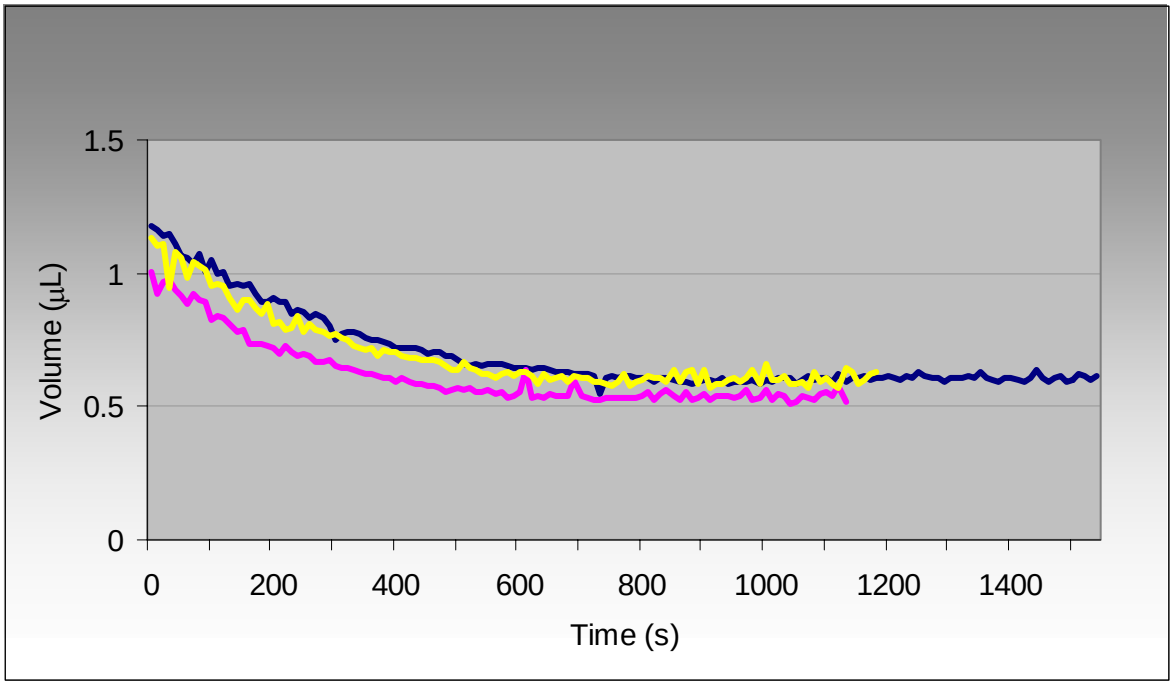

Diagram 3.9: Three evaporation experiments with 50% PEG 400 solution.

Calculations were made at the part of each graph from start to 500 s. The results were put into table X.

Table X: Data of the evaporation experiments shown in diagram 3.9.

	50% PEG 400 1	**50% PEG 400 2**	**50% PEG 400 3**
Function of The regression line	y= -0.00097x+1.114	y=-0.00084x+0.931	Y=-0.00091x+1.055
R^2	0.955461	0.930943	0.929577
Speed of evaporation	0.00097 µL/s	0.00084 µL/s	0.00091 µL/s

The average evaporation speed in the first part of the experiment was 0.0009 µL/s. This speed is slightly lower than for pure water and can be explained by the strong water/polymer intermolecular interactions, holding the water molecules back from taking off at the surface and due to slow diffusion from the interior of the droplet to the surface where the evaporation process is taking place.

Solutions of 25% and 50% PEG 10 000 were treated in the same way as previous evaporation experiments.

As can be seen in diagram 3.10 a and b, the evaporation process came to a halt after 300-500 seconds (depending on the initial volume) in the case of the 25% solution, and after 50-150 seconds when dealing with the 50% solution.
75% of the25% PEG 10 000 droplet constituents is made up of water and after the evaporation of the water the droplet turned into a solid due to gelatinization of the polymer as can be seen in the left picture of figure 11.

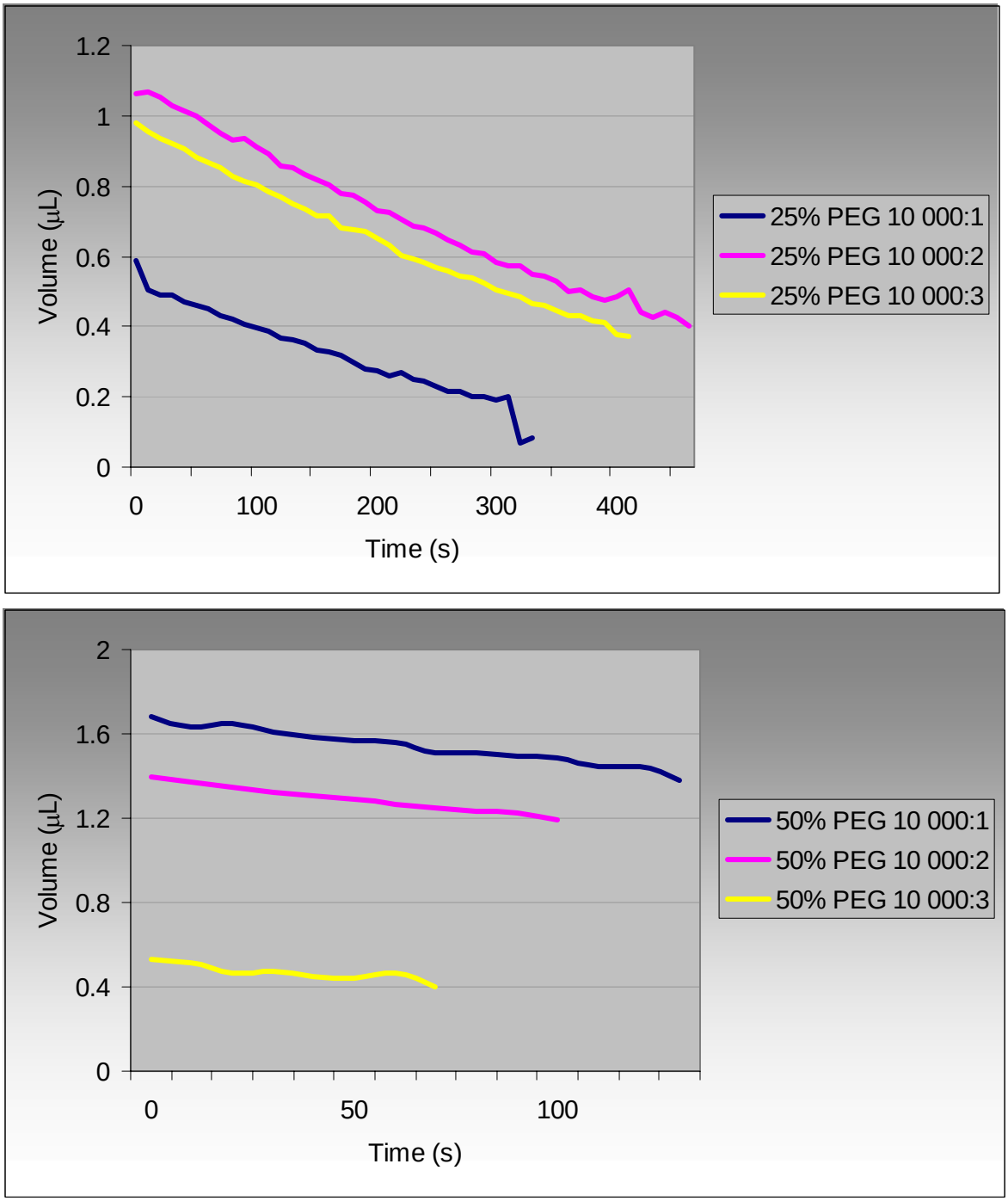

Diagram 3.10: The evaporation of a) 25% PEG 10000, b) 50% PEG 10000.

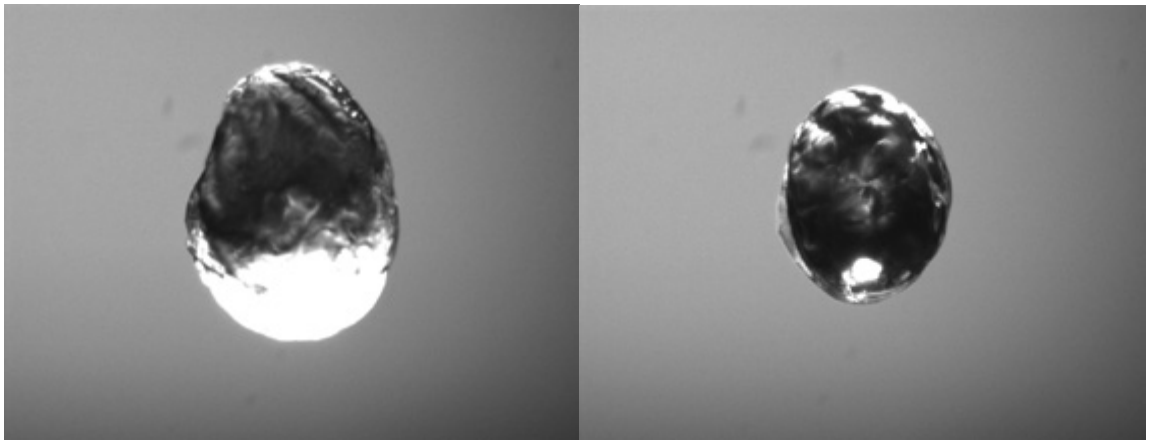

Figure 11: Left picture: 25% PEG 10 000 turning into a solid. Right picture: 50% PEG 10 000.

In the case of the 50% PEG 10 000 solution (fig 11, right picture) gelatinization occurred in the same way as described above but the evaporation came to a halt at a sooner stage due to its lower water content.

3.4 Compensation of evaporation

When performing a LevMac experiment you want to keep the droplet volume as constant as possible in order to keep the concentrations of the droplet constituents under control.

One way to keep a stable droplet volume is by the use of dispensers for filling up the levitated droplet in order of compensating for the liquid that is evaporating.

Evaporation is dependent on temperature so different droplet ejection frequency settings have to be used if the temperature in the instrument varies significantly during an experiment.

The volume of the ejected dispenser droplets, typically in the range of 40-100 pL, is dependent on the size of the nozzle, the shape of the voltage pulse, and liquid parameters like surface tension, viscosity, and density [17].

In a first experiment, the volume of the dispenser droplets was to be established in order to get a hint of which dispenser settings to use for keeping the droplet volume stable.

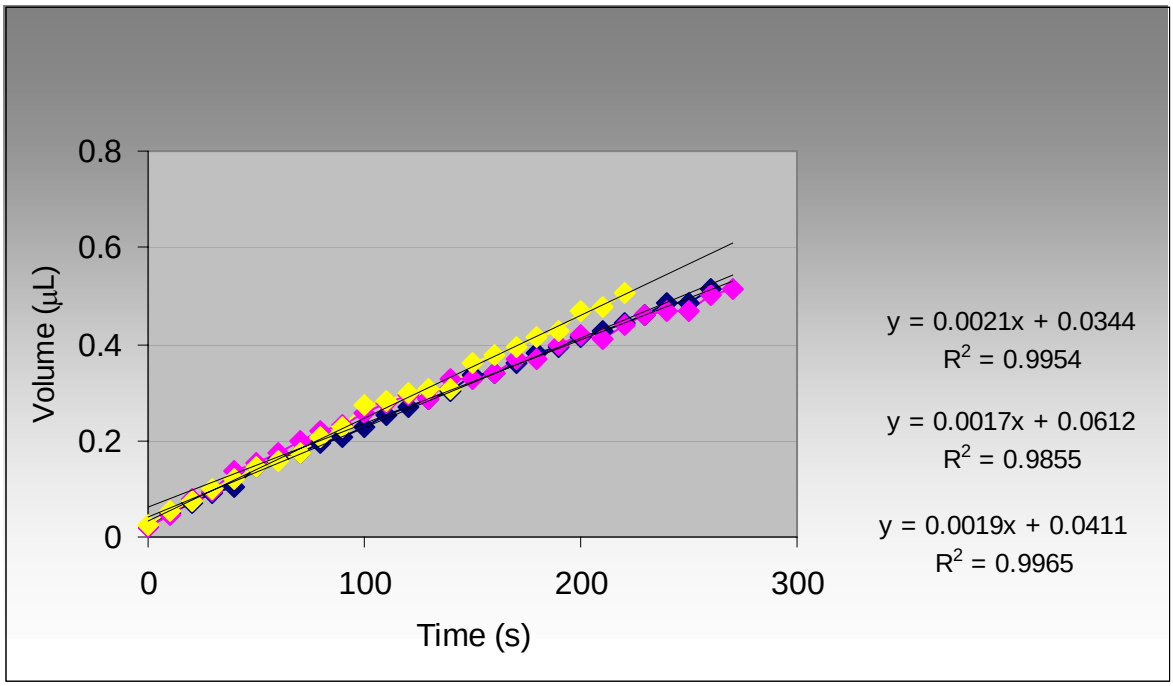

Diagram 3.11: The filling up of a node with 50 Hz addition.

A stable beam of dispenser droplets of 50 Hz was adjusted to continuously hit a node in order to fill the node with water.

From the volume measurements, graphs were plotted into diagram 3.11 and an average droplet size was calculated. With the droplet ejection frequency set on 50 Hz, the average filling up speed of dispenser droplets was calculated to be 0.0019 µL/s, giving an average droplet volume of 40 pL.

The ejected dispenser droplet volume predicted by the manufacturers was about 65 pL and the smaller volume calculated in this experiment could possibly be due to fast evaporation of the tiny droplets on their trajectory into the levitated droplet.

In a second experiment different droplet ejection frequencies were tried in order to find one to match the evaporation speed. The one showing the best agreement with the evaporation speed at room temperature was the 19 Hz addition frequency. Three runs with this frequency are shown in diagram 3.12.

With the calculated dispenser droplet volume of 40 pL and a frequency of 19 Hz, the replenish to the levitated droplet becomes 0.0008 µL/s which shows good agreement with the evaporation experiments in section 3.3 where the average water evaporation speed was calculated to be 0.001 µL/s.

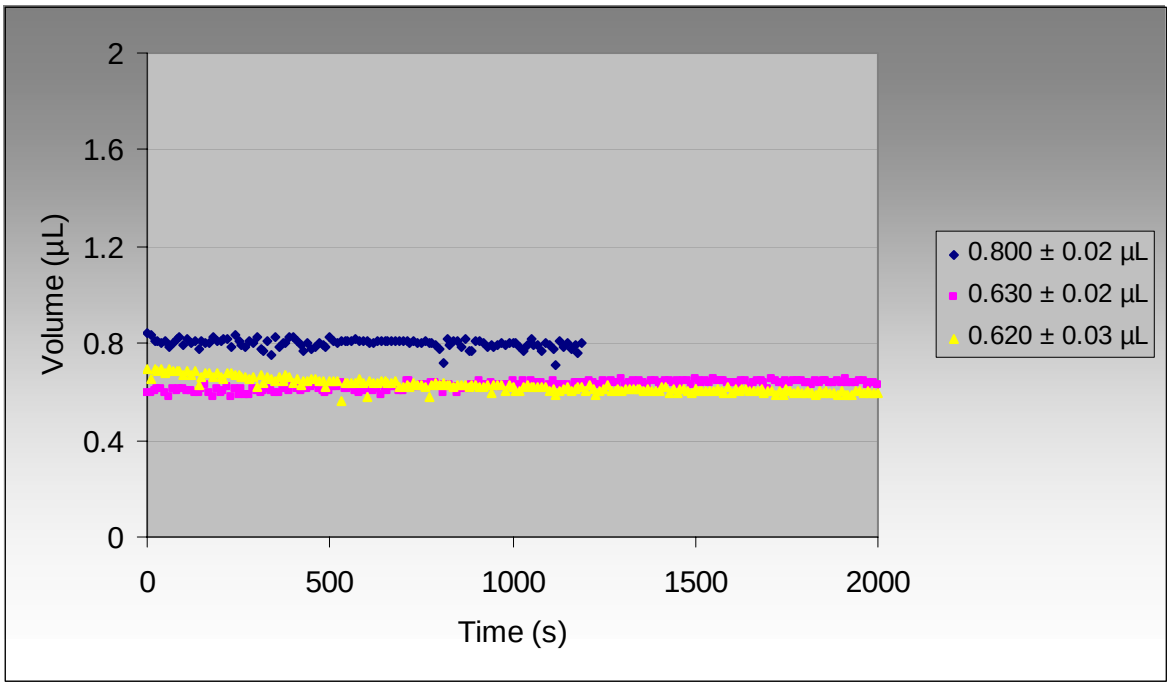

Diagram 3.12: Constant droplet volume provided by 19 Hz dispenser additions.

3.5 Prevention of evaporation

In some cases, it is desirable being able to perform an experiment without making any additions to the levitated droplet. Examples of experiments of this kind can be found in section 4.2.

In miniaturized systems the surface to volume ratio is large, and fast evaporation is associated with it. Different precautions in order to hinder the evaporation process are needed when not making any additions to the droplet or else the droplet will evaporate.

Ways of preventing evaporation can be the addition of a hygroscopic material to the sample, mixing the liquid with a lower vapor pressure solvent, topping the solution with a low vapor pressure non mixing liquid, or working in a solvent-saturated environment [26].

In this experiment glycerol was used as a solvent of lower vapor pressure to cover the levitated water droplet.

Glycerol is a solution that is not suited for dispensing due to its physical properties. It can be metered with a Hamilton syringe or a pipette tip and can be added to the sample droplet by bringing the desired volume hanging at the end of the tip near the nodal point of the stationary ultrasonic field [10]. The glycerol and the levitated droplet are then merged together and could be replaced in the node as one droplet.

3.5.1 Behaviour of glycerol

In a first experiment pure glycerol was left in the levitator in order to get a picture of its behavior when exposed to evaporation.

As can be seen in diagram 3.13, pure glycerol droplets show no tendency to evaporate.

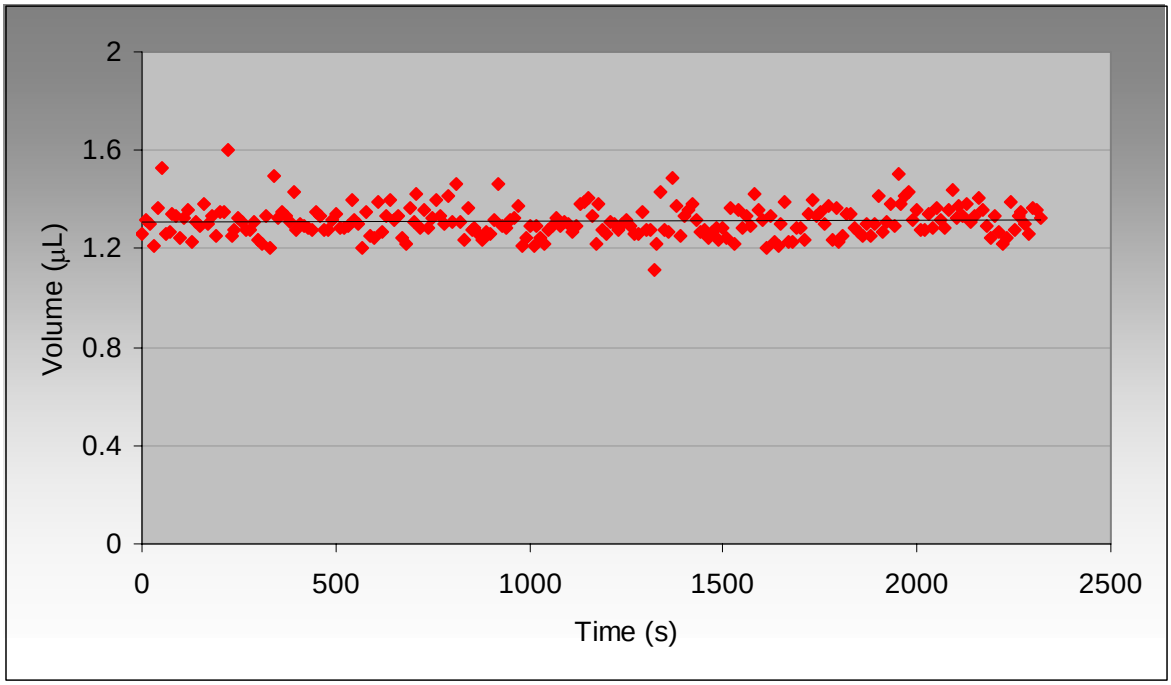

Diagram 3.13: An attempt of evaporating a droplet of pure glycerol.

3.5.2 Positioning of large glycerol droplets

When trying to hinder evaporation by covering the sample droplet with glycerol the combined droplet tends to get relatively big because enough glycerol must be added to cover the entire sample droplet.

As a first test, attempts were made of positioning the largest possible glycerol droplet in the levitator, without changing or optimizing the levitator settings. This could provide guidelines of suitable volumes of glycerol with which to cover samples droplets.

Results, presented in table XI, showed that glycerol/sample droplets of a total volume of about 1.7 µL are suitable to use in the LevMac in order to prevent evaporation.

It is possible to position larger droplets, but, in order to minimize the risk of losing valuable sample, it can be wise to keep the total droplet volume in this area.

Table XI: Table showing the attempts of positioning large droplets of glycerol.

Test	Volume (μL)
1	1.545
2	1.559
3	1.664
4	1.676
5	1.763
6	1.813
Average:	**1.7**

3.5.3 Glycerol covered water droplets

To evaluate if droplet evaporation could be prevented by covering it with glycerol, three experiments were made.

In each experiment a levitated water droplet was left to evaporate down to a suitable volume.

A glycerol droplet was caught from a test tube with a GELoader tip. The tip with the glycerol droplet was then approached to the levitated water droplet. When holding the glycerol droplet close enough, the water droplet and the glycerol merged together on the tip.

The new larger combined water/glycerol droplet was then reinserted into the node. The process can be followed in diagram 3.14 a-c.

The results show that a good way of hindering the evaporation of a levitated sample droplet can be to cover it with glycerol

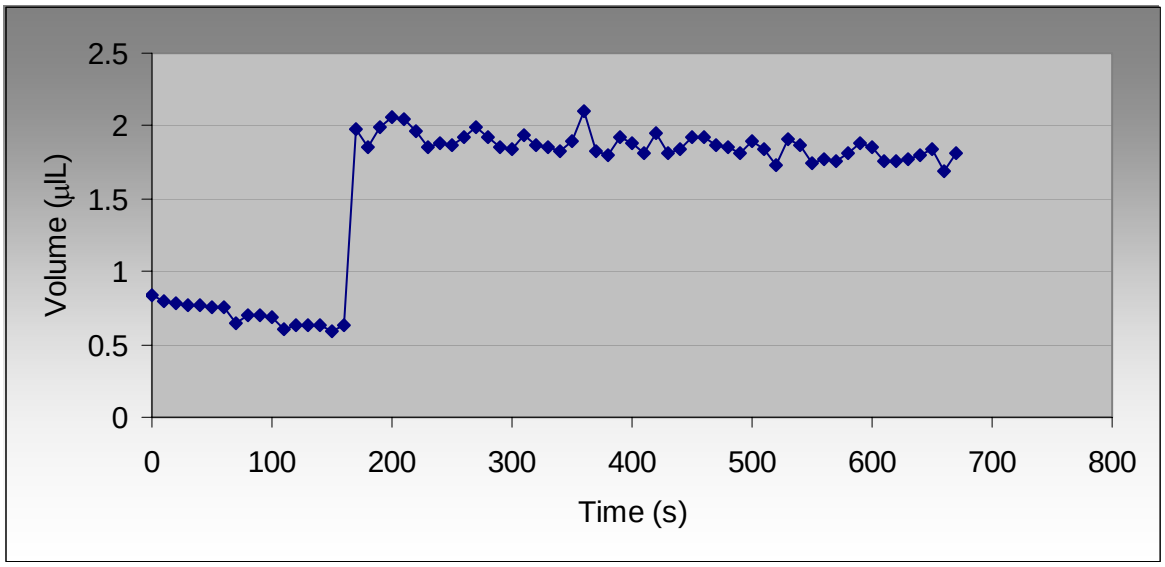

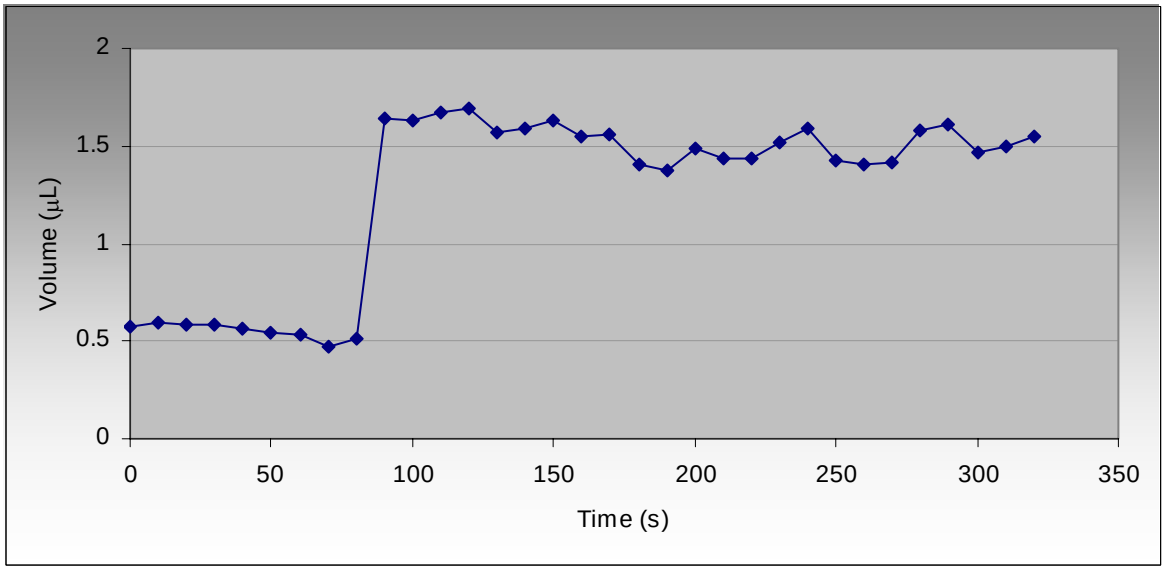

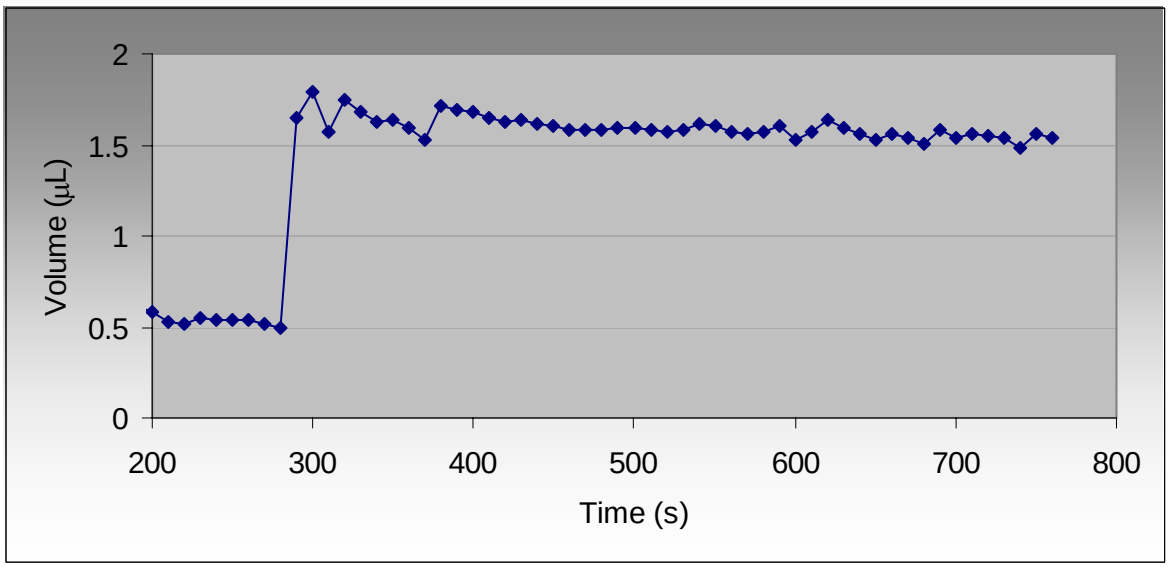

Diagram 3.14a-c: In experiment a), a 0.6 µL water droplet was covered with 1.4 µL of glycerol. In experiment b), a water droplet of 0.5 µL was covered with 1.1 µL of glycerol. In experiment c), a 0.5 µL water droplet was covered with 1.3 µL of glycerol.

3.6 The detection system

3.6.1 Optimization of the light intensity

The RALS detection system has the light source placed at 90 degrees from the camera objective. The system is sensitive to reflections from the light in the levitated droplets. The results of this phenomenon are a spreading of the data points giving false values of the volume and scattering, and sometimes missed measurement values. These reflections are different for liquids of different properties. Glycerol has a pronounced behavior of reflections and is therefore used in the following experiments.

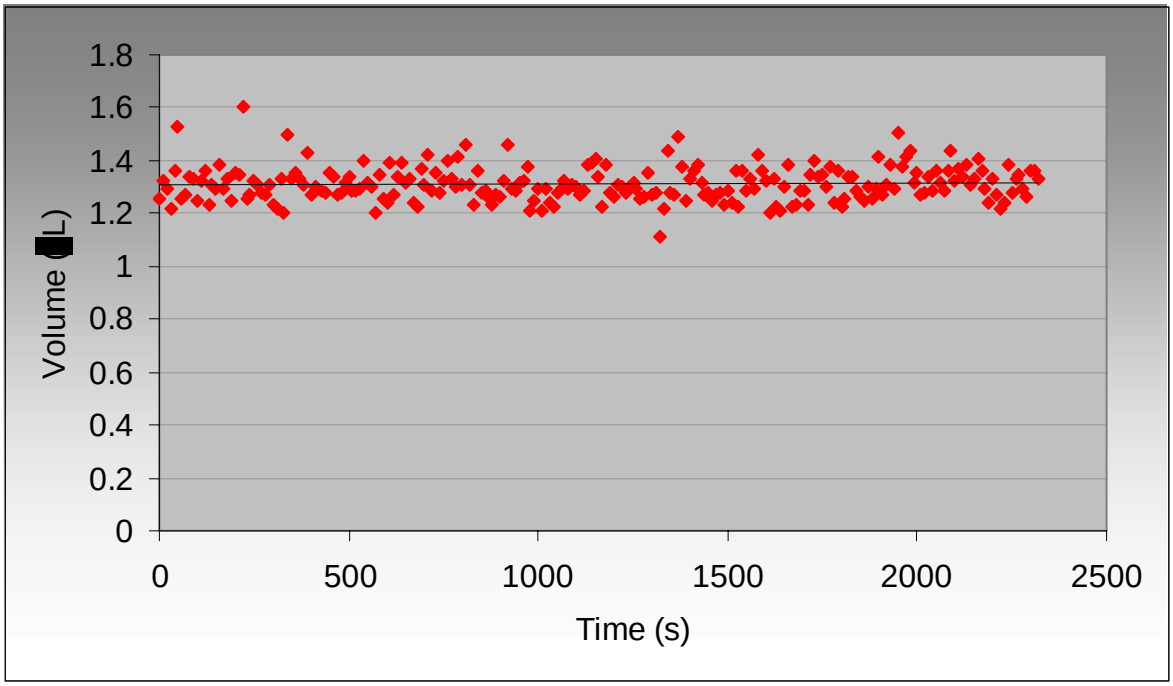

Diagram 3.15: Diagram showing the volume measurements of a glycerol droplet using 90 degrees light scattering as detection system.

As can be seen in diagram 3.15, the distribution of the measurements is not the best. The standard deviation for the volume measurements having the light source at 90 degrees was calculated to be 0.07 µL.

The light source in the LevMac is movable and after changing the position of the light from 90 degrees to a smaller angel a new run, presented in diagram 3.16, with a droplet if glycerol were made.

The improvement was noticeable. The standard deviation from the second run was 0.01 µL, an improvement of 14%.

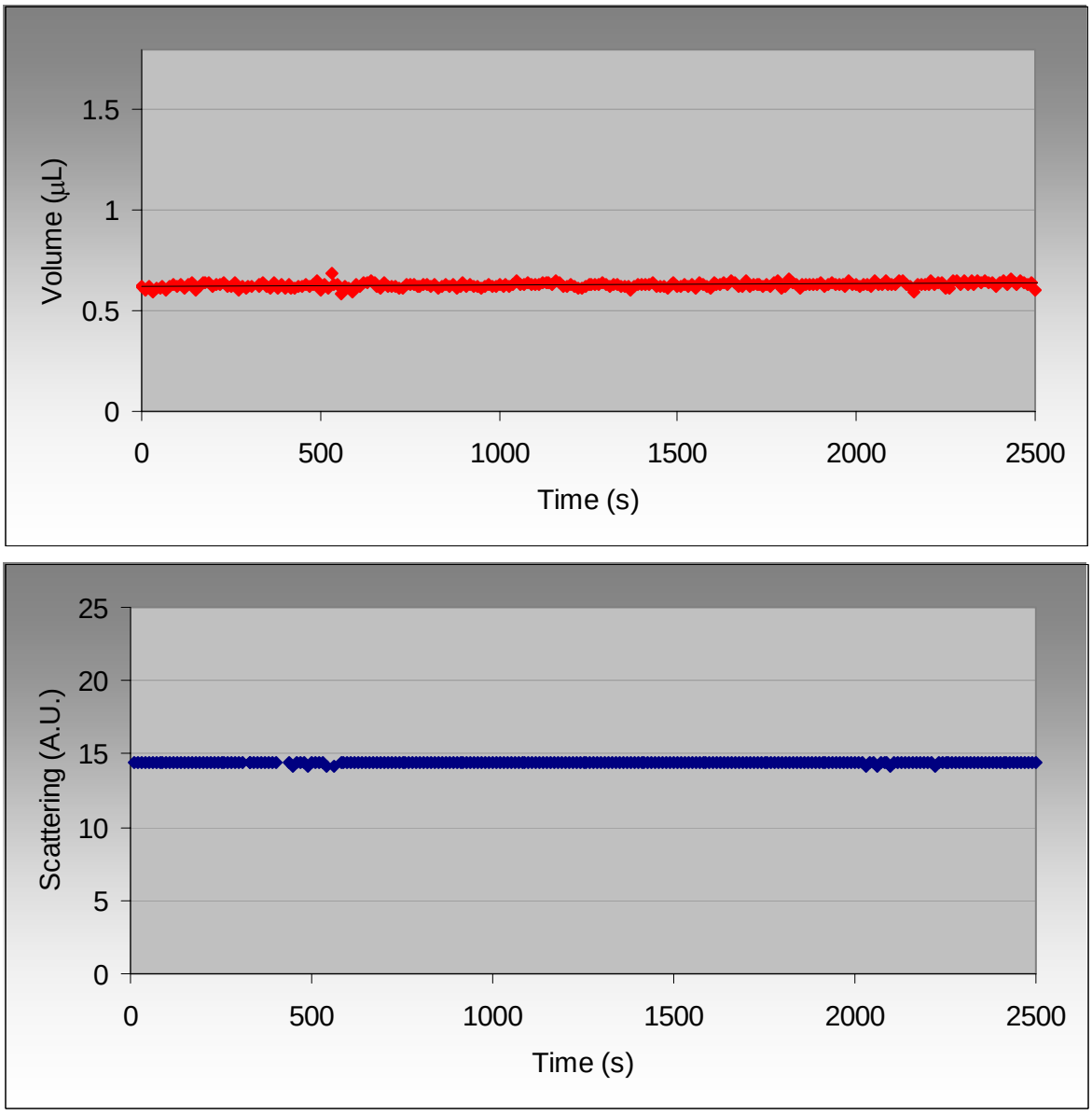

Diagram 3.16a-b: Glycerol droplet being detected using small angel light scattering, a) volume measurements, b) scattering measurements.

3.6.2 Limit of detection

The limit of detection (LOD) of the volume and scattering measurements using the LevMac method was calculated from the experimental data in diagram 3.16, using the formula that LOD = 3 × the standard deviation.

Table XII: The limit of detection for the LevMac instrument.

	Limit of detection
Volume measurements	0.03 µL
Scattering measurements	0.1 A.U.

3.6.3 Precipitation of ammonium sulfate

In order to evaluate the performance of the LevMac instrument in protein crystallization experiments, a similar approach was first tested using an aqueous solution of ammonium sulfate.

Three droplets of 3.5 M ammonium sulfate were left in the levitator where the water content was evaporating, leading to precipitation and crystallization of the salt. Measurements of volume and light scattering were made every tenth second on pictures taken by the instrumental camera. Figure 12 shows the precipitation process.

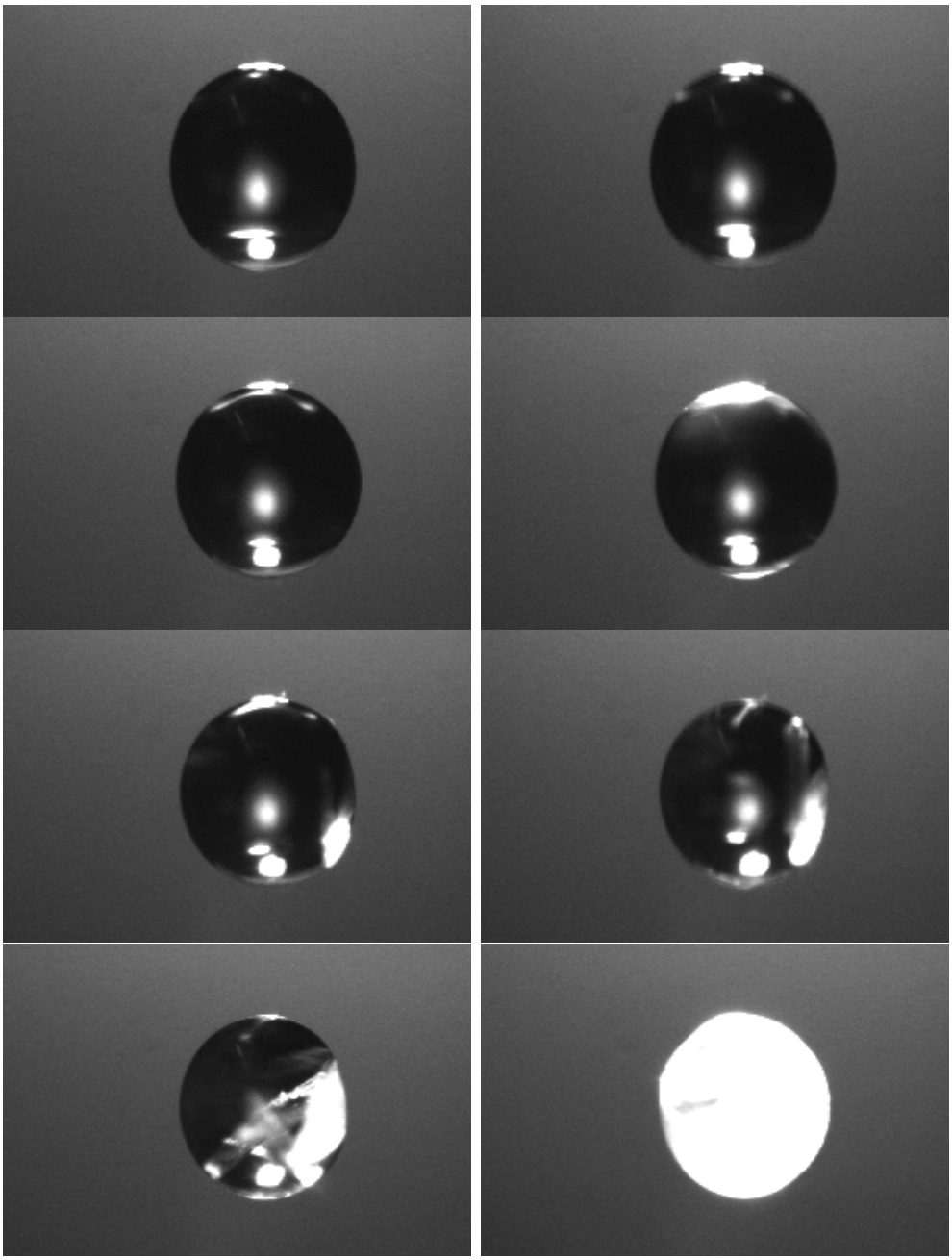

Figure 12: Pictures taken at 0, 40, 80, 120, 140, 160, 170, and 180 s.

The pictures in figure 12 were taken at the red data points in diagram 3.17.

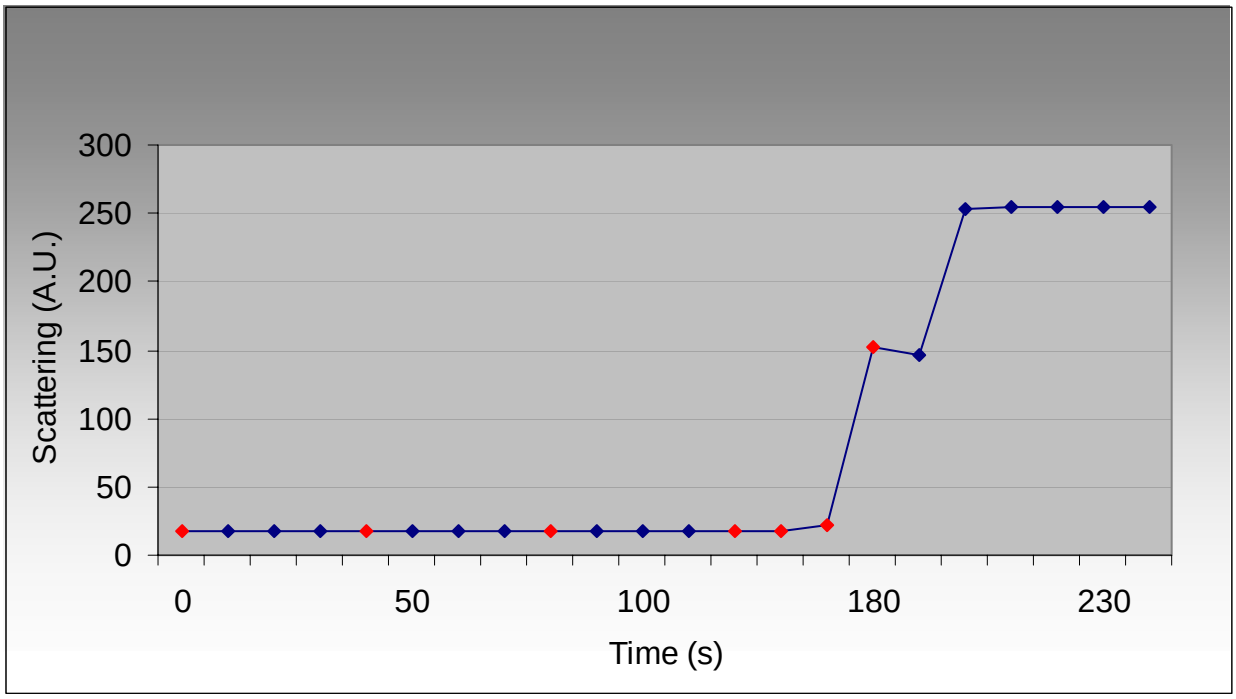

Diagram 3.17: Diagram showing the precipitation of an ammonium sulfate droplet. The red data points corresponds to the pictures taken during the experiment, shown in figure 12.

In order to get a hint of the measurement accuracy of the instrument, calculations on the water solubility of ammonium sulfate were performed. The concentration of the experiment droplets of 3.5 M ammonium sulfate corresponds to 462.49 g/L. The water solubility of ammonium sulfate is 754 g/L at 20ºC (Merck).

Performing the three precipitation experiments seen in diagram 3.18, gave the following results

Table XIII: Table showing the start volume of the ammonium sulfate droplets, the volume at the start of precipitation, and the water solubility for the experiments shown in diagram 3.18.

Experiment	Start volume (µL)	Volume at the start of precipitation (µL)	Water solubility (g/L)
a.	0.913	0.567	745
b.	0.841	0.531	732
c.	1.242	0.809	710

The average water solubility of ammonium sulfate calculated from the three experiments above was 729 g/L ±18 g. Compared with the tabulated value of

754 g/L, the LevMac values are slightly lower, but show an acceptable agreement.

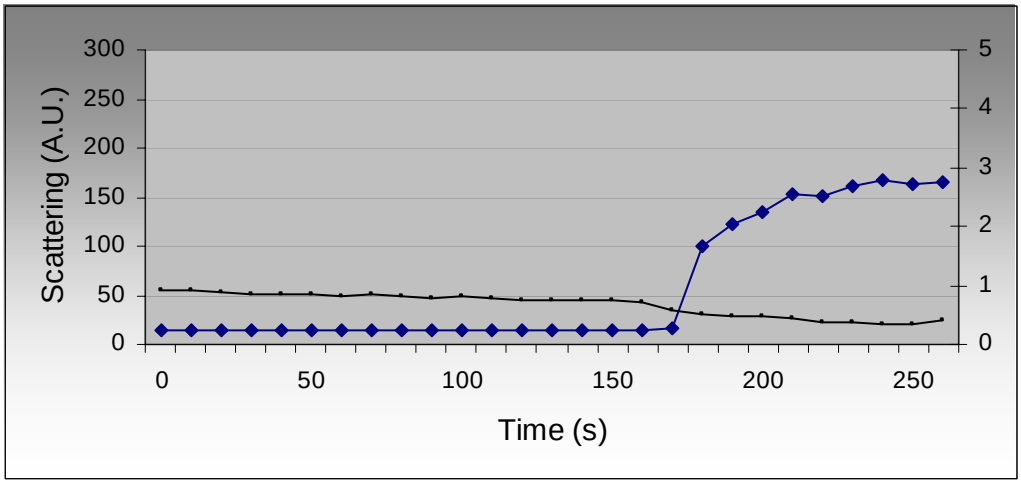

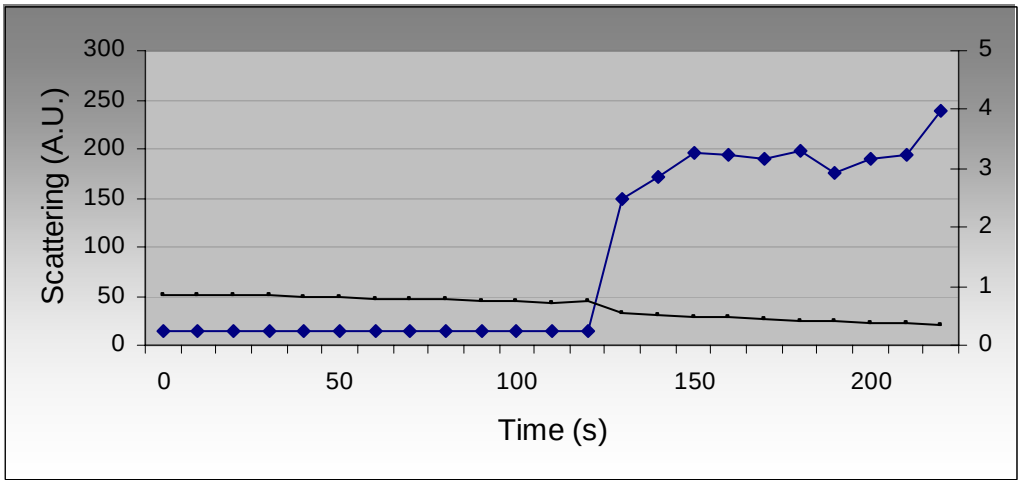

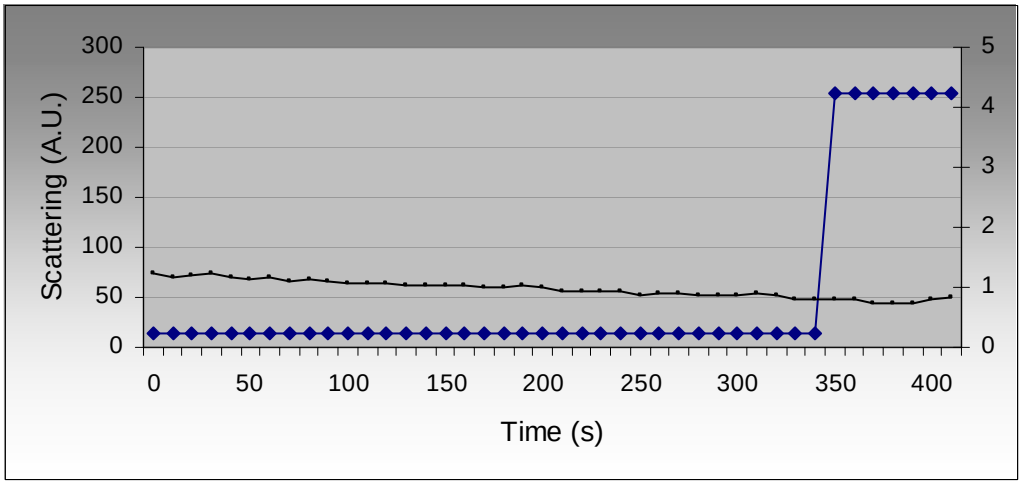

Diagram 3.18a-c: Three precipitation curves of ammonium sulfate droplets.

4 Protein experiments

A methodology for 2D crystallization of membrane proteins was to be developed for the LevMac instrument. As discussed in section 1.2.5, membrane proteins are complicated when trying to crystallize them.

Detergents are used to extract proteins from membranes, and during further purification to obtain samples suitable for crystallization. During this process the membrane protein structure and function are affected by the loss of interaction with the lipids. The most efficient way to reconstitute membrane proteins into a lipid bilayer in order to obtain 2D crystals is the removal of detergent from a protein-lipid-detergent ternary mixture [27].

There are mainly three ways to remove detergent; dialysis, adsorption to biobeads, and dilution. However, all of these methods have their limitations. For dialysis, the molecular weight cut-off of the membranes has to be chosen sufficiently low to prevent diffusion of proteins and lipids, thus only permitting detergent monomers to pass through the dialysis membrane. The high efficiency of detergent adsorption to biobeads frequently results in too fast detergent removal leading to aggregation. The major drawback of the dilution approach is the inability to remove the detergent completely [27].

A new approach based on complexion by cyclodextrins is used here. The ability of cyclodextrins to remove detergent from ternary mixtures (lipid, detergent, and protein) in order to get 2D crystals was proven in [27].

α-, β-, or γ-cyclodextrins are ring shaped molecules made of 6, 7, and 8 glucose molecules respectively. The non-polar environment inside the ring enables cyclodextrin to encapsulate hydrophobic or amphiphilic molecules like cholesterol or detergents. The reconstitution rate is directly related to the amount of cyclodextrin added. The higher affinity of the inclusion compounds of cyclodextrin for detergents than for lipids prevents the LPR (lipid-to-protein ratio) to change during reconstitution [27].

A cyclodextrin partner (α-, β- or γ-cyclodextrin) with a sufficiently high binding affinity can be found for most detergents. The affinity of a detergent molecule for a cyclodextrin is largely determined by the fit of its hydrophobic moiety with the cyclodextrin cavity. Full functional reconstitution of membrane proteins with any kind of detergent is therefore possible [27].

Here, methyl-β-cyclodextrin (MBCD) was selected for its high solubility and its high affinity for a wide range of detergents commonly used in membrane protein chemistry. MBCD solutions of different concentrations were obtained

by dilution of appropriately combined stock solutions with reagent grade water produced by a Milli-Q-system.

Previous experiments with MBCD [27] show that faster detergent removal rates (2 hours and less) result in low quality crystals.

The capability of cyclodextrin to complex any kind of detergent molecule is a crucial advantage over the dialysis method in the removal of low CMC detergents.

The nature of the detergent, the detergent removal rate, and the detergent removal technique affect size and quality of the resulting crystals. Even if detergent is removed in an efficient way there is no guarantee that 2D crystals will form during the reconstitution process.

One advantage of the cyclodextrin method is the accuracy of the detergent removal allowing us to control the kinetics of the whole process in a very precise way. The detergent removal rate is controlled by the amount of cyclodextrin added and does not depend on the CMC of the detergent. Another advantage of the cyclodextrin method lies in its applicability in systematic screenings for crystallization conditions. The sample volume can be very small allowing us to work with small amounts of protein per condition. This is especially advantageous with compounds that are expensive or not available in large quantities.

In figure 13, 2D crystallization using MBCD is illustrated. Free detergent molecules are trapped by the MBCD rings. This decreases the amount of detergent in detergent-lipid, and detergent-lipid-protein complexes. The protein is incorporated in the lipid bilayer to avoid exposure of the hydrophobic part of the molecule to the aqueous medium. The subsequent addition of phospholipase A2 degrades lipids from the bilayer allowing the protein to pack in a denser arrangement. The degradation products are bound by MBCD and can therefore not take part in the resolubilization of the protein.

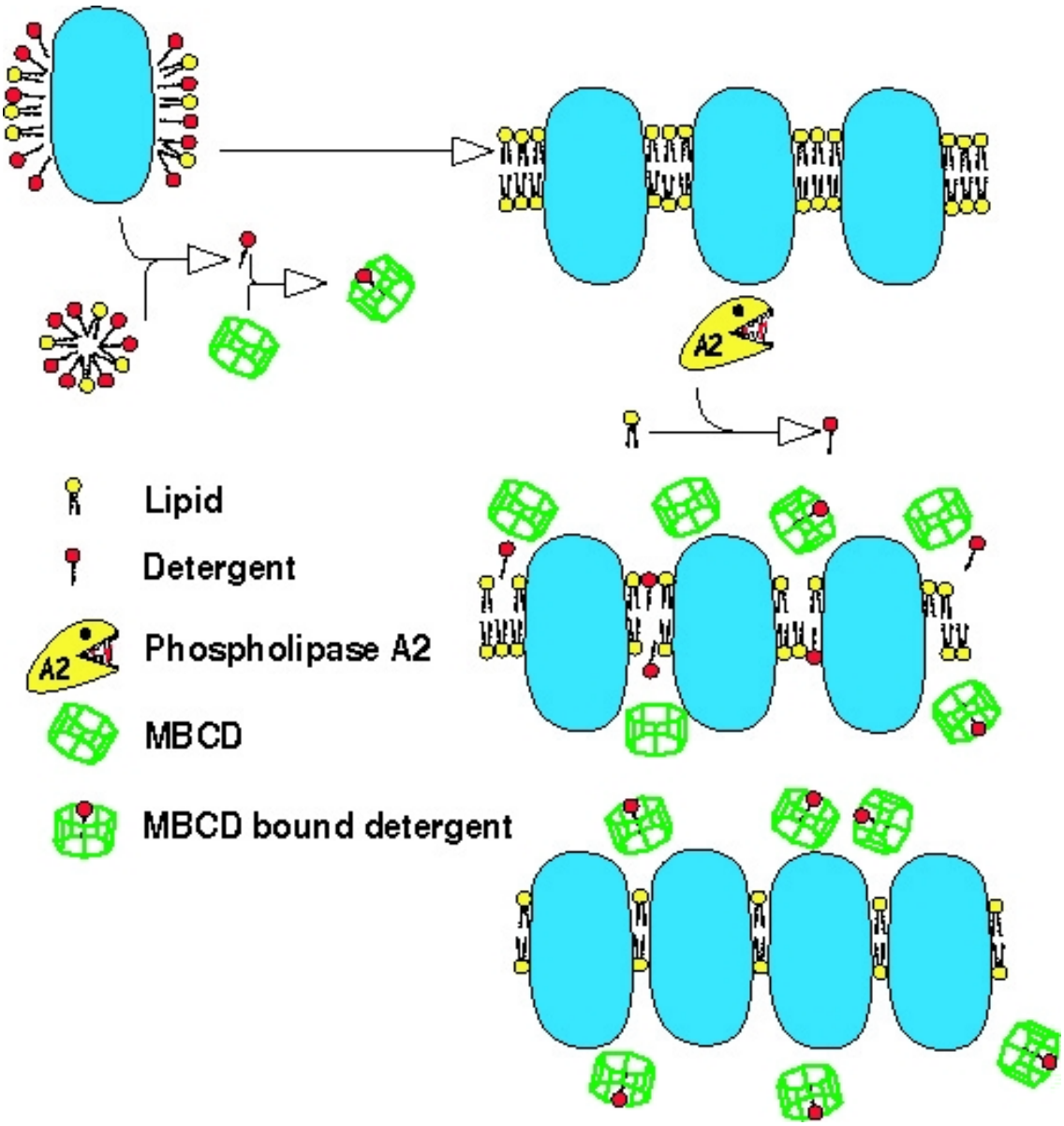

Figure 13: Picture showing the reconstitution of membrane proteins into a lipid bilayer using cyclodextrin.

4.1 Membrane protein evaporation

To find the right settings and to be able to calculate the added MBCD concentrations, evaporation studies were performed on both the protein solution and the mixture of protein solution and cyclodextrin.

Using the protein solution, three runs were performed, and the average evaporation speed in the region from 1µl – 0.5 µL was found to be 0.001 µL/s ± 0.0002 µL.

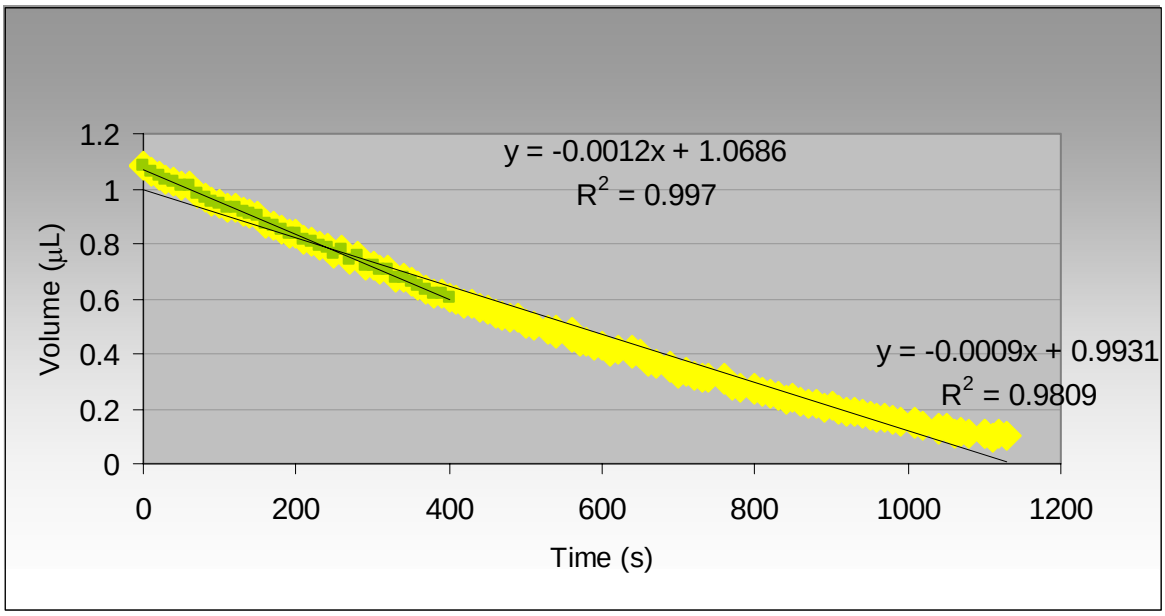

Diagram 4.1: Evaporation of a protein droplet.

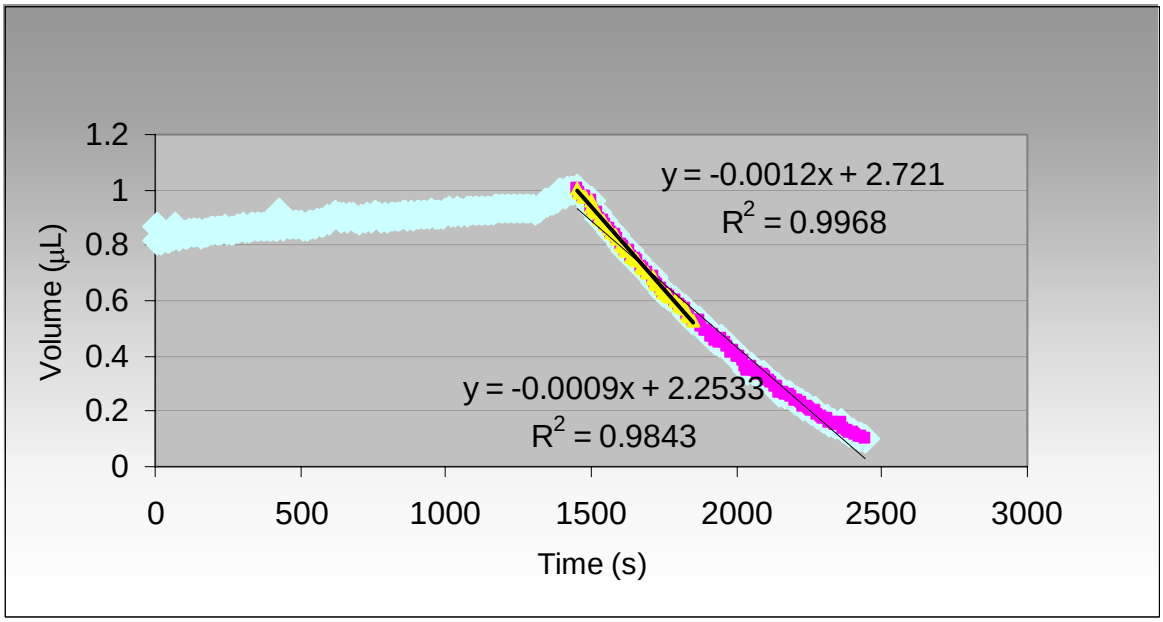

Diagram 4.2: Addition of MBCD to a protein droplet (0-1500 s) and consequent evaporation of the resulting protein-MBCD droplet (1500-2500).

With the MBCD-protein droplets, an evaporation rate of 0.001 µL/s ± 0.00007 µL was established. Based on these results it is safe to make the assumption that during a protein experiment, the droplet will evaporate with a rate of 0.001 µL per second. The dispenser droplet addition rate thus has to be adjusted accordingly to prevent the droplet from shrinking.

4.2 Tests on prevention of evaporation using glycerol mixtures

Some experimenrs were performed on protein droplets being left in a levitator without any replenishing additions. Instead the protein droplets were covered with different mixtures of glycerol and cyclodextrin. Different mixtures were evaporated (diagram 4.3) for an evaluation of the evaporation behavior.

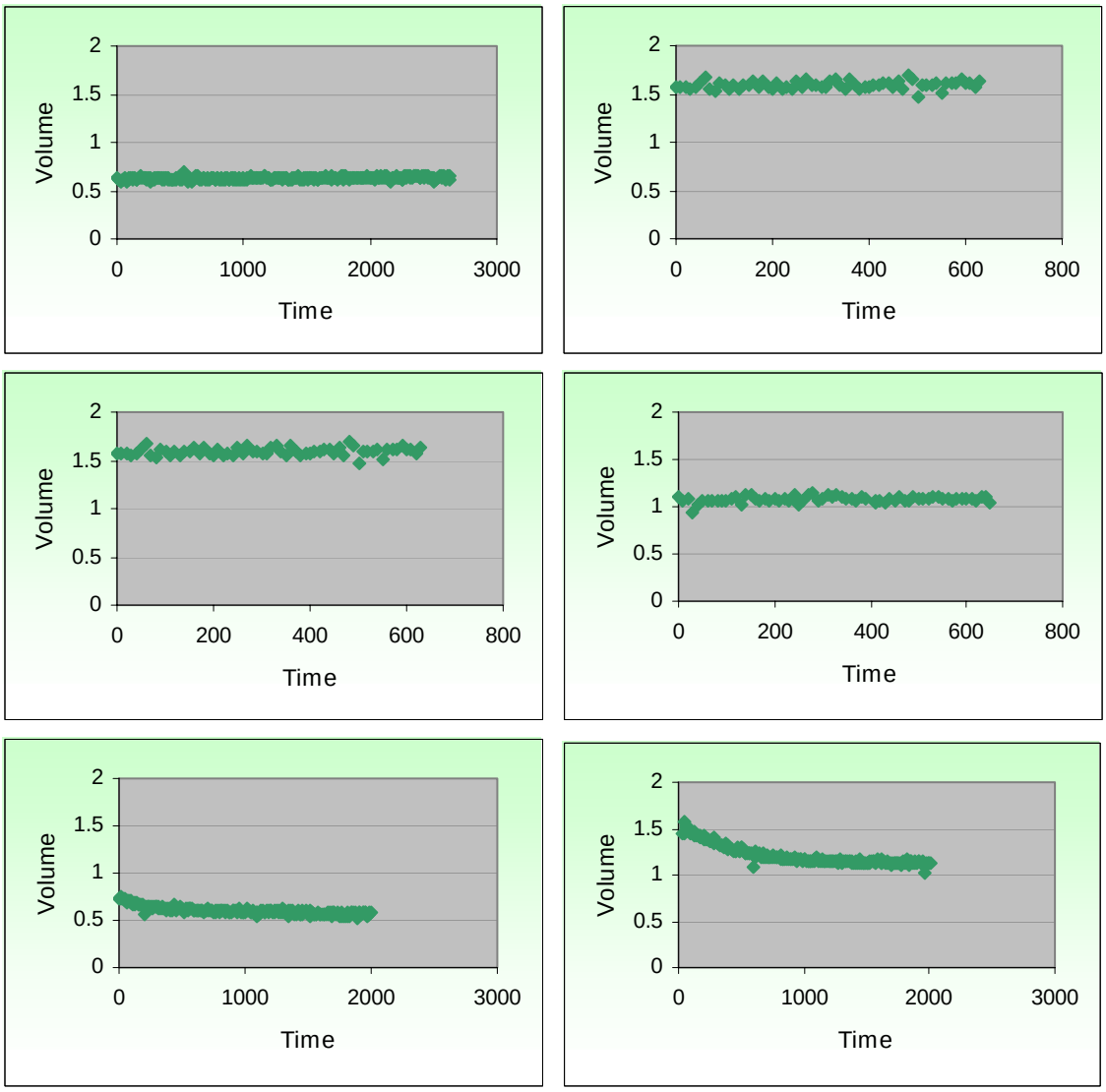

Diagram 4.3: Evaporation studies on different glycerol solutions. The two diagrams on the top is pure glycerol droplets. In the middle diagrams droplets of a solution containing 900 µL glycerol and 100 µL MBCD were evaporated. The bottom diagrams were made on droplets of a solution containing 600 µL glycerol and 400 µL MBCD.

Droplets of ternary mixtures containing the protein HasA-HasR, the lipid DLPC in lipid-to-protein ratio 1, and the detergents C8E4, OG, or DDM were covered with a glycerol/MBCD mixture and left in a levitator for various periods of time. The idea was to have the glycerol surrounding the protein releasing its cyclodextrin slowly during the day.

Table XIV: Table showing experiments of droplets covered with glycerol mixtures.

Experi-ment	Deter-Gent	Vol. (µL)	Time (h)	Covered with
3	C8E4 0.25%	0.5	7	1µL of 6 µL MBCD3% and 94 µL glycerol
4	C8E4 0.25%	0.5	7	1µL of 100 µL MBCD3% and 900µL glycerol.
6	OG 1%	0.5	15	1µL of 400 µL MBCD3% and 600µL glycerol.
7	C8E4 0.25%	0.5	15	1µL of 100 µL MBCD3% and 900µL glycerol
8	DDM 0.25%	0.5	Over night	1µL of 100 µL MBCD3% and 900µL glycerol
10	C8E4 0.25%	0.5	Over night	1µL of 100 µL MBCD3% and 900µL glycerol
11	DDM 0.25%	0.5	3	1µL of 100 µL MBCD3% and 900µL glycerol

The experiments resulted in aggregates, meaning the cyclodextrin exchange was effective, but too fast for 2D crystals to form. Further experiments with different glycerol-MBCD mixture ratios should be tested to establish the suitable experimental conditions in this approach.

4.3 Tests on detergent removal using MBCD addition by dispenser

A droplet of ternary protein-lipid-detergent solution was placed in the levitator. The MBCD solution was added from a flow-through dispenser with volume and scattering measurements taken every tenth second.
After each experiment, the droplet was collected with a GELoader tip and transferred to a 25 µL glass capillary. The capillary was instantly put into a perforated plastic test tube and frozen in liquid nitrogen where it was kept until stored in a -90ºC freezer.

To get an idea of the instrument performance and to be sure of when the reaction took place, the limit of detection was calculated from 100 data points in the beginning of three different protein experiments (diagram 4.4). The standard deviations from these experiments were 0.014, 0.018, and 0.039, giving an average LOD of 0.07 A.U.

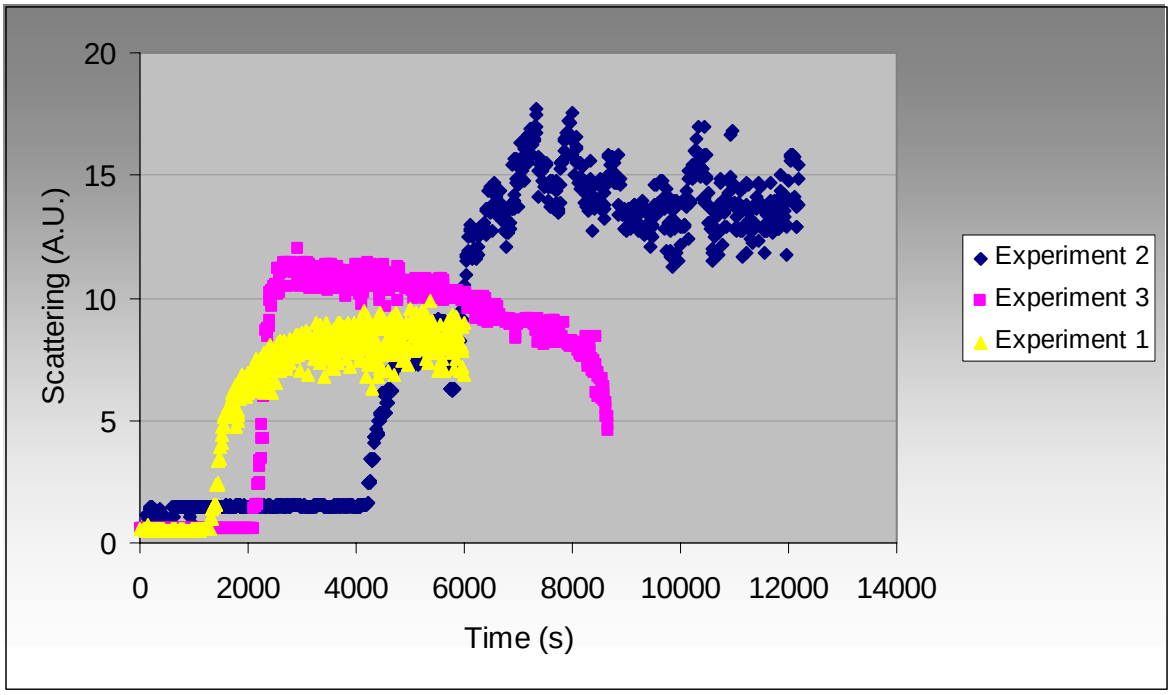

Diagram 4.4: Three 2D crystallization experiments with the addition of 0.25% MBCD.

An evaluation of the three experiments showed that the instrument was working for its purpose, but the formation of aggregates (figure 14) shows that the process was too fast for high quality crystals to form.

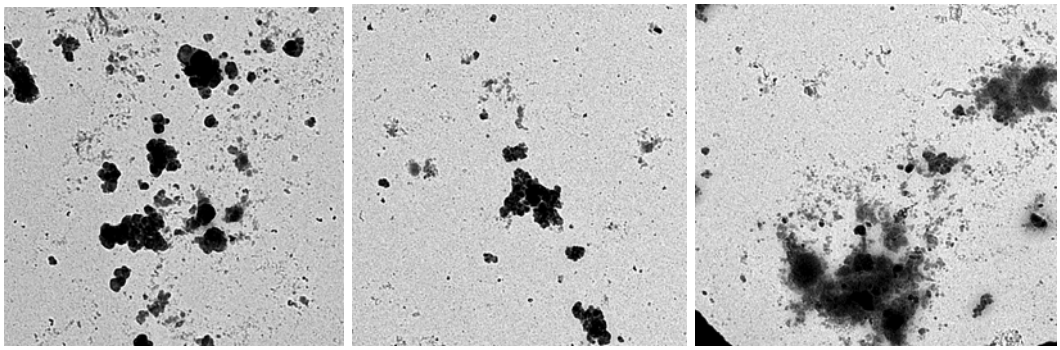

Figure 14: Aggregates formed in a levitated droplet off ternary protein-lipid-detergent mixture with additions of MBCD from the dispenser.

In order to produce high quality crystals the method has to be optimized. First, you want the start of reconstitution to begin as soon as possible in order to save valuable analysis time. Then, you want the slope of the reconstitution curve to be as shallow as possible in order to get a slow reconstitution process.

Four experiments using the same solution (C8E4_DLPC_LPR1) with 0.25% MBCD additions were made. In diagram 4.5 it is shown that experiment 7 got the shallowest curve but a late start of precipitation. In experiment 7, water was used for addition between 4000 and 5600 seconds to slow down the process.

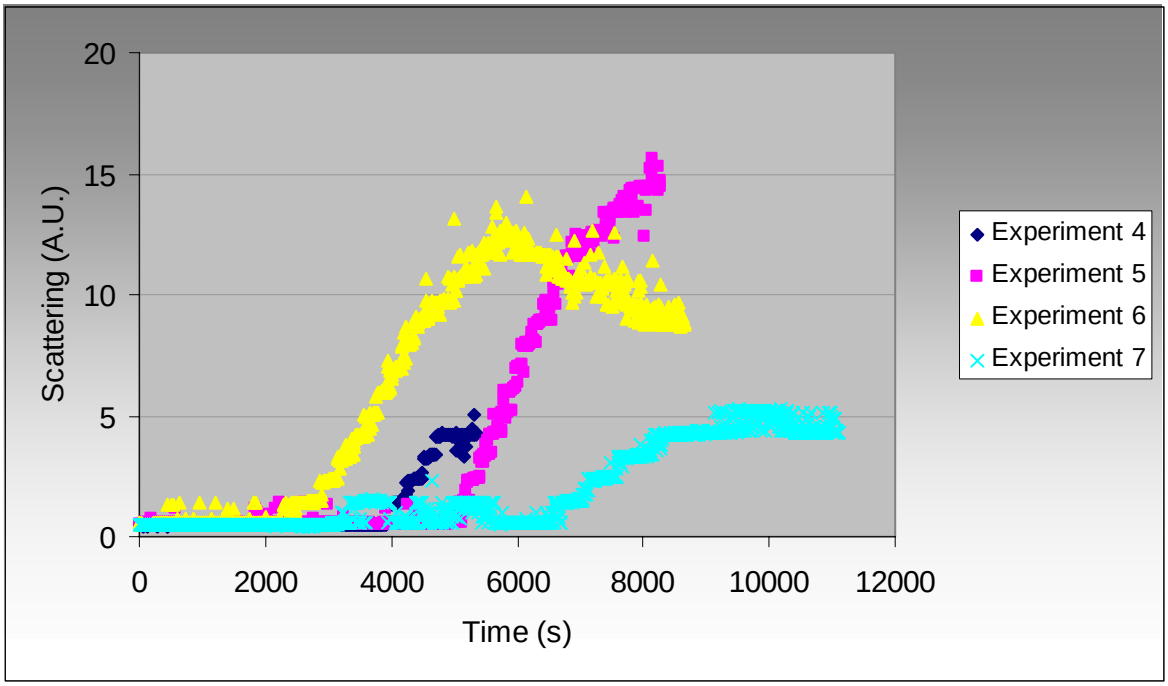

Diagram 4.5: Four experiments were made using C8E4_DLPC_LPR1. In all experiments 0.25% MBCD was used as addition. In experiment 7, a water addition between 4000 and 5600 seconds was used to slow down the reconstitution process.

Five experiments were now performed where the starting concentration of MBCD were increased in order to get a faster start of precipitation. The results are shown in diagram 4.6.

In experiment 9, the 3% addition was exchanged for water at 690 seconds. In experiment 10, 3% MBCD were used from start and until 500 seconds of the reaction. Between 500-2300 seconds, water was used as addition to slow the process down, and after 2300 seconds the addition was changed to 0.25% MBCD. In experiment 12, 3% MBCD was used between 0-1150 seconds and at 2950 the 0.25% MBCD solution was used for the rest of the experiment.

From these experiments it can be concluded that the 3% solution can be used initially as a way of speeding the reaction up, and that by switching to a solution of lower concentration, the speed of reaction can be slowed.

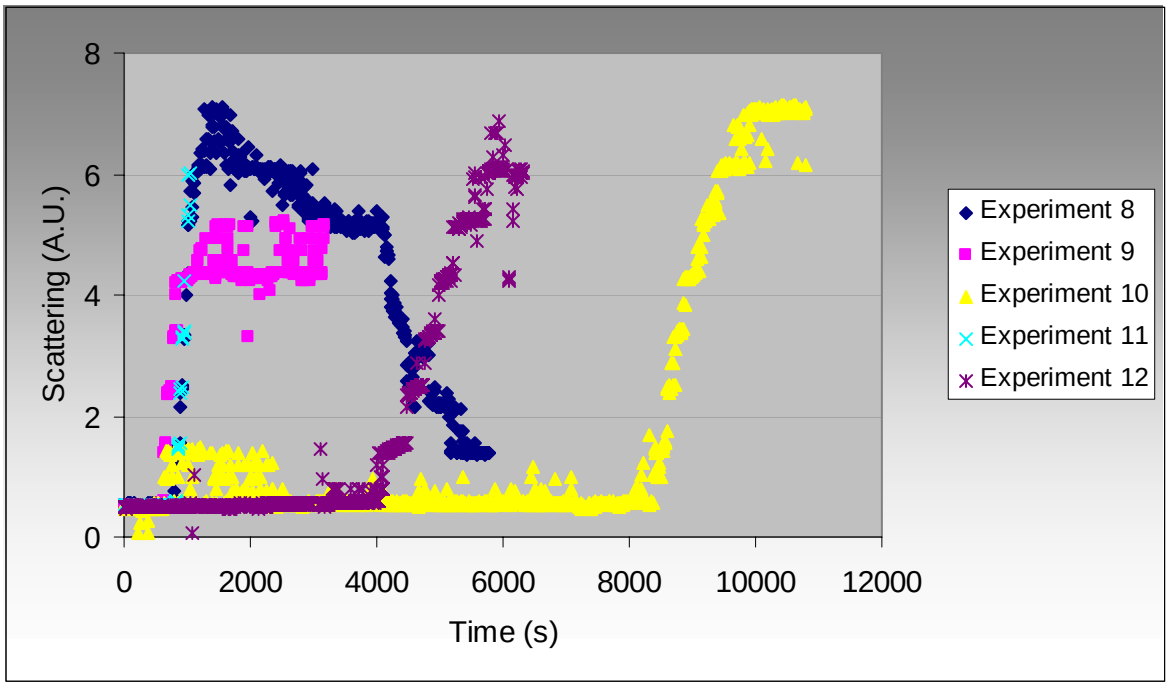

Diagram 4.6: Five experiments using C8E4_EC_LPR1. In experiment 8, 9, and 11, 3% MBCD additions were made all the way in order of getting a fast start of the reconstitution. In experiment 10 and 12, 3% was used in the beginning but was exchanged to 0.25% MBCD in order of getting a slower reconstitution process.

Comparing the two experiments in diagram 4.7 shows that addition of 3% MBCD gives a faster start of reaction than an addition of 0.25%. the 0.25% solution also gives the reaction longer time to reach the plateau, which is better for the crystallization reaction.

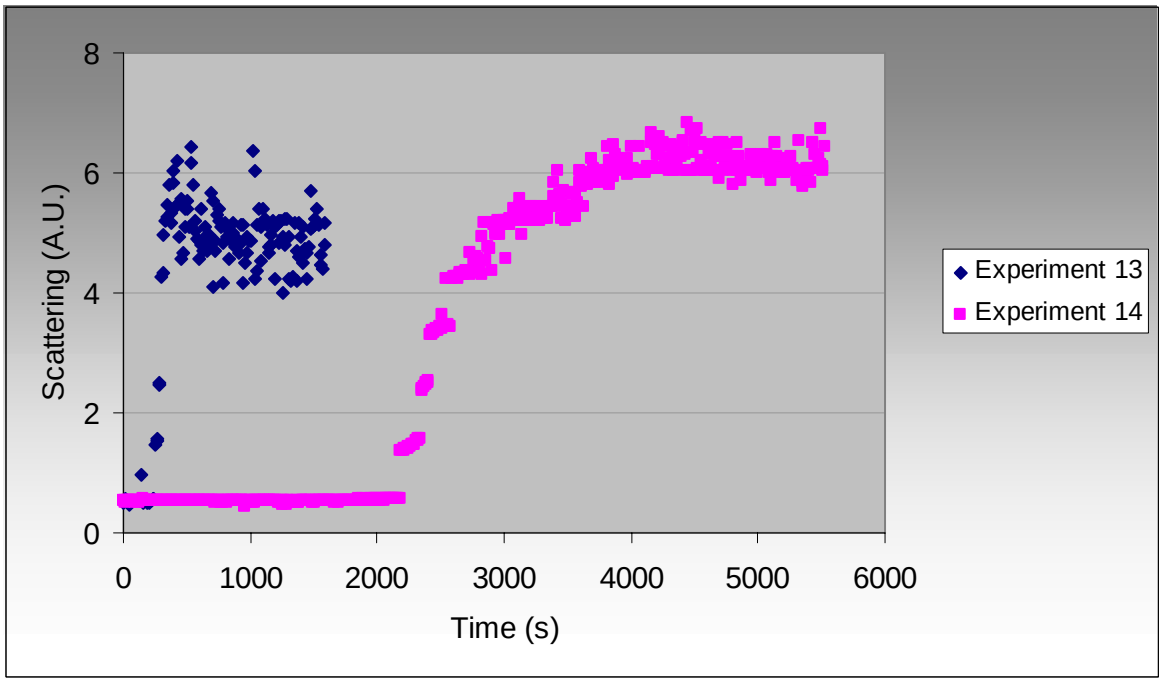

Diagram 4.7: A comparison of 0.25% and 3% MBCD additions to DDM_DLPC_LPR1.

Now different optimizations by using more and more dilute solutions and by doing the switches of dispenser MBCD solutions at different times were made. Some of these results are shown in diagram 4.8.

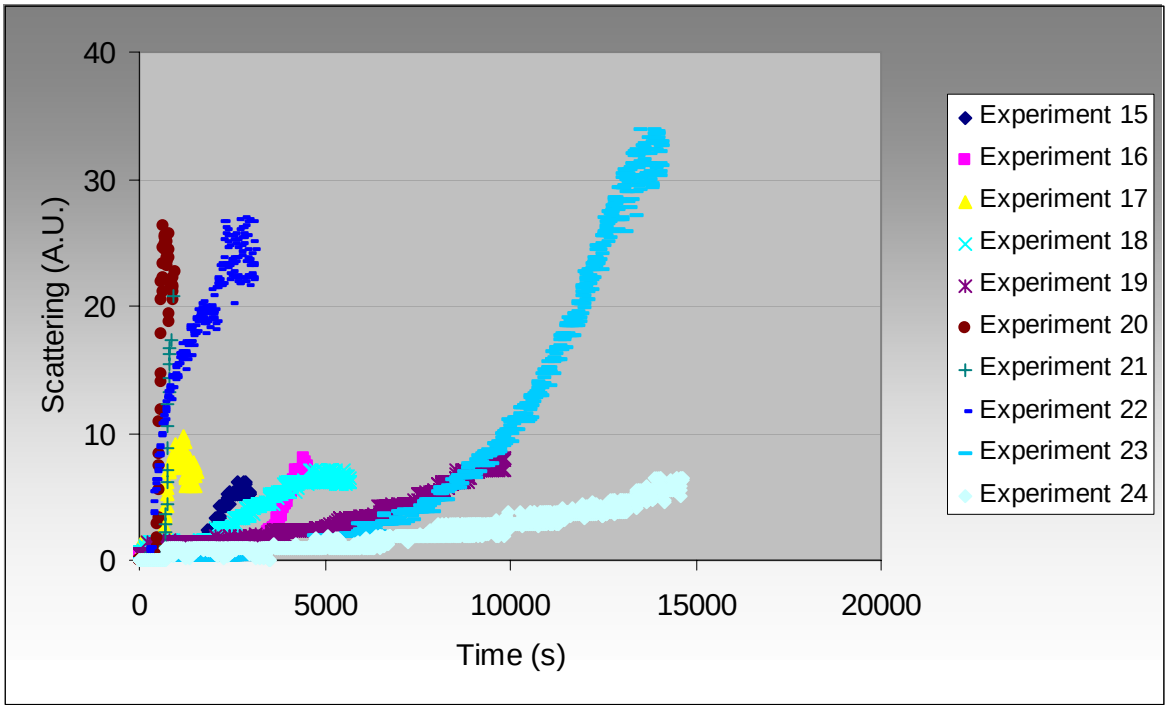

Diagram 4.8: All the protein samples used in this diagram contained DDM_EC_LPR1. In experiment 15 and 16, 0.25% and 0.1% MBCD were used. In experiment 17, 20, and 21, 1% MBCD were used as addition. In experiment 18, 1% and 0.01% were used. In experiment 19, 22, 23, and 24, 1% and 0.005% MBCD solutions were used.

In experiment 24, 1% MBCD was used from start to 230 seconds. Between 231 and 6500 seconds 0.005% MBCD was used, and after that the addition was changed to 0.0025%. This experiment was aborted at 15000 seconds but would, if continued, give the best result so far.

The results are obvious. By using a higher concentration of MBCD (e.g.3%) the reconstitution process starts almost immediately and proceeds quickly, providing aggregates. By using more and more diluted MBCD solutions as the reaction proceeds, the reconstitution process is slowed and levels off.

From the results obtained, it is clear that the reconstitution behavior in the levitated drop can be predicted in a reliable and reproducible way. Due to limited time, it has not been possible within this thesis work to obtain EM images of most experiments, but it is clear already from the scattering results and the few EM images obtained so far that the method is being validated. Future experiments should focus on repeating the process for other proteins and get more EM images.

5 Acknowledgements

First I would like to thank my supervisor Sabina Santesson at Crystal Research AB, Lund, for introducing me to this project and for all time and effort spent on me, I wish you all the best with your future projects.

I also want to thank Hervé-W. Rémigy for providing us with protein samples and for sharing interesting facts of his work.

I would like to send my gratitude to my examiner, Margareta Sandahl, for inspiration and encouragement during my years of studying.

Thank you to my friends and family for being patient with me and my lack of time for you, a special thanks to my mum for all Thursday coffees.

Finally, with all of my heart, thank you Roger for always believing in me, for taking care of everything during these years, for not complaining over my late nights, my books being everywhere, or my lack of time for you, thank you for being the one you are.

6 References

1) *MAX-lab – the bright link to microcosm*, A Swedish National Laboratory, Max 2001.
2) *Crystal Research AB*, http://www.crystalresearch.se/
3) Ljungen O, *Microscale Sample Preparation in Chip-Based Chemical Analysis,* UPTEC X 03 016 Jun 2003
4) Rooij NF, *Recent Advances in Technology and Application of Microsystems,* Institute of Microtechnology, University of Neuchâtel, CH 2000 Neuchâtel, Switzerland
5) Nikolajeff F, *The use of micro-optics for miniaturized chemical and biomedical analysis systems,* Åmic AB, Uppsala Science Park, Sweden
6) *Här skapas framtidens teknik,* Tekniksektionen, Instutitionen för materialvetenskap, Ångströmslaboratoriet, Uppsala
7) Madou M.J, Cubicciotti R, *Scaling Issues in Chemical and Biological Sensors,* Proceedings of the IEEE, Vol 91, NO. 6, June 2003
8) Wood BR, Heraud P, Stojkovic S, Morrison D, Beardall J, McNaughton D, *A Portable Raman Acoustic Levitation Spectroscopic System for the Identification and Environmental Monitoring of Algal Cells,* Anal. Chem, 2005, 77, 4955-4961
9) Santesson S, Nilsson S, *Airborne chemistry: acoustic levitation in chemical analysis,* Anal Bioanal Chem (2004) 378: 1704-1709
10) Lavén M, Wallenborg S, Velikyan I, Bergström S, Djodjic M, Ljung J, Berglund O, Edenwall N, Markides K.E, Långström B, *Radionuclide Imaging of Miniaturized Chemical Analysis Systems,* Anal. Chem 2004, 76, 7102-7108
11) Eberhardt R, Neidhart B, *Acoustic levitation device for sample pretreatment in microanalysis and trace analysis,* Fresenius J Anal Chem (1999) 365: 475-479
12) Yarin A.L, Weiss D.A, Brenn G, Rensink D, *Acoustically levitated drops: drop oscillation and break-up driven by ultrasound modulation,* International Journal of Multiphase Flow 28 (2002) 887-910
13) Priego-Capote F, Luque de Castro MD, *Analytical uses of ultrasound II. Detectors and detection techniques,* Trends in Analytical Chemistry, Vol 23, No. 10-11, 2004
14) Laurell T, Wallman L, Nilsson J, *Design and development of a silicon micro fabricated flow-through dispenser for on-line picolitre sample handling,* J.Micromech. Microeng. 9 (1999) 369-376
15) Önnerfjord P, Nilsson J, Wallman L, Laurell T, Marko-Varga.G, *Picoliter Sample Preparation in MALDI-TOF MS Using a*

Micromachined Silicon Flow-Through Dispenser, Anal. Chem 1998, 70, 4755-4760
16) Bergkvist J, Lilliehorn T, Nilsson J, Johansson S, Laurell T, *Miniaturized Flowthrough Microdispenser With Piezoceramic Tripod Actuation,* Journal of Microelectromechanical systems, Vol 14, NO 1, February 2005
17) Santesson S, *Miniaturized Bioanalytical Chemistry in Acoustically Levitated droplets,* Department of Technical Analytical Chemistry, Lund Institute of Technology, Lund University, 2004
18) Kundrot C.E, *Review: Which strategy for a protein crystallization project?* Cellular and Molecular Life Science 61 (2004) 525-536
19) Bard J, Ercolani K, Svenson K, Olland A and Somers W, *Automated systems for protein crystallization,* Methods 34 (2004) 329-347
20) Mueller U, Nyarsik L, Horn M, Rauth H, Przewieslik T, Saenger W, Lehrach H, Eickhoff H, *Development of a technology for automation and miniaturization of protein crystallization,* Journal of Biotechnology 85 (2001) 7-14
21) Baird J.K, *Theory of protein crystal nucleation and growth controlled by solvent evaporation,* Journal of Crystal Growth 204 (1999) 553-562
22) Drenth J, Tardieu A, *Nucleation – The Birth of a Protein Crystal,* http://laue.lec.csis.es/esatt/birth_of_crystal.htm, 2006-01-21
23) Baird J.K, *Theory of protein crystal nucleation and growth controlled by solvent evaporation,* Journal of Crystal Growth 204 (1999) 553-562
24) Crystallization of membrane proteins, College of liberal arts and sciences, Arizona state University.
25) 2D crystallization of membrane proteins, Physical chemistry, “curie” – UMR CNRS/Institut Curie
26) Madou M.J, Cubicciotti R, *Scaling Issues in Chemical and Biological Sensors,* Proceedings of the IEEE, Vol 91, NO. 6, June 2003
27) Signorell G.A, Kaufmann T.C, Kukulski W, Engel A, Rémigy H-W, *Controlled 2D Crystallization of Membrane Proteins using Methyl-β-Cyklodextrin,* M.E. Müller Institute for Microscopy at the Biozentrum, University of Basel, Basel, Switzerland.

Appendix 1

Complete table over the positioning experiments presented in section 3.1.2. Twenty tests were performed with thirteen solutions and average values were calculated.

Test	A	B	C	D	E	F	G	H	I	J	K	L	M	N
1	5.1	5.2	4.8	5	4.9	4.9	4.8	4.9	4.9	4.9	4.9	4.8	6.5	7.7
2	4.9	5.2	4.8	4.9	4.9	4.9	4.8	4.9	4.9	4.9	4.9	4.8	6.8	6.5
3	4.9	5.2	4.8	4.8	4.9	4.9	4.8	4.9	4.9	4.9	4.9	4.8	6.3	7.8
4	5	5.2	4.8	5.2	4.9	4.9	4.8	4.9	4.9	4.9	4.9	4.8	6.3	8
5	4.9	5.2	4.8	4.9	4.9	4.9	4.8	4.9	4.9	4.9	4.9	4.8	7.8	6.7
6	5	5.2	4.8	4.9	4.9	4.9	4.8	4.9	4.9	4.9	4.9	4.8	7.5	7.5
7	4.9	5.2	4.8	4.9	4.9	4.9	4.8	4.9	4.9	4.9	4.9	4.8	6.5	10.2
8	4.9	5.2	5.1	4.9	4.9	4.9	4.8	4.9	5.1	4.9	4.9	4.8	6.7	7.9
9	4.9	5.2	4.8	4.9	4.9	4.9	4.8	5.1	4.9	4.9	4.9	4.8	5.9	6.5
10	4.9	5.2	4.8	4.9	4.9	4.9	4.8	5.2	4.9	4.9	4.9	4.8	7.3	8.7
11	4.9	5.2	4.8	4.9	4.9	4.9	4.8	4.9	4.9	4.9	4.9	4.8	6.5	7.9
12	4.9	5.2	5.2	4.9	4.9	4.9	4.8	5.1	4.9	4.9	4.9	4.8	6.2	10.1
13	4.9	5.2	4.8	4.9	4.9	4.9	4.8	5.5	4.9	4.9	4.9	4.8	6.3	9.2
14	4.9	5.2	4.8	4.9	4.9	4.9	4.8	5.5	4.9	4.9	4.9	4.8	7.2	9.2
15	4.9	5.2	4.8	4.9	4.9	4.9	4.8	4.9	5.2	4.9	4.9	4.8	6.3	10.2
16	4.9	5.2	4.8	4.9	4.9	4.9	4.8	5.3	4.9	4.9	4.9	4.8	68	9.3
17	4.9	5.2	4.8	4.9	4.9	4.9	4.8	5.1	5	4.9	4.9	4.8	6.9	9.6
18	4.9	5.2	4.8	4.9	4.9	4.9	4.8	4.9	4.9	4.9	4.9	4.8	7.2	10.5
19	4.9	5.2	4.8	4.9	4.9	4.9	4.8	5.2	4.9	4.9	4.9	4.8	6.9	10.7
20	4.9	5.2	4.8	4.9	4.9	4.9	4.8	5.1	4.9	4.9	4.9	4.8	7.5	94
Min HF	**4.9**	**5.2**	**4.8**	**4.8**	**4.9**	**4.9**	**4.8**	**4,9**	**4,9**	**4.9**	**4.9**	**4.8**	**4.9**	**4.9**
HF needed	**4.9**	**5.2**	**4.8**	**4.9**	**4.9**	**4.9**	**4.8**	**5,05**	**4,9**	**4.9**	**4.9**	**4.8**	**6.77**	**8.68**
Std dev	**0.05**	**0**	**0.11**	**0.07**	**0**	**0**	**0**	**0,20**	**0,08**	**0**	**0**	**0**	**0.51**	**1.35**

A	Water	**H**	100% PEG 400
B	Ethanol	**I**	50% PEG 1000
C	100% MPD	**J**	20% PEG 1500
D	3,5 M Ammonium Sulfate	**K**	25% PEG 6000
E	3,4 M Sodium Malonate	**L**	25% PEG 10 000
F	2 M Sodium Chloride	**M**	1% dMBCD
G	50% PEG 400	**N**	Water using Hamilton syringe

Appendix 2

Complete table over the min – max intervals presented in section 3.2.1.2.

Water						
Slope	**Amplitude**			**Average**		**Difference**
6	-	-	-	-	min	
6	-	-	-	-	max	-
7	16.2	15.8	15.8	15.9	min	
7	17.5	17.6	17.2	17.4	max	1.5
8	12.5	12.5	12.4	12.5	min	
8	16.1	16.8	16.8	16.6	max	4.1
9	14.8	15	15	14.9	min	
9	15.9	16	15.9	15.9	max	1
10	15.4	15.4	15.5	15.4	min	
10	16.9	16.8	16.8	16.8	max	1.4
Amplitude	**Slope**			**Average**		**Difference**
12	-	-	-	-	min	
12	-	-	-	-	max	-
13	-	-	-	-	min	
13	-	-	-	-	max	-
14	-	-	-	-	min	
14	-	-	-	-	max	-
15	7.2	7.4	7.1	7.2	min	
15	10.4	10.4	10.4	10.4	max	3.2
16	6.5	6.5	6.6	6.5	min	
16	10.4	10.4	10.4	10.4	max	3.9
17	6.2	6.2	6.3	6.2	min	
17	7.2	7.2	7	7.1	max	0.9
18	6.1	6.2	6.2	6.2	min	
18	6.6	6.5	6.4	6.5	max	0.3
19	6.1	6.1	6.1	6.1	min	
19	6.2	6.3	6.2	6.2	max	0.1
20	6.3	6.2	6.3	6.3	min	
20	6.3	6.3	6.3	6.3	max	0.0

50% PEG 400						
Slope	**Amplitude**			**Average**		**Difference**
6	-	-	-	-	min	
6	-	-	-	-	max	-
7	-	-	-	-	min	
7	-	-	-	-	max	-
8	16.6	16.8	16.8	16.7	Min	
8	18.4	18.4	18.3	18.4	max	1.6
9	16.6	16.8	16.8	16.7	min	
9	18	18	18.1	18.0	max	1.3
10	16.6	16.6	16.6	16.6	min	
10	18.1	18	17.9	18.0	max	1.4
Amplitude	**Slope**			**Average**		**Difference**
12	-	-	-	-	min	
12	-	-	-	-	max	-
13	-	-	-	-	min	
13	-	-	-	-	max	-
14	-	-	-	-	min	
14	-	-	-	-	max	-
15	-	-	-	-	min	
15	-	-	-	-	max	-
16	-	-	-	-	min	
16	-	-	-	-	max	-
17	7.8	7.5	7.6	7.6	min	
17	10.4	10.4	10.4	10.4	max	2.8
18	6.8	6.9	6.9	6.9	min	
18	10.4	10.4	10.4	10.4	max	3.5
19	6.8	7.1	6.9	6.9	min	
19	10.4	10.4	10.4	10.4	max	3.5
20	6.9	6.8	6.7	6.8	min	
20	10.4	10.4	10.4	10.4	max	3.6
21	6.7	6.8	6.7	6.7	min	
21	8	8	8	8.0	max	1.3
22	6.7	6.7	6.7	6.7	min	
22	7.1	7.3	7.3	7.2	max	0.5
23	6.7	6.7	6.7	6.7	min	
23	7.1	7.1	7.1	7.1	max	0.4
24	6.7	6.7	6.7	6.7	min	
24	6.7	6.8	6.8	6.8	max	0.1

25% PEG 1000						
Slope	**Amplitude**			**Average**		**Difference**
6	-	-	-	-	Min	
6	-	-	-	-	Max	-
7	17.1	17	17.2	17.1	Min	
7	17.9	18.1	18	18.0	Max	0.9
8	16.1	16.1	16.1	16.1	Min	
8	17.3	17.6	17.5	17.5	Max	1.4
9	16.1	16.1	16	16.1	Min	
9	17.4	17.5	17.5	17.5	Max	1.4
10	17.3	17.3	17.2	17.3	Min	
10	17.4	17.2	17.3	17.3	Max	0.0
Amplitude	**Slope**			**Average**		**Difference**
12	-	-	-	-	Min	
12	-	-	-	-	Max	-
13	-	-	-	-	Min	
13	-	-	-	-	Max	-
14	-	-	-	-	min	
14	-	-	-	-	max	-
15	-	-	-	-	min	
15	-	-	-	-	max	-
16	7.8	7.7	7.8	7.8	min	
16	10.4	10.4	10.4	10.4	max	2.6
17	7.1	7.1	7.1	7.1	min	
17	7.2	7.2	7.3	7.2	max	0.1
18	6.2	6.1	6.2	6.2	min	
18	6.2	6.2	6.4	6.3	max	0.1
19	6.2	6.2	6.2	6.2	min	
19	6.4	6.4	6.4	6.4	max	0.2

3,5 M Ammonium sulfate						
Slope	**Amplitude**			**Average**		**Difference**
6	-	-	-	-	min	
6	-	-	-	-	max	-
7	-	-	-	-	min	
7	-	-	-	-	max	-
8	18.2	18	18	18.1	min	
8	18.6	18.4	18.3	18.4	max	0.4
9	18.2	18.1	17.7	18.0	min	
9	21.2	21	21.4	21.2	max	3.2
10	21	20.9	20.9	20.9	min	
10	21.2	21.4	21.8	21.5	max	0.5
Amplitude	**Slope**			**Average**		**Difference**
12	-	-	-	-	min	
12	-	-	-	-	max	-
13	-	-	-	-	min	
13	-	-	-	-	max	-
14	-	-	-	-	min	
14	-	-	-	-	max	-
15	-	-	-	-	min	
15	-	-	-	-	max	-
16	-	-	-	-	min	
16	-	-	-	-	max	-
17	-	-	-	-	min	
17	-	-	-	-	max	-
18	9.1	9.1	9.4	9.2	min	
18	10.4	10.4	10.4	10.4	max	1.2
19	7.5	7.2	7.4	7.4	min	
19	8	8.1	8.2	8.1	max	0.7
20	6.7	6.7	6.7	6.7	min	
20	6.7	6.8	6.8	6.8	max	0.1

3,4 M Sodium Malonate						
Slope	**Amplitude**			**Average**		**Difference**
6	-	-	-	-	Min	
6	-	-	-	-	Max	-
7	-	-	-	-	Min	
7	-	-	-	-	Max	-
8	16.6	16.7	16.9	16.7	Min	
8	17.4	17.2	17.3	17.3	Max	0.6
9	16.3	16.2	16.3	16.3	Min	
9	16.8	16.9	16.8	16.8	Max	0.6
10	16.4	16.3	16.4	16.4	Min	
10	16.6	16.9	16.9	16.8	Max	0.4
Amplitude	**Slope**			**Average**		**Difference**
12	-	-	-	-	Min	
12	-	-	-	-	Max	
13	-	-	-	-	Min	
13	-	-	-	-	Max	
14	-	-	-	-	Min	
14	-	-	-	-	max	
15	-	-	-	-	min	
15	-	-	-	-	max	
16	-	-	-	-	min	
16	-	-	-	-	max	
17	-	-	-	-	min	
17	-	-	-	-	max	
18	-	-	-	-	min	
18	-	-	-	-	max	
19	8.1	8.2	8.4	8.2	min	
19	10.4	10.4	10.4	10.4	max	2.2
20	6.9	7.2	7.2	7.1	min	
20	6.9	6.8	6.9	6.9	max	-0.2

50% MPD						
Slope	**Amplitude**			**Average**		**Difference**
6	-	-	-	-	min	
6	-	-	-	-	max	-
7	16.7	16.4	16.3	16.5	min	
7	17.2	17.3	16.8	17.1	max	0.6
8	15.1	15.1	15.3	15.2	min	
8	15.7	15.8	15.7	15.7	max	0.6
9	15	14.9	14.2	14.7	min	
9	15.4	15.1	15.6	15.4	max	0.7
10	15.4	15.4	15.3	15.4	min	
10	15.4	15.4	15.7	15.5	max	0.1
Amplitude	**Slope**			**Average**		**Difference**
12	-	-	-	-	min	
12	-	-	-	-	max	-
13	-	-	-	-	min	
13	-	-	-	-	max	-
14	-	-	-	-	min	
14	-	-	-	-	max	-
15	7.4	7.8	7.8	7.7	min	
15	10.4	10.4	10.4	10.4	max	2.7
16	7.1	6.9	7.1	7.0	min	
16	8.2	8	7.9	8.0	max	1
17	6.7	6.7	6.8	6.7	min	
17	7.2	7.2	7.2	7.2	max	0.5
18	6.5	6.5	6.6	6.5	min	
18	6.7	6.7	6.7	6.7	max	0.2
19	6.3	6.3	6.3	6.3	min	
19	6.5	6.4	6.4	6.4	max	0.1
20	6.2	6.2	6.3	6.2	min	
20	6.3	6.2	6.2	6.2	max	0

Appendix 3

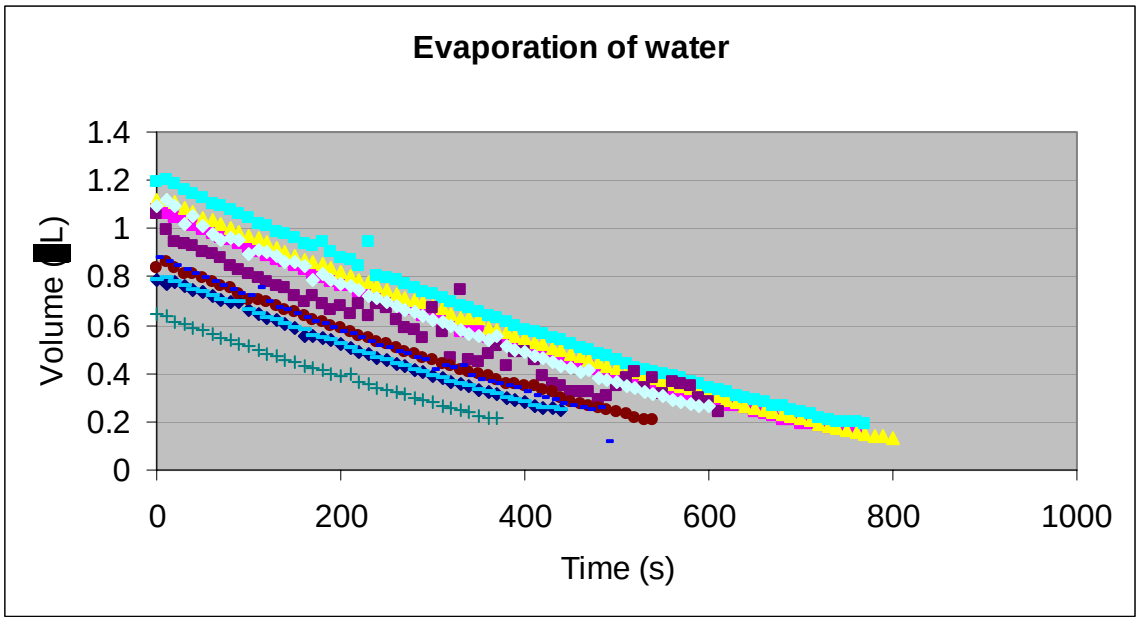

Diagram showing the evaporation curves of ten water droplet evaporation experiments.

	Speed of evaporation (µL/s)	R^2
Water 1	0,0012953	0,9953771
Water 2	0,0012209	0,9898471
Water 3	0,0012595	0,9923648
Water 4	0,0013555	0,9902677
Water 5	0,0011687	0,9298295
Water 6	0,0012300	0,9954370
Water 7	0,0011800	0,9956240
Water 8	0,0013600	0,9902770
Water 9	0,0013000	0,9957000
Water 10	0,0014100	0,9930000
Average:	**0,0013**	
Std.dev:	**0,000081**	

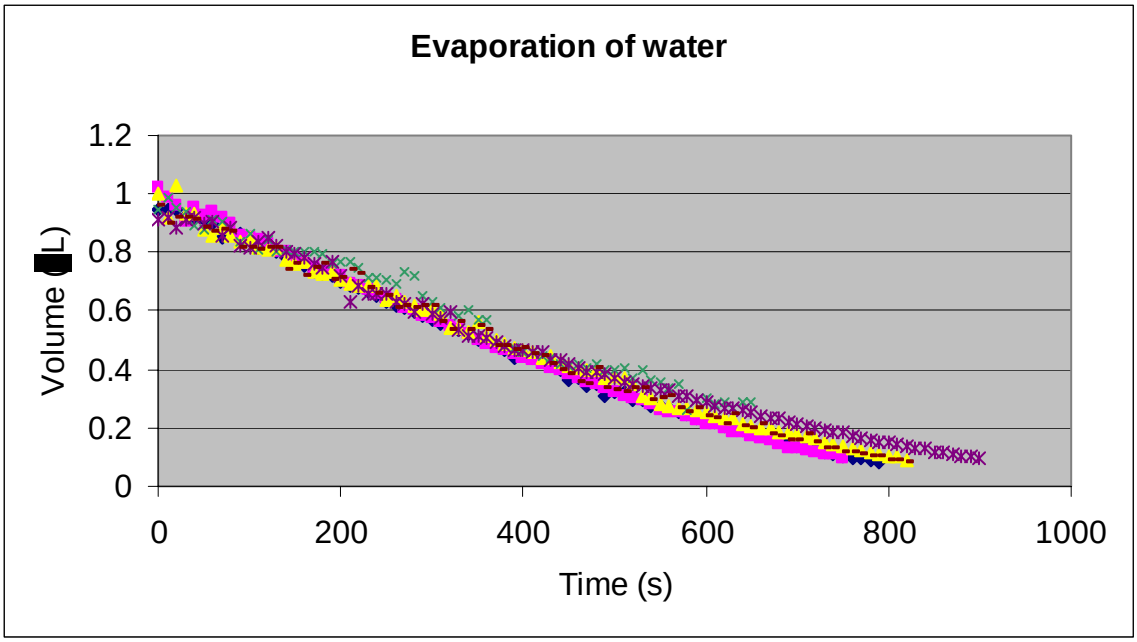

Diagram showing the evaporation curves of six water droplet evaporation experiments.

	Speed of evaporation (mL/s)	R^2
Water 1	0.0011	0.9889
Water 2	0.0012	0.9637
Water 3	0.0012	0.9907
Water 4	0.0011	0.9885
Water 5	0.0011	0.9813
Water 6	0.001	0.9797
Average	**0.0011**	
Std dev	**0.00008**	

Appendix 4

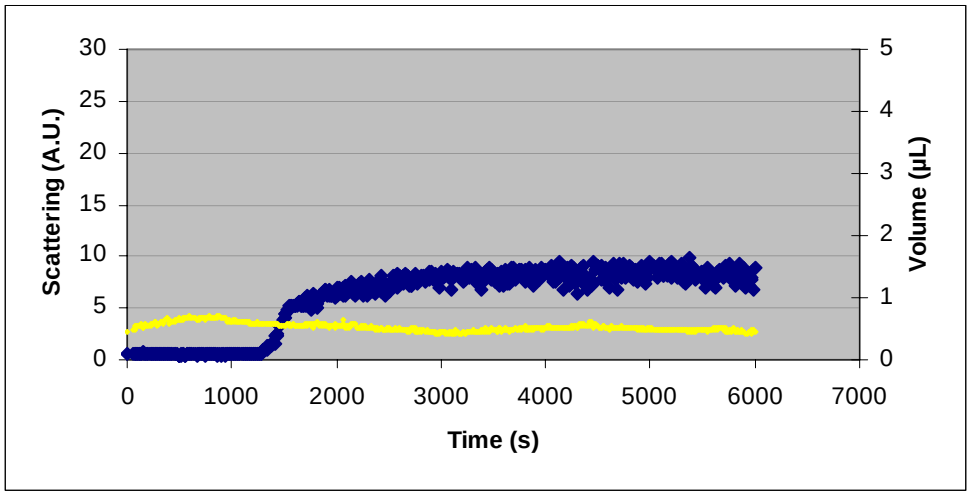

Diagram 1: Experiment 1) DDM_DLPC1_exp_NO 1 0

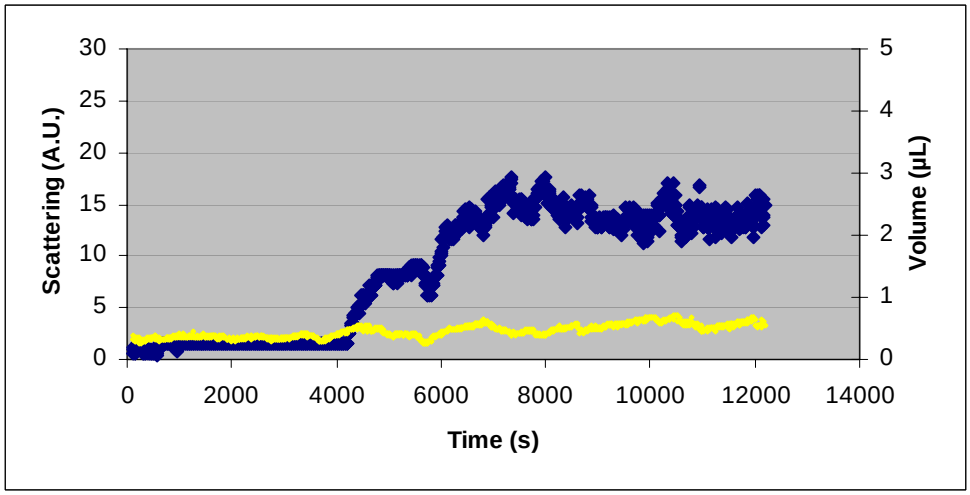

Diagram 2: Experiment 2) HasAHasR_C8E4_DLPC_1 5

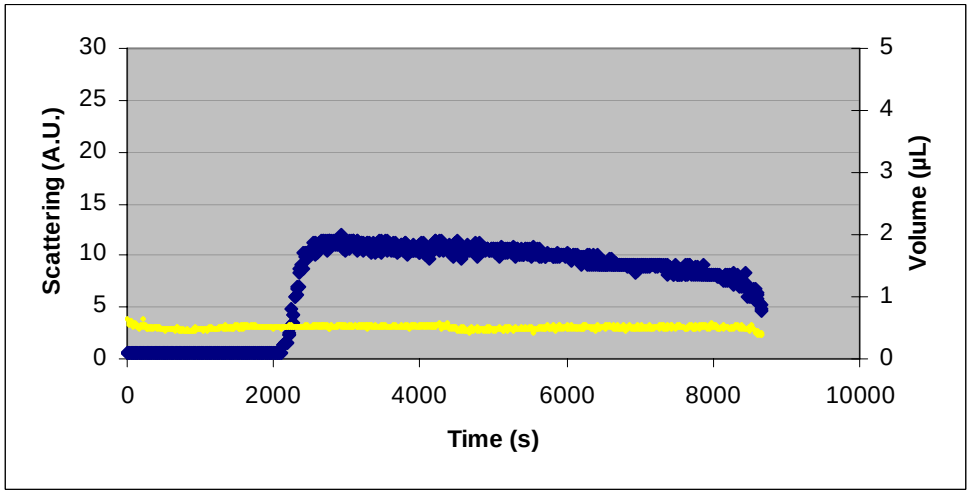

Diagram 3: Experiment 3) HasAHasR_C8E4_DLPC_1 7

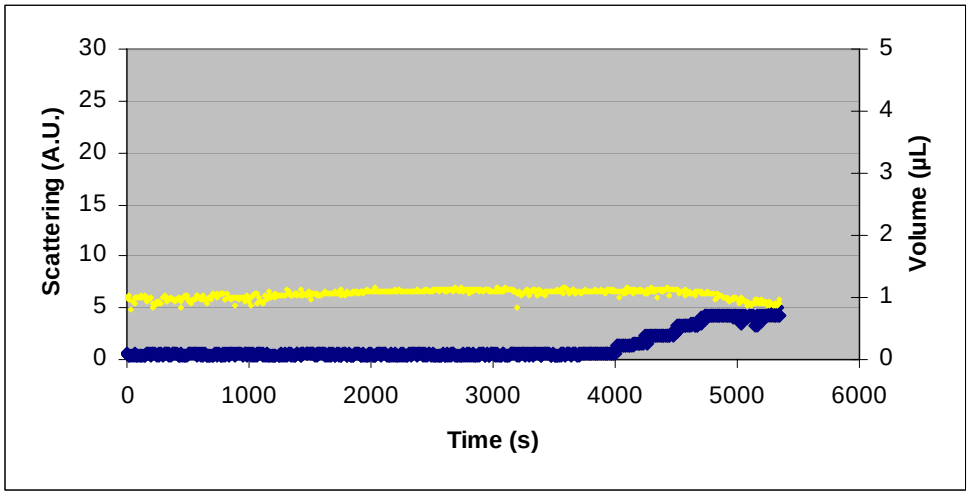

Diagram 4: Experiment 4) C8E4_DLPC_LPR1_060330_exp_2

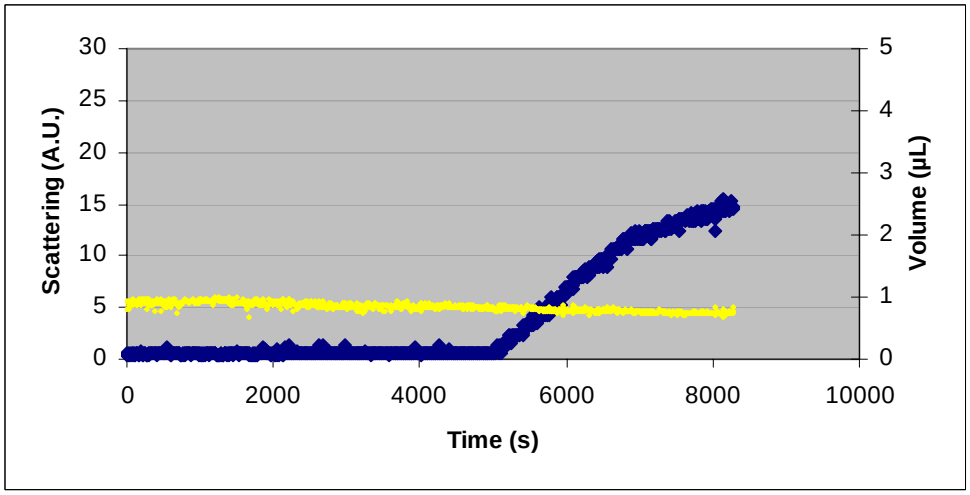

Diagram 5: Experiment 5) C8E4_DLPC_LPR1_060330_exp3

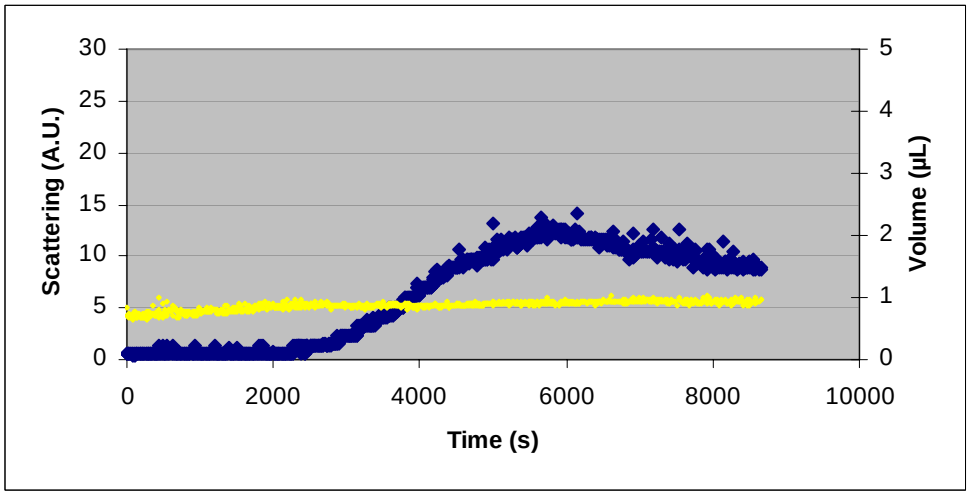

Diagram 6: Experiment 6) C8E4_DLPC_LPR1_060330_exp_4

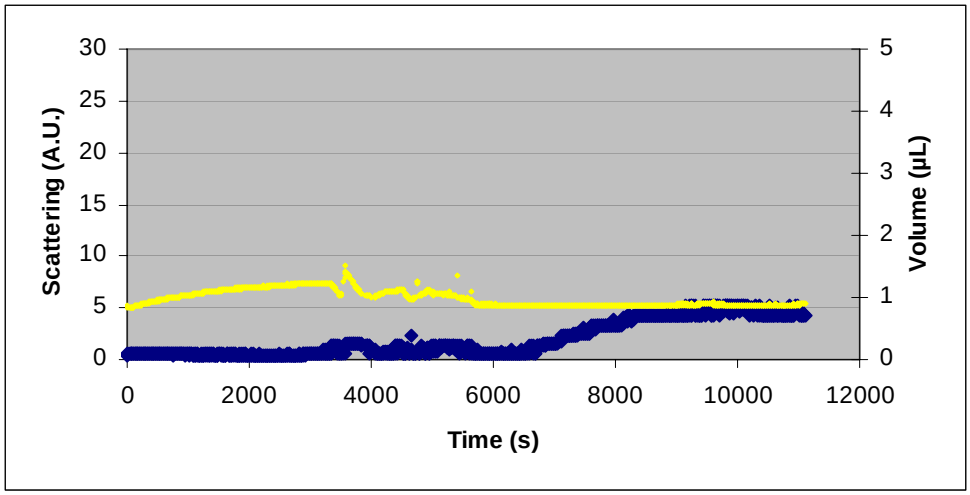

Diagram 7: Experiment 7) C8E4_DLPC_LPR1_060331_exp5

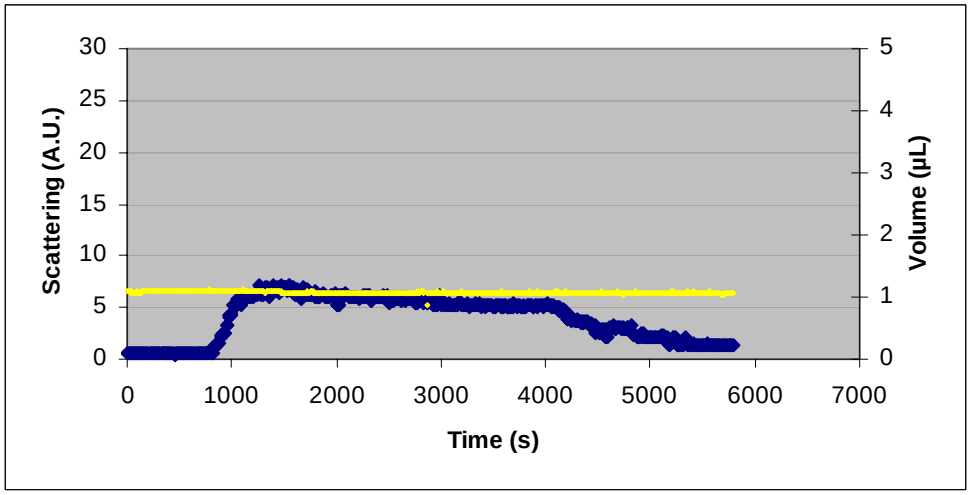

Diagram 8: Experiment 8) C8E4_EC_LPR1_060403_exp_1

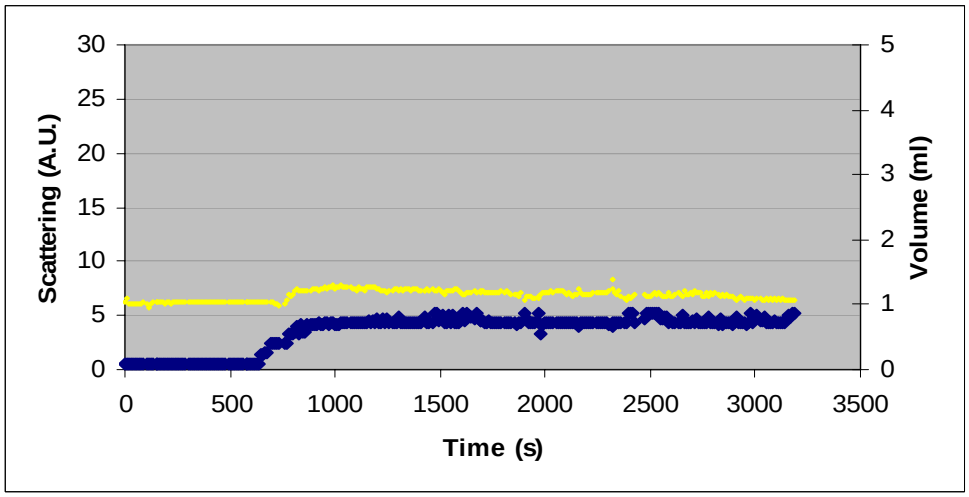

Diagram 9: Experiment 9) C8E4_EC_LPR1_060403_exp2

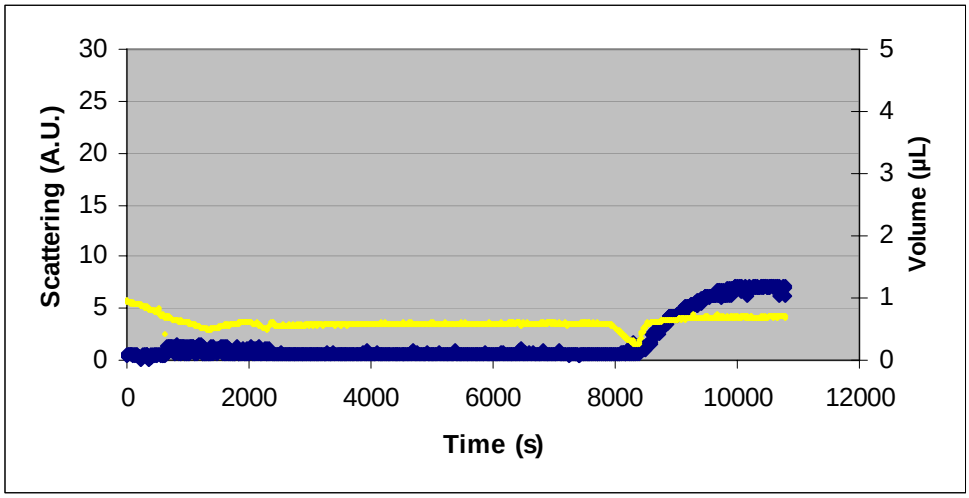

Diagram 10: Experiment 10) C8E4_EC_LPR1_060403_ep_4

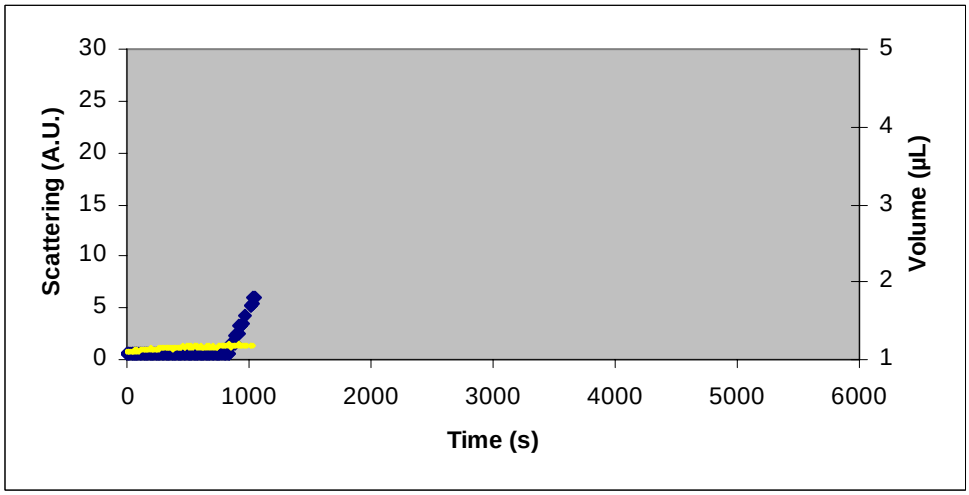

Diagram 11: Experiment 11) C8E4_EC_LPR1_060404_exp_6

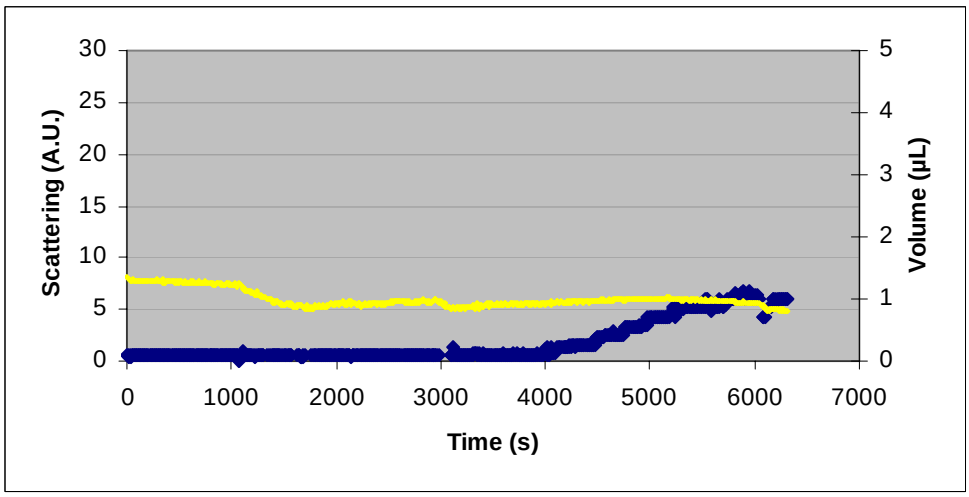

Diagram 12: Experiment 12) C8E4_EC_LPR1_060404_exp_7

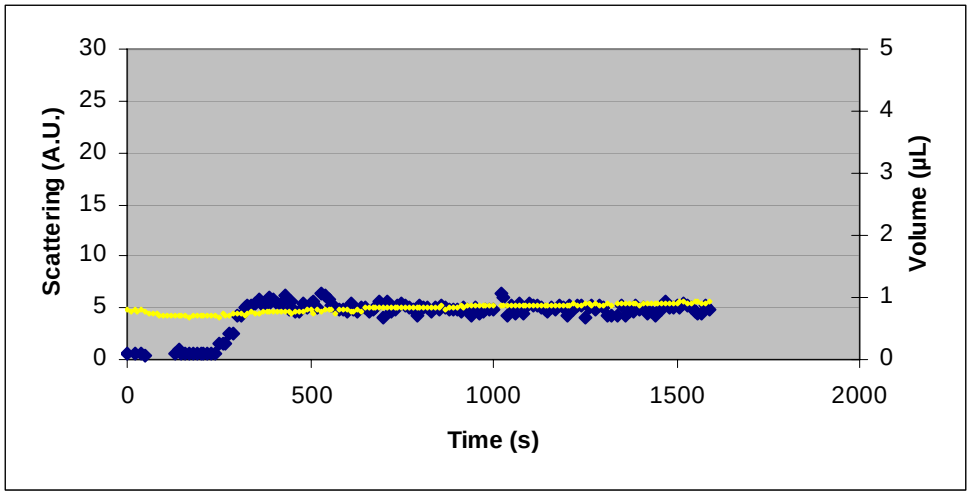

Diagram 13: Experiment 13) DDM_DLPC_LPR1_060406_exp_2

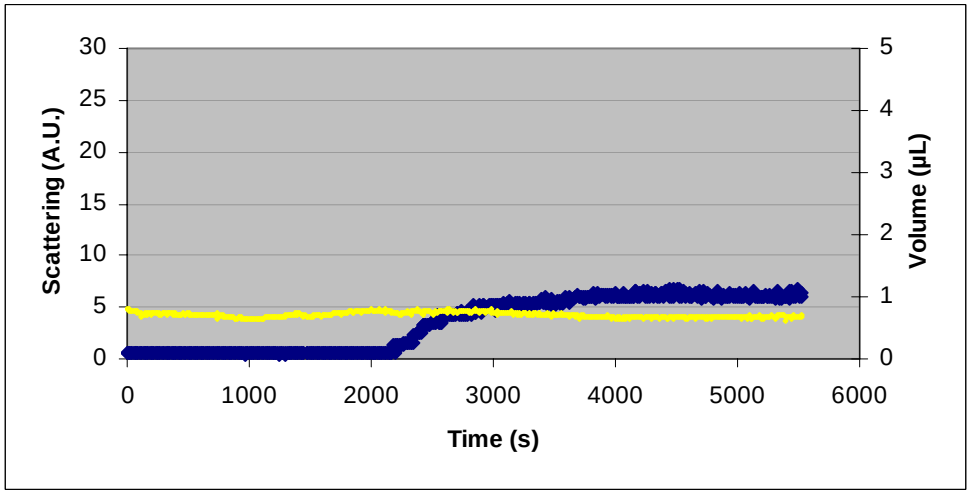

Diagram 14: Experiment 14) DDM_DLPC_LPR1_060406_exp_3

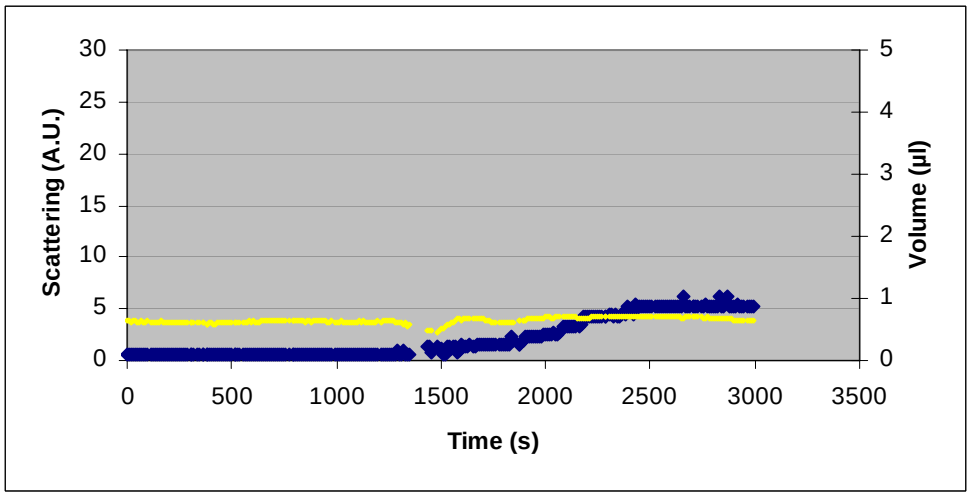

Diagram 15: Experiment 15) DDM_EC_LPR1_060406_exp_8

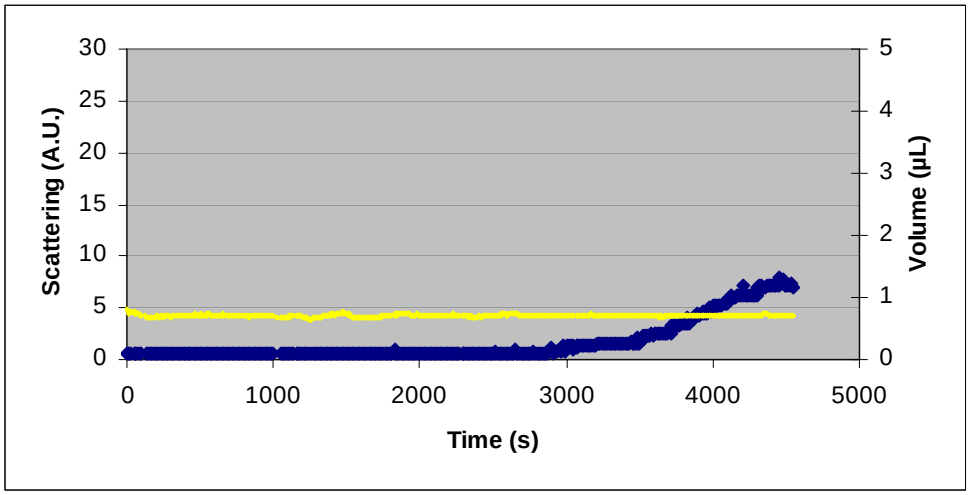

Diagram 16: Experiment 16) DDM_EC_LPR1_060406_exp_9

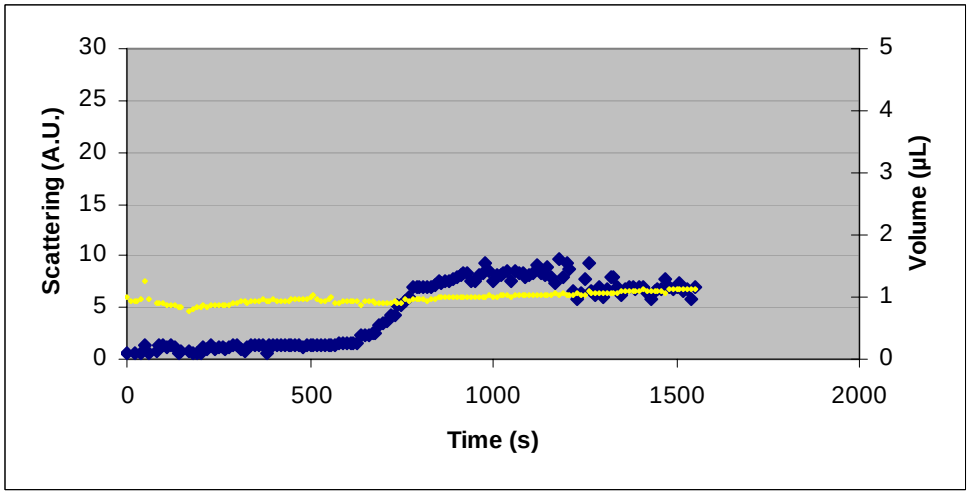

Diagram 17: Experiment 17) DDM_EC_LPR1_060407_exp_10

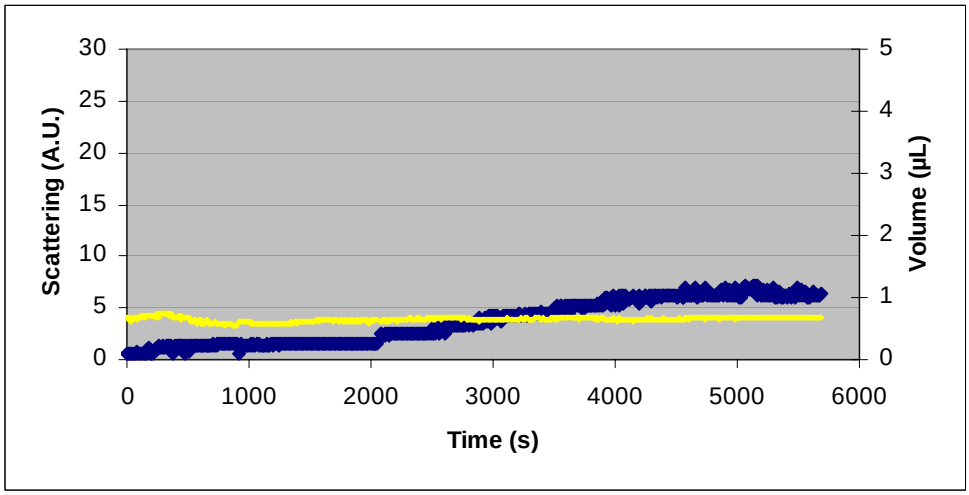

Diagram 18: Experiment 18) DDM_EC_LPR1_060407_exp_11

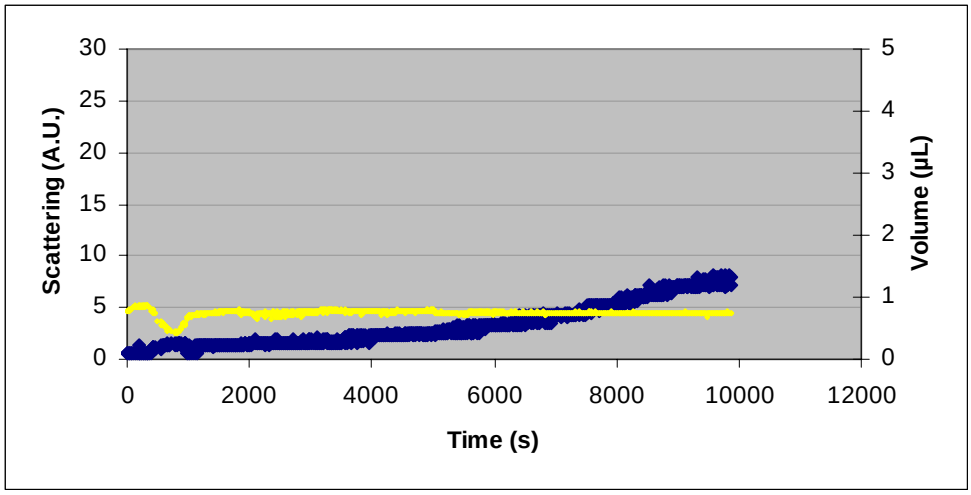

Diagram 19: Experiment 19) DDM_EC_LPR1_060407_exp_14

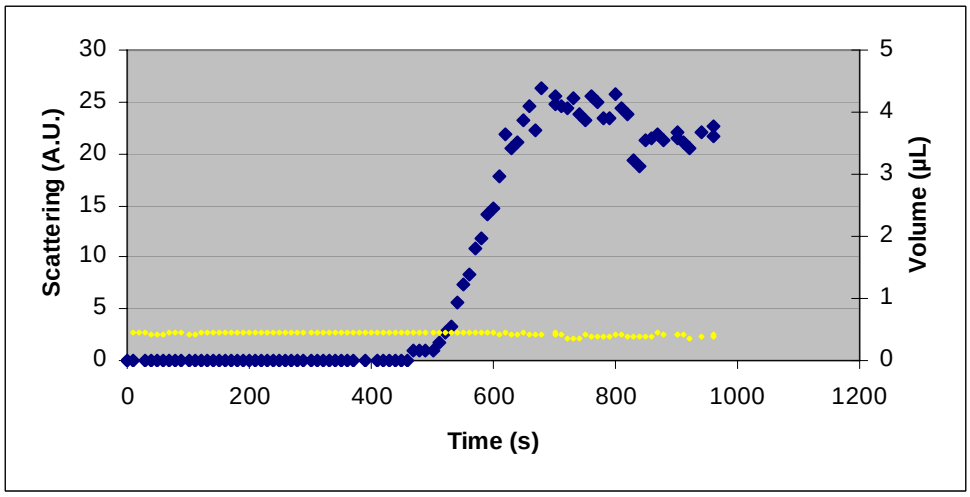

Diagram 20: Experiment 20) DDM_EC_LPR1_060425_exp_2

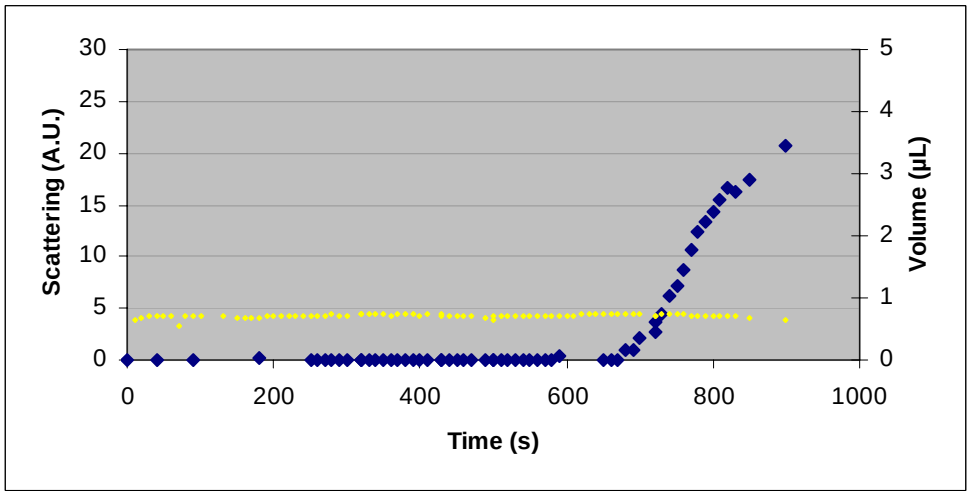

Diagram 21: Experiment 21) DDM_EC_LPR1_060426_exp_1

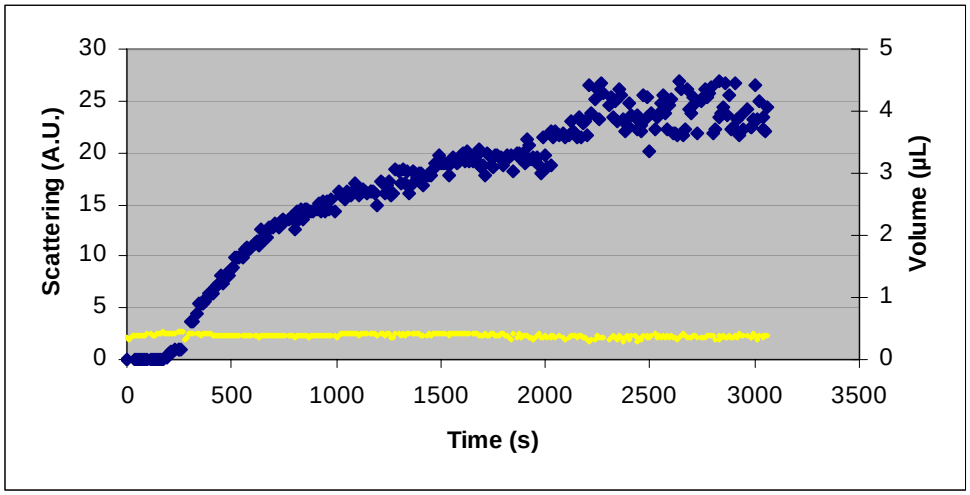

Diagram 22: Experiment 22) DDM_EC_LPR1_060426_exp_2

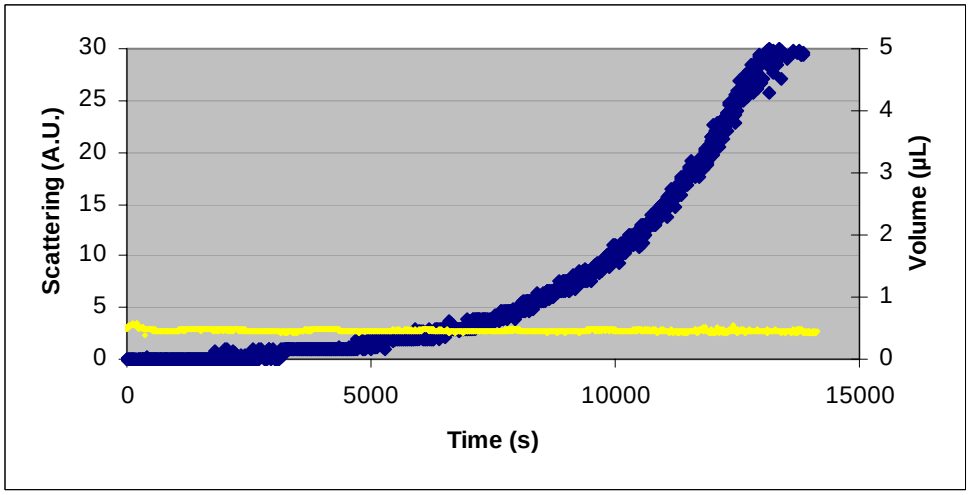

Diagram 23: Experiment 23) DDM_EC_LPR1_060426_exp_3

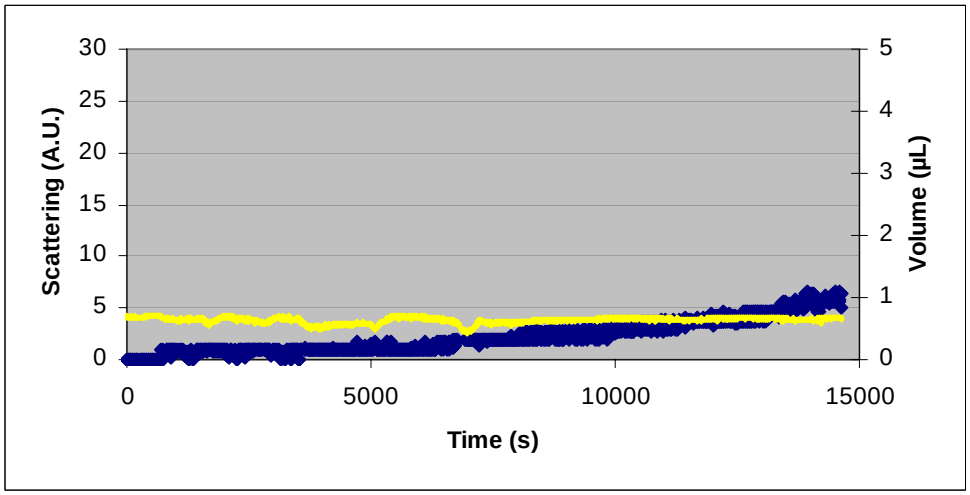

Diagram 24: Experiment 24) DDM_EC_LPR1_060427_exp_1

Experiment	4	5	6	7
Start of precipitation)	4010 sec	5050 sec	2280sec	6710 sec
Concentration of MBCD used	0.25%	0.25%	0.25%	0.25%
Addition from start until precipitation	8.051 µL 0.25%	12.233 µL 0.25%	6.28 µL 0.25%	5.596 µL 0.25%
Conc. MBCD at the start of precipitation	1.86%	3,92%	1.73%	1.59%
Time to reach the plateau	12 min	34 min	55 min	28 min

Experiment	8	9	10	11	12
Start of precipitation	830 sec	650 sec	650 sec	850 sec	3970 sec
Concentration of MBCD used	3%	3%	3%, 0.25%	3%	3% 0.25%
Addition from start until precipitation	0.844µL 3%	0.791 µL 3%	0.412 µL 3%	1.025 µL 3%	1.213 µL 3% 1.535 µL 0.25%
Conc. MBCD at the start of precipitation	2.3%	2.3%	1.55%	2.63%	3.6%
Time to reach the plateau	6 min	4 min	24 min	3 min	32 min

Experiment	13	14
Start of precipitation	250 sec	2180 sec
Concentration of MBCD used	3%	0.25%
Addition from start until start of precipitation	0.279µL 3%	2.562 µL 0.25%
Conc. MBCD at the start of precipitation	1.26%	0.87%
Time to reach the plateau	2 min	12 min

Experiment	15	16	17	18	19	20
Start of precipitation	1320 sec	2890 sec	640 sec	2080 sec	3550 sec	460 sec
Concentration of MBCD used	0.25% 0.1%	0.25% 0.1%	1%	1% 0.01%	1% 0.005	1%
Addition	1.367µL 0.25%	1.096 µL 0.25% 1.986 µL 0.1%	1.198 µL 1%	0.575 µL 1% 2.08 µL 0.01%	0.349 µL 1% 4,926 µL 0.005	0.501 µL 1%
Conc. MBCD at the start of precipitation	0.56%	0.66%	1.36%	0.82%	0.44%	1.13%
Time to reach the plateau	20 min	26 min	3 min	42 min	105 min	4 min

Experiment	21	22	23	24
Start of precipitation	590 sec	260 sec	1970 sec	750 sec
Concentration of MBCD used	1%	1% 0.005%	1% 0.005%	1% 0.005% 0.0025 %
Addition	0.858 µL 1%	0.405 µL 1%	0.385 µL 1% 1.882 µL 0.005%	0.222 µL 1% 0.517 µL 0.005%
Conc. MBCD at the start of precipitation	1.19%	0.91%	0.77%	0.32%
Time to reach the plateau	5 min	28 min	200 min	226 min